

Abstract

The Essential Protein Sts1 Facilitates 26S Proteasome Nuclear Import by a Unidirectional Mechanism in *Saccharomyces cerevisiae*

Carolyn Allain Breckel

2023

Maintenance of the delicate balance between protein translation and degradation is imperative to preserving proper cellular homeostasis. The ubiquitin-proteasome system represents one of the major pathways for protein quality control and is conserved across eukaryotes. The proteasome is a large protein complex that is responsible for proteolysis of various degradation target proteins, and most cellular proteasomes are localized to the cell nucleus. In the budding yeast *Saccharomyces cerevisiae*, proper localization of the proteasome to the nucleus is essential to viability; therefore, the mechanism by which proteasomes enter the nucleus is also of considerable interest. Here, we show that the essential yeast protein Sts1 is responsible for acting as a bridge between fully assembled proteasomes and the classical nuclear transport machinery. Sts1 possesses a bipartite nuclear localization signal that is sufficient for recruitment of the nuclear transport factor karyopherin- α . Subsequent interaction with karyopherin- β mediates entry into the nucleus through the nuclear pore complex, ferrying the 26S proteasome cargo bound to Sts1. Strikingly, Sts1 is degraded by the proteasome in a ubiquitin-independent manner, likely due to unstructured domains at its N- and C-termini, and its ability to bind to the proteasome directly. Sts1 degradation appears to be triggered only in the nucleus upon the action of RanGTP removing the karyopherin proteins and freeing the Sts1 N-terminal

domain for proteasomal degradation. Importantly, this mechanism is likely exclusive to proliferative yeast growth and appears to be a single turnover event. Additionally, we examine the cross-species complementation between Sts1 and its structural homolog in the fission yeast *Schizosaccharomyces pombe* Cut8, as well as its apparent functional homolog from mammalian cells, AKIRIN2. These experiments indicate that Sts1 is an essential unidirectional proteasome nuclear import factor in budding yeast.

The Essential Protein Sts1 Facilitates 26S Proteasome Nuclear Import by a Unidirectional
Mechanism in *Saccharomyces cerevisiae*

A Dissertation
Presented to the Faculty of the Graduate School
of
Yale University
In Candidacy for the Degree of
Doctor of Philosophy

By
Carolyn Allain Breckel

Dissertation Director: Mark Hochstrasser

May 2023

Copyright © 2023 by Carolyn Allain Breckel

All rights reserved.

Table of Contents

Table of Contents	v
List of Figures.....	viii
List of Abbreviations Used	xi
Acknowledgments	xiii
Chapter 1: An introduction to the ubiquitin-proteasome system and karyopherin-mediated nuclear import.....	1
1.1 The ubiquitin-proteasome system	1
1.2 Nuclear import	8
1.3 The Sts1 adaptor protein	13
Chapter 2: Materials and Methods	18
2.1 <i>S. cerevisiae</i> strain construction and growth.....	18
2.2 Plasmid constructions	19
2.3 Antibodies and immunoblotting	19
2.4 Viability assay (plasmid shuffle) and plasmid curing.....	20
2.5 Serial dilution growth assay	21
2.6 Protein expression level analysis	21
2.7 Protein purification	22
2.8 Binding assays and pull-down assays with purified proteins	24
2.9 Degradation assays with purified proteins	25
2.10 Live cell microscopy and nuclear/cytoplasmic signal quantification	26
2.11 Cycloheximide-chase analysis	27
2.12 Anchor Away yeast protein degradation assays	27
Chapter 3: Sts1 structural domains	30
3.1 Introduction.....	30
3.2 Results.....	32
3.2.1 Sts1 contains a non-canonical bipartite NLS that is sufficient for recruitment of karyopherin- α	32
3.2.2 The Sts1 three-helix domain likely mediates homodimerization	40

3.2.3 The Sts1 six-helix bundle is sufficient for proteasome interaction.....	48
3.2.4 The Sts1 C-terminus may regulate proteasome interaction	55
3.3 Discussion.....	58
Chapter 4: Sts1 mediates proteasome nuclear transport	61
4.1 Introduction.....	61
4.2 Results.....	64
4.2.1 Sts1 preferentially binds to 26S proteasomes	64
4.2.2 Sts1 binds the karyopherin- α/β heterodimer and is disrupted by RanGTP.....	67
4.2.3 The karyopherin complex can import proteasome-free Sts1	73
4.2.4 Sts1 does not contribute to proteasome reimport from PSGs	77
4.3 Discussion.....	81
Chapter 5: Sts1 is degraded by the proteasome following completion of nuclear import	87
5.1 Introduction.....	87
5.2 Results.....	90
5.2.1 Sts1 undergoes proteasomal ubiquitin-independent degradation	90
5.2.2 Availability of the N-terminus is required for Sts1 degradation.....	92
5.2.3 Sts1 degradation is initiated by RanGTP	96
5.2.4 Sts1 degradation only occurs in the cell nucleus	99
5.3 Discussion.....	104
Chapter 6: Structural and functional conservation of Sts1	108
6.1 Introduction.....	108
6.2 Results and Discussion	110
6.2.1 Cut8 and AKIRIN2 do not complement an <i>STS1</i> deletion	110
6.2.2 Cut8 can bind to karyopherin- α proteins.....	116
6.2.3 Conservation of proteasome nuclear import adaptors	120
Chapter 7: Conclusions and Outlook	122
7.1 Conclusions.....	122
7.2 Future Studies	124
Appendix 1: Yeast strains used in this study	132

Appendix 2: Plasmids used in this study.....135
References.....137

List of Figures

Chapter 1

Figure 1.1 The ubiquitin-proteasome system.....	2
Figure 1.2 The 26S proteasome.....	6
Figure 1.3 Nuclear import and export pathways.....	9
Figure 1.4 Predicted structure and domain architecture of Sts1.....	16

Chapter 3

Figure 3.1 Sts1 contains a bipartite NLS.....	34
Figure 3.2 The Sts1 N-terminus is sufficient for Srp1 recruitment and nuclear localization of the proteasome.....	39
Figure 3.3 Sts1 likely forms a homodimer that is important to cell viability.....	42
Figure 3.4 Sts1-EE is sufficient to disrupt the Sts1-Srp1 complex.....	45
Figure 3.5 Sts1-EE affects proteasome localization <i>in vivo</i>	47
Figure 3.6 Sts1 dimerization mutants do not impact proteasome expression.....	49
Figure 3.7 Srp1 is required for Sts1 to bind to the 26S proteasome within its six-helix bundle domain.....	51
Figure 3.8 The six-helix bundle mutant <i>sts1-2</i> results in a proteasome interaction and localization defect.....	53
Figure 3.9 Sts1(1-276) rescues <i>sts1</i> Δ but results in cytoplasmic proteasome localization.....	56

Chapter 4

Figure 4.1 Sts1 preferentially binds to 26S proteasomes.....	65
---	----

Figure 4.2 Srp1 can weakly bind purified RP and CP <i>in vitro</i>	66
Figure 4.3 Sts1 forms a transport-competent complex with Srp1 and Kap95 that is disrupted by RanGTP.....	69
Figure 4.4 The Anchor Away system sequesters proteasomes to various cellular compartments.....	74
Figure 4.5 Sts1 can undergo nuclear import without bound proteasomes.....	76
Figure 4.6 Sts1 does not contribute to the reimport of proteasomes from PSGs.....	78
Figure 4.7 Cytoplasmic foci observed during glucose starvation do not contain Sts1-GFP.....	82

Chapter 5

Figure 5.1 Sts1 is a ubiquitin-independent proteasome substrate.....	91
Figure 5.2 The free Sts1 N-terminus is required for its ubiquitin-independent degradation.....	94
Figure 5.3 Sts1 ubiquitin-independent degradation is initiated by RanGTP.....	98
Figure 5.4 Ran may be able to bind and hydrolyze ATP.....	100
Figure 5.5 Sts1 proteasomal degradation occurs in the nucleus following nuclear import.....	102
Figure 5.6 Sts1 degradation in the nucleus but not the cytoplasm is observed by radioactive pulse-chase.....	103

Chapter 6

Figure 6.1 Sts1 and its homologs do not complement each other <i>in vivo</i>	112
---	-----

Figure 6.2 Cut8 is more stable compared to Sts1 in *S. cerevisiae*.....114

Figure 6.3 Sts1 and Cut8 are unable to achieve proteasome nuclear accumulation in their reciprocal species.....115

Figure 6.4 Cut8 is degraded in a ubiquitin-dependent manner in *S. cerevisiae*.....117

Figure 6.5 Cut8 can bind to karyopherin- α proteins.....119

Chapter 7

Figure 7.1 Model of Sts1 and karyopherin- α/β -mediated nuclear import of 26S proteasomes and subsequent Sts1 ubiquitin-independent degradation in the nucleus.....125

List of Abbreviations Used

Abbreviation

BSA	Bovine serum albumin
cNLS	Classical nuclear localization signal
CP	Core Particle
DMSO	Dimethyl sulfoxide
DTT	Dithiothreitol
DUB	Deubiquitylating enzyme
ECL	Enhanced chemiluminescence
EDTA	Ethylenediaminetetraacetic acid
GAP	RanGTPase-activating protein
GEF	Guanine nucleotide exchange factor
GSH	Glutathione
GST	Glutathione S-transferase
HECT	Homologous to E6-AP Carboxy Terminus
IBB	Importin- β binding (domain)
IBR	In-between RING (domain)
INM	Inner nuclear membrane
IPTG	Isopropyl β -D-1-thiogalactopyranoside
MBP	Maltose-binding protein
NaOH	Sodium hydroxide
N/C	Ratio of nuclear to cytoplasmic signal
NES	Nuclear export signal
NLS	Nuclear localization signal
NPC	Nuclear pore complex
NTR	Nuclear transport receptor
OD ₆₀₀	Optical density (measured at wavelength 600 nm)
PAGE	Polyacrylamide gel electrophoresis
PMSF	Phenylmethylsulfonyl fluoride
PQC	Protein quality control

PSG	Proteasome storage granule
RBR	RING Between RING
RING	Really Interesting New Genes
RP	Regulatory Particle
RRM	RNA recognition motif
SC	Synthetic complete
SD	Synthetic defined
SDS	Sodium dodecyl sulfate
SUMO	Small ubiquitin-like modifier
SV40	Simian virus 40
UPS	Ubiquitin-proteasome system
WT	Wild type
YPD	Yeast-peptone-dextrose
5-FOA	5'-Fluororotic acid
6His	Hexahistidine affinity tag

Acknowledgments

There are a number of individuals who have aided me throughout my time in graduate school and I would like to thank them for their support and assistance. First, I would like to thank my mentor, Mark Hochstrasser, for his direction, encouragement, and leadership; I am grateful to have had an advisor so willing to teach me and help me to grow. Additionally, I would like to thank the members of my thesis committee, Mark Solomon and Christian Schlieker for their advice and helpful suggestions over the years. I also would like to thank Cordula Enenkel for serving as my outside reader and offering a critical eye to the final work.

I owe a debt of gratitude to the current and former members of the Hochstrasser lab. Each person in this group contributed to my scientific development and created a wonderful environment to work in every day. I am particularly grateful to Chris Hickey, Lauren Budenholzer, Jason Berk, and Zane Johnson for teaching me new techniques, offering excellent feedback and ideas in support of my project, and especially for their endless patience.

I would also like to thank my “forced friends” for their kindness and company over all these years. To Cat, Josh, and Lukas: thank you for all of the climbing sessions, game nights, and picnics. I am so grateful for your friendship.

I owe the greatest thanks and gratitude to my family for inspiring me and providing many years of unending support. To my parents specifically, for your love and your sacrifice for my success and happiness. Finally, I would like to thank my husband, Andrew, for staying by my side through so much, and simply being everything I could have wanted.

Chapter 1: An introduction to the ubiquitin-proteasome system and karyopherin-mediated nuclear import

Portions of this chapter were previously published in Breckel CA & Hochstrasser M. (2021). Ubiquitin Ligase Redundancy and Nuclear-Cytoplasmic Localization in Yeast Protein Quality Control. *Biomolecules* **11**, 1821.

1.1 The ubiquitin-proteasome system

Cells depend on the proper maintenance of protein homeostasis, including regulation of protein levels in response to external stimuli or during development and clearance of damaged or dysfunctional proteins. Genomic mutations or errors during transcription or translation can produce erroneously folded proteins that are incapable of carrying out their functions, and various chemical and physical stressors can similarly induce protein misfolding (Goldberg, 2003). In eukaryotes, misfolded proteins are managed by various protein quality control (PQC) systems that repair or degrade them. When abnormal proteins cannot be refolded, their degradation is accomplished in large part by the actions of the ubiquitin-proteasome system (UPS) (Hochstrasser, 1996). Such aberrant proteins often form intracellular aggregates that can be toxic to cells if they are not cleared in a timely fashion (Yang and Hu, 2016; Folger and Wang, 2021).

Regulation of protein homeostasis (“proteostasis”) is mediated in part by the UPS, which degrades aberrant proteins that cannot be refolded. Protein substrates are marked for degradation by the 26S proteasome through covalent attachment of the conserved small protein ubiquitin (Hochstrasser 1996; Hochstrasser 2009). Ubiquitylation of a protein is carried out by a cascade of enzymes: a ubiquitin-activating enzyme (E1), one or more ubiquitin-conjugating enzymes (E2), and one or more ubiquitin ligases (E3) (Figure 1.1).

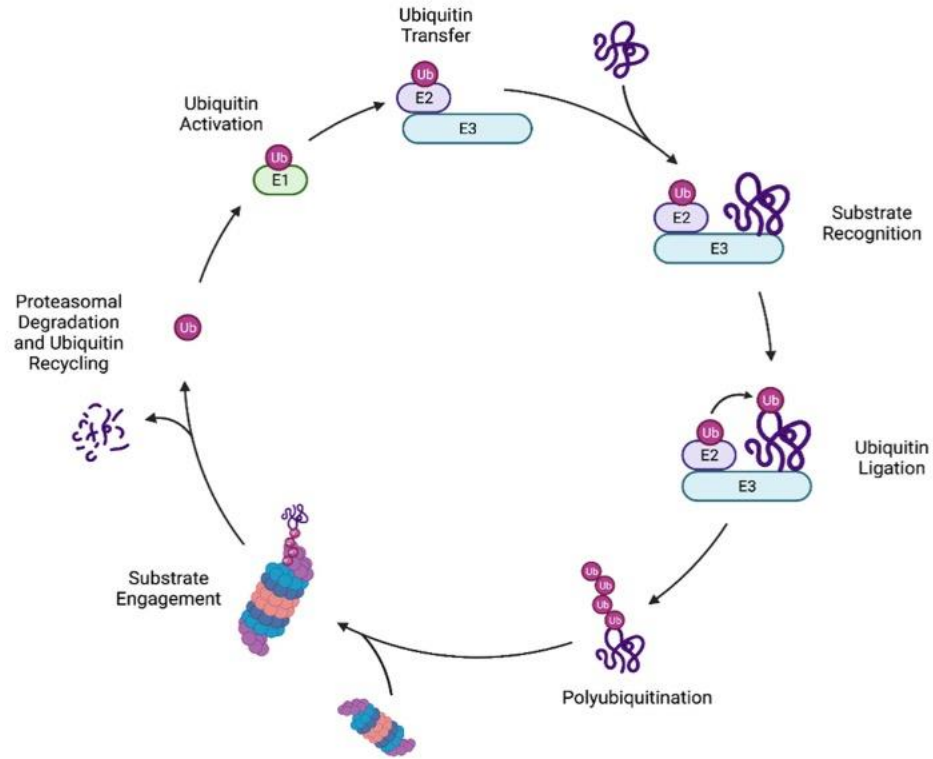


Figure 1.1: The ubiquitin-proteasome system.

Ubiquitin is activated by a ubiquitin-activating enzyme (E1) and is transferred to a ubiquitin-conjugating enzyme (E2). A ubiquitin ligase (E3) recognizes a protein substrate and simultaneously binds the E2-Ub conjugate. The E3 enzyme mediates transfer of the ubiquitin to a substrate protein. Multiple rounds of ubiquitylation can be performed on a given substrate to create poly-ubiquitin chains. Ubiquitylated substrates are recognized by the proteasome. Substrates are deubiquitylated, unfolded, and translocated into the proteasome core for degradation. Substrate peptides are released, and intact ubiquitin molecules are recycled. Image from Breckel & Hochstrasser, 2021.

The E1 first forms a high-energy thioester bond between the ubiquitin C-terminus and its own active site cysteine residue in an ATP-dependent manner. This activated ubiquitin is then transferred to an E2 cysteine side chain via a transthioylation reaction. Finally, an E3 enzyme binds both the protein substrate and the E2-Ub conjugate and promotes the transfer of ubiquitin to a substrate lysine residue (Deshaies and Joazeiro, 2009; Fredrickson and Gardner, 2012). In yeast, there is only one ubiquitin-activating enzyme (Uba1) along with 11 ubiquitin-conjugating enzymes, and roughly 100 ubiquitin ligases, reflecting the wide range of substrates that must be recognized by E3 enzymes, often for specific proteasome-mediated degradation (Finley et al., 2012; Jackson et al., 2000).

There are three main classes of ubiquitin ligases: HECT (Homologous to E6-AP Carboxy Terminus), RING (Really Interesting New Gene), and RBR (RING Between RING). The HECT-type E3 ligases interact directly with E2 conjugating enzymes and mediate the transfer of a ubiquitin moiety from the E2 to the HECT domain of the E3 ligase. Loading of the ubiquitin moiety primes the E3 ligase for ubiquitylation of a bound protein substrate (Bernassola et al., 2008). While HECT ubiquitin ligases serve as a catalytic intermediate, RING ubiquitin ligases are metalloenzymes that coordinate zinc ions to create a platform for E2 enzymes to directly transfer the ubiquitin moiety to the substrate protein (Metzger et al., 2013). RBR ubiquitin ligases are a newer class of E3 enzymes that function through the action of three domains: a RING domain, an in-between RING domain (IBR), and a RING2 domain. This trio allows for the RING domain to bind both the E2 and ubiquitin to mediate ubiquitin transfer to the RING2 domain, priming the E3 enzyme for substrate attachment (Wenzel and Klevit, 2012). The mechanisms by which ubiquitin ligases recognize misfolded proteins for degradation are closely tied to the type

of degradation signal or “degron” that is displayed by the substrate protein (Hochstrasser 1996; Finley et al., 2012). The various ubiquitin ligases have specific affinity for certain degron sequences or general features of misfolded proteins such as exposed hydrophobicity. Different ubiquitin ligases are also localized to specific cellular compartments such as the nucleus, cytoplasm, or endoplasmic reticulum, and may contribute to unique protein quality control pathways depending on their resident compartment (Breckel and Hochstrasser, 2021).

A target protein can be ubiquitylated at a single residue (mono-ubiquitylation), mono-ubiquitylated at several residues (multi-ubiquitylation), or have a chain of ubiquitin moieties appended to a single protein site (poly-ubiquitylation) (Pickart, 2000). Although protein lysyl ubiquitylation is most common, it is also possible for serine, threonine, cysteine, or the substrate N-terminal methionine amino group to be used as ubiquitin attachment sites (Cadwell and Coscoy, 2005). There is considerable variability in the possible poly-ubiquitin chains that can be formed. A ubiquitin moiety can be covalently attached to one of the seven lysine residues on another ubiquitin molecule (K6, K11, K27, K29, K33, K48, and K63), producing unbranched (homotypic) or branched (heterotypic) poly-ubiquitin chains (Hochstrasser 2009). An unbranched poly-ubiquitin chain is composed of a single linkage type, while a branched poly-ubiquitin chain can contain several different amide (isopeptide) linkages (Yau and Rape, 2016). Protein ubiquitylation can have various consequences depending on the ubiquitin configuration on the protein substrate. Protein mono-ubiquitylation has been associated with many processes, including DNA repair, autophagy, and membrane trafficking, while poly-ubiquitylation often directs protein substrates to the proteasome (Sadowski et al., 2012; Pohl and Dikic, 2019). Poly-

ubiquitin chains of various linkages can mark substrates for degradation, but the majority of proteasome-mediated degradation is mediated by K48 and K11 ubiquitin chains (Finley et al., 2012). An important facet of ubiquitylation is that it is readily reversible due to the action of deubiquitylating enzymes (DUBs), of which there are at least 21 in budding yeast (Burrows et al., 2012; Mapa et al., 2018).

Proteasomes are conserved across eukaryotes and archaea and represent a major site of enzymatic activity in cells (Tomko and Hochstrasser, 2013; Majumder et al., 2019; Finley 2009; Müller et al., 2019). The proteasome itself is a ~2.5 MDa multimeric protein complex that is composed of two main subcomplexes: the 19S regulatory particle (RP), and the 20S core particle (CP). The fully assembled 26S proteasome is composed of the 20S CP and one or two RPs capping either end of the cylindrical CP. The RP can be further broken down into two subcomplexes known as the lid and base (Figure 1.2) (Coux et al., 1996; Lu et al., 2015). The lid is responsible for ubiquitylated substrate recognition where the yeast subunit Rpn11 acts as a deubiquitylating enzyme that removes ubiquitin chains from proteasome-bound substrates (Thrower et al. 2000; Verma et al., 2002; Saeki 2017). The base is responsible for ATP-dependent substrate unfolding through its AAA+ ATPase ring (Glickman et al., 1998; Kunjappu and Hochstrasser, 2014). Unfolded substrates are then translocated into the CP for proteolysis. The protein target is degraded, but the ubiquitin moieties are recycled (Ravid and Hochstrasser, 2008).

Though most proteolytic target proteins are recognized and degraded by the proteasome via ubiquitylation, an increasing number of proteins have been identified as ubiquitin-independent proteasome substrates. Ubiquitin-independent degradation has been observed both as degradation mediated solely by the 20S core particle or proceeding

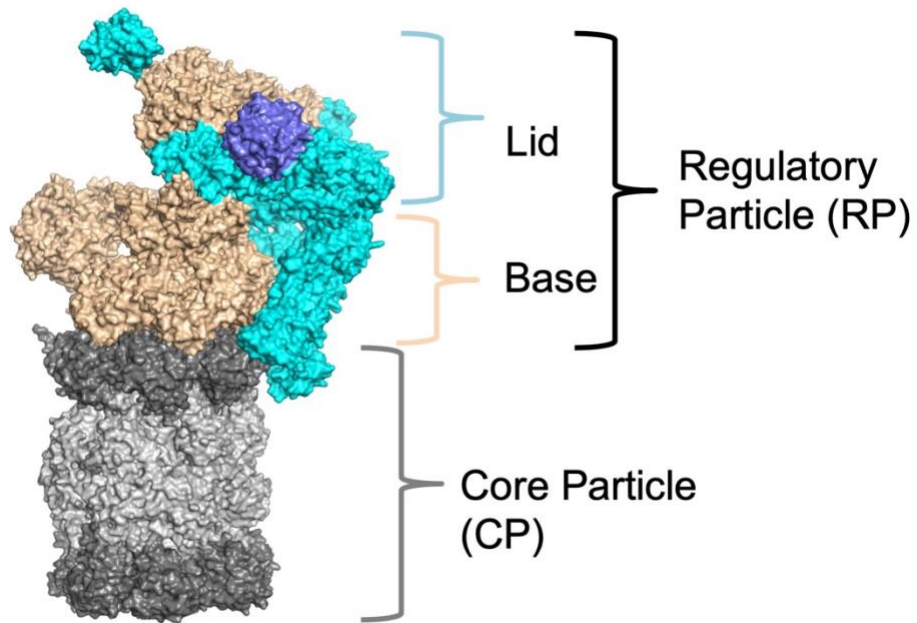


Figure 1.2: The 26S proteasome.

The 26S proteasome is composed of two major subcomplexes: the 20S core particle and the 19S regulatory particle. The CP is colored in grey with the α -rings colored in dark grey and the β -rings colored in light grey. The RP comprises the base (shown in tan) and the lid (shown in light blue). In this view, one of the ubiquitin-binding subunits, Rpn10, is colored in dark blue. Image generated using PDB 3JCP, adapted from Budenholzer et al., 2017.

through ubiquitin-independent interaction with the 26S proteasome regulatory particle. Several intrinsically disordered proteins have been identified as 20S-dependent proteolytic substrates, including the mammalian cell cycle inhibitor p21 (Chen et al., 2007; Sánchez-Lanzas & Castaño, 2014; Ben-Nissan & Sharon, 2014). Such substrates likely do not require the proteasome RP to unfold the target proteins prior to CP proteolysis, instead being engaged directly through the unfolded domains passively diffusing into the CP pore (Erales and Coffino, 2014; Liu et al., 2002; Liu et al., 2006). In mammals, the CP is also able to interact with several different regulators other than the proteasome RP. These include PA28 $\alpha\beta$, REG γ , and PA200, species that can bind to the CP α -rings and mediate 20S activation and gate-opening (Babbitt et al., 2005; Ma et al., 1992). Similar requirements for unstructured domains have been observed for ubiquitin-independent substrates of the 26S proteasome. For these species, common characteristics include the availability of a disordered domain that, as with 20S substrates, may be engaged by the CP to initiate degradation (Jariel-Encontre et al., 2008; Erales and Coffino, 2014). This is typically accomplished by the substrate protein first binding to the proteasome RP directly. This ability to interact with the RP likely eliminates the need for a poly-ubiquitin chain for proteasome recognition of the substrate (Yu et al., 2016). Though many questions still exist, ubiquitin-independent degradation remains an important proteasome-associated function.

Though the ubiquitin-proteasome system is responsible for specific proteolysis, in the case of large protein aggregates or damaged organelles, the cell can instead degrade these substrates through autophagy. The macroautophagy pathway encloses substrates in double-membrane sacs called autophagosomes that subsequently fuse with the vacuole

(equivalent to the mammalian lysosome) where their contents are digested. Autophagy is typically induced under stress conditions such as starvation (Nakagowa et al., 2009; Li and Kane, 2009). Under nitrogen starvation, autophagosomes usually engulf random volumes of cytoplasm; however, autophagy can be selective, and such mechanisms often also employ ubiquitin as a specificity tag (Nakagowa et al., 2009; Li and Kane, 2009).

1.2 Nuclear import

Nuclear transport is a highly conserved cellular pathway that is mediated by various nuclear transport factors (NTRs). In classical nuclear import, the karyopherin- α and karyopherin- β proteins (also called importins) form an α/β heterodimer to mediate cargo transport (Figure 1.3). NTRs can recognize distinct sequences in cargo proteins, known as nuclear localization signals (NLSs) or nuclear export signals (NESs), to initiate cellular trafficking (Cautain et al., 2014). Classical nuclear localization signals (cNLSs) are generally composed of basic amino acid patches (primarily lysine and arginine), either in a single short patch (monopartite) or in two distinct patches separated by a linker sequence (bipartite) (Kalderon et al., 1984; Dingwall and Laskey, 1991; Robbins et al., 1991). In monopartite NLSs, such as the simian virus 40 (SV40) T-antigen NLS, karyopherin- α binds to the basic NLS sequence across its major concave binding pocket (Conti et al., 1998; Kobe 1999). In contrast, bipartite NLS sequences engage both the major binding pocket as well as a secondary minor binding site of karyopherin- α with each basic sequence (Conti et al., 1998; Kobe 1999; Fontes et al., 2000; Conti and Kuryian, 2000). Importantly, bipartite NLS sequences typically rely on both basic sequences for full nuclear import functionality, while separate monopartite NLSs maintain nuclear transport capabilities

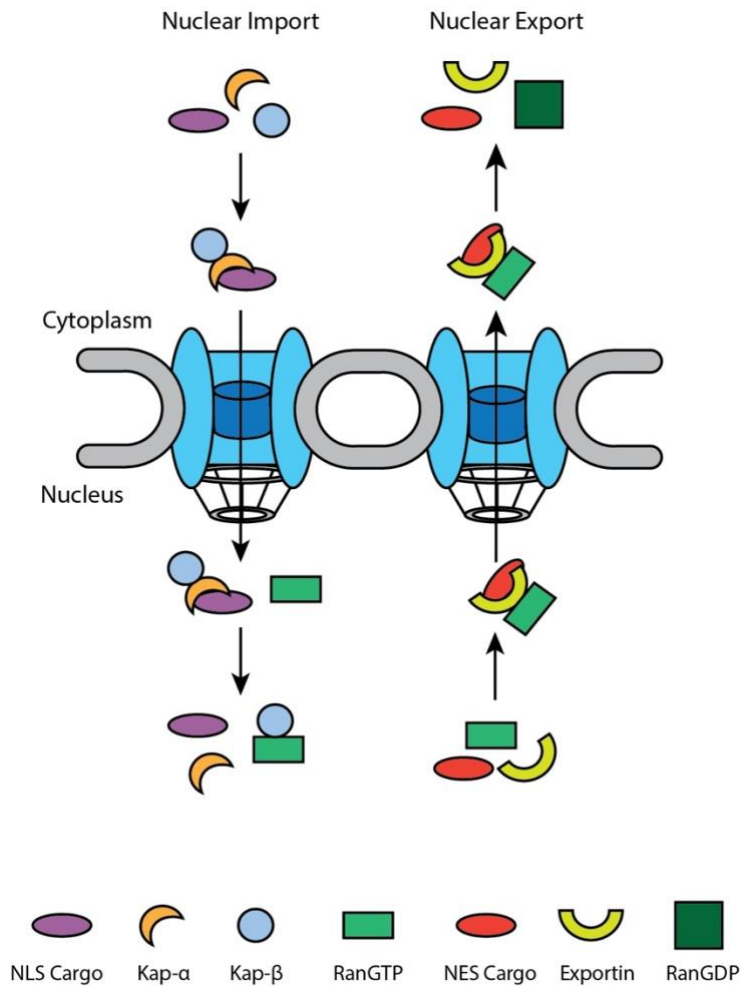


Figure 1.3: Nuclear import and export pathways.

Nuclear import: Karyopherin- α receptors recognize NLS sequences in cargo proteins and subsequently recruit karyopherin- β , forming a heterodimer. Karyopherin- β mediates nuclear entry through the nuclear pore complex. The transport complex is disassembled by RanGTP in the nucleus and the cargo is released. Nuclear export: Exportin receptors bind to NES sequences in cargo proteins and mediate export through the nuclear pore complex with the aid of RanGTP. Once in the cytoplasm, GTP hydrolysis releases the cargo protein, producing RanGDP.

even when one basic patch has been mutated (Lange et al., 2010). Nuclear export signals (NESs) behave opposite to NLSs, mediating interactions with karyopherin- β -related exportin proteins to transport cargo from the nucleus out into the cytoplasm. NESs are typically composed of hydrophobic amino acids and were first identified in the HIV-1 Rev protein and protein kinase inhibitor A (Fisher et al., 1995; Wen et al., 1995).

For classical NLS-containing proteins, the NTR karyopherin- α binds the NLS sequence of a target protein in the cytoplasm, thus triggering recruitment of the karyopherin- β transport protein to the karyopherin- α importin- β -binding (IBB) domain (Leung et al., 2003; Conti et al., 1998; Kalderon et al., 1984; Cingolani et al., 1999). The α/β heterodimer mediates import of the cargo protein to the nucleus through the nuclear pore complex (NPC). This is achieved via transient interactions between karyopherin- β and the disordered Phe-Gly-repeat regions of nucleoporin proteins within the NPC (Bayliss et al., 2000; Enenkel et al., 1995). The hydrophobic filaments of nucleoporins form a restrictive matrix inside the NPC which prevent the passive diffusion of proteins larger than ~40 kDa (Lott et al., 2010; Ribbeck et al., 2002; Bayliss et al., 2000; Suntharalingam and Went, 2003; Went and Rout, 2010).

Once inside the nucleus, karyopherin- β is released from its binding partner through interaction with the active GTP-bound form of the small Ras-like GTPase Ran. Nuclear transport is mediated by a gradient across the nuclear membrane between the two forms of the Ran with high RanGTP in the nucleus and high RanGDP in the cytoplasm (Moore et al., 1998; Chook et al., 2011). These two populations are maintained by the RanGTPase-activating protein (GAP) in the cytoplasm, which promotes GTP hydrolysis, and the Ran guanine nucleotide exchange factor (RanGEF) in the nucleus that mediates the exchange

of GDP for GTP (Hopper et al., 1990; Kunzler et al., 2000). RanGTP interaction with karyopherin- β triggers cargo release in the nucleus, and the import factors are subsequently recycled to the cytoplasm, in some cases by association with exportin proteins, for repeated rounds of nuclear import (Lee et al., 2005; Kobe 1999; Matsuura and Stewart, 2004; Nachury and Weis 1999; Stewart 2007; Gorlich et al., 1996). The various factors involved in nuclear import and export are illustrated in Figure 1.3.

In the budding yeast *Saccharomyces cerevisiae*, roughly 80% of proteasomes accumulate in the nucleus and the maintenance of this nuclear population is important to cell survival (Pack et al., 2014; Tsuchiya et al., 2013; Budenholzer et al., 2020). Nuclear localization of proteasomes is generally evolutionarily conserved across eukaryotes (Wojcik and DeMartino, 2003; Laporte et al., 2008). In the fission yeast *Schizosaccharomyces pombe* and the green alga *Chlamydomonas reinhardtii*, proteasomes concentrate at the inner nuclear envelope; mammalian proteasome localization, while often also mostly nuclear, varies among different cell types (Wojcik and DeMartino, 2003; Laporte et al., 2008; Pack et al., 2014; Wilkinson et al., 1998; Chowdury and Enenkel, 2015; Albert et al., 2017). The need for the concentration of proteasomes in the nucleus is not well understood. One possibility is the high number of transcription factors present in the nucleus that must be rapidly turned over, as well as the important contributions of the UPS to DNA replication and repair (Ulrich et al., 2010). Another possibility is that misfolded proteins in the nucleus are a greater threat than in other compartments. Studies in mammalian cells have shown that misfolded protein aggregates can be cytotoxic to cells because they sequester their interaction partners (Zhu et al., 2000; Yang and Hu, 2016; Folger and Wang, 2021). These can include proteasome subunits, chaperone and co-

chaperone proteins, transcription factors, and RNA. The functions of these species can be compromised, and nuclear processes may be particularly sensitive to these deficits. Though the presence of proteasomes in the cell nucleus appears to be imperative to proteostasis, the means by which proteasomes enter the nucleus have remained controversial.

Several proteasome subunits in the RP base and CP contain nuclear localization signals, though it is not clear whether all of these NLS sequences would be accessible in the fully assembled 26S proteasome structure (Enenkel, 2014; Lehmann et al., 2002; Tanaka et al., 1990; Wendler et al., 2004). While the RP base and certain CP assembly precursors can be transported into the nucleus independently of the 26S proteasome complex, the RP lid contains no known NLS sequence and yet still primarily localizes to the nucleus (Wendler and Enenkel, 2019; Isono et al., 2007). How the lid is able to enter the nucleus is currently unclear, though current hypotheses speculate that it is imported by piggybacking on the base or fully assembled proteasome or using an adaptor protein that contains an NLS sequence. Though there is debate in the field whether proteasomes are predominantly imported as various subcomplexes and later assembled in the nucleus, 26S proteasomes are competent for karyopherin-mediated nuclear transport (Pack et al., 2014; Budenholzer et al., 2020).

Transport of proteins into the nucleus require entry through NPCs, which span the nuclear envelope. As noted above, the NPC interior is composed of the disordered FG repeat-rich domains of nucleoporin proteins, which create a roughly 9 nm aqueous channel and prevent the passive diffusion of proteins larger than ~40 kDa (Paine et al., 1975; Feldherr and Akin, 1997; Feldherr et al., 1984; Wentz and Rout, 2010). As described above, larger proteins that cannot diffuse through the NPC require nuclear import factors

to ferry them through the pores, which are able to accommodate cargo up to 26 nm in diameter, though the dynamic nature of the NPC suggests that the pore may dilate and admit larger cargo (Dworetsky and Feldherr 1988; Feldherr et al., 1998; Strambio-de-Castillia and Rout, 2002; Zimmerli et al., 2021).

The fully assembled 26S proteasome, roughly cylindrical in shape, has a diameter of approximately 15 nm, suggesting that it may be able to pass through the NPC (Förster et al., 2013; Wendler and Enenkel 2019). A bulky nuclear import cargo of this size necessitates the use of karyopherin-mediated active transport to translocate through the restrictive NPC channel. In fact, current studies indicate that large nuclear import targets require increasing amounts of NLS sequences to mediate their efficient nuclear translocation (Paci et al., 2020). The existence of cNLSs in some but not all of the proteasome subunits and subcomplexes suggests that fully assembled 26S proteasomes can be imported in a classical NLS import pathway (Shulga et al., 1996; Chen and Madura, 2014).

1.3 The Sts1 adaptor protein

The large size of the proteasome and the presence of nuclear localization signals in several of its subunits implies the contribution of the karyopherins to proteasome nuclear accumulation. Importantly, the proteasome lid does not possess an NLS sequence in any of its subunits, raising the question of how it is able to accumulate in the nucleus when separated from the fully assembled complex (Wendler and Enenkel, 2019; Isono et al., 2007). If the lid is a karyopherin-mediated import cargo, it likely must bind to an adaptor

protein or chaperone that contains an NLS sequence of its own. In *S. cerevisiae*, a possible candidate for this lid import adaptor is the small essential protein Sts1.

Originally identified as a suppressor of the temperature-sensitive secretory pathway mutant *sec23-11*, Sts1 (Sec Twenty-three Suppressor-1) has been loosely connected to several cellular pathways including co-translational degradation, ER to Golgi trafficking, and cell division (Ha et al., 2014; Liang et al., 1993; Amrani et al., 1996; Houman and Holm, 1994). In one study, Sts1 was shown to be a suppressor of the temperature-sensitive mutant *srp1-49*, a mutant of the yeast karyopherin- α protein Srp1, and a direct interaction partner of Srp1 (Tabb et al., 2000). This karyopherin mutant is reportedly still able to import cNLS-containing cargo, at least after short periods at the restrictive temperature (Shulga et al., 1996; Chen and Madura, 2014). Additionally, the Tabb et al. study also identified the proteasome lid subunit Rpn11 as a high-copy suppressor of the *srp1-49* growth defect and showed that overexpression of either Sts1 or Rpn11 in *srp1-49* yeast alleviated the observed degradation defect of a model substrate, ubiquitin-Pro- β -galactosidase (Tabb et al., 2000). Sts1 is a primarily nuclear protein, possesses a nuclear localization signal, and is able to bind to both Srp1 and the proteasome *in vitro*, as well as affect the localization of the proteasome *in vivo* (Tabb et al., 2000; Romero-Perez et al., 2007; Chen et al., 2011; Ha et al., 2014). These data suggested that the karyopherin pathway and Sts1 could function together in proteasome nuclear import, with Sts1 serving as a possible Srp1 adaptor.

No structural data for Sts1 currently exists, and sequence similarity searches indicate that there does not exist a homologous protein in mammals or other tetrapods, despite the essential nature of Sts1 in baker's yeast (Budenholzer et al., 2020). In such

searches, a likely homolog of Sts1 can be identified in the fission yeast *Schizosaccharomyces pombe*. This protein, Cut8, is a protein required at high temperatures in *S. pombe* that has been suggested to function as an anchor protein that tethers the proteasome to the inner nuclear membrane (Tatebe and Yanagida, 2000; Takeda and Yanagida, 2005). The crystal structure of the central portion of Cut8 has been solved; this α -helical core is flanked by largely disordered segments (Takeda et al., 2011). Cut8 was reported to assemble into a homodimer, weaving monomers together through one of its two helical domains. From comparisons to the crystal structure of Cut8 and the use of AlphaFold2 structure prediction software, we have identified several predicted structural domains in Sts1 (Takeda et al., 2011; Jumper et al., 2021; Varadi et al., 2022) (Figure 1.4). Like Cut8, the Sts1 central region is predicted to be composed of two α -helical domains and possesses disordered domains at both its N- and C-termini. As this study will discuss, the different predicted structural domains of Sts1 confer disparate yet important functions in proteasome nuclear import. A summary of these domains as well as a predicted structure of Sts1 from AlphaFold2 is represented in Figure 1.4.

Despite the well-characterized connections between Sts1, the karyopherin pathway, and the proteasome, the mechanism of proteasome import has remained elusive. In this thesis I will investigate the role that Sts1 plays in karyopherin-mediated proteasome nuclear import. I will describe unique features of each of the predicted Sts1 binding domains and the essential nature of Sts1-mediated nuclear import of the proteasome. I will also describe evidence for the contribution of the karyopherin- α/β heterodimer and the RanGTPase cycle to proteasome nuclear import. In addition, this work suggests that Sts1-mediated nuclear import is unidirectional and terminates with the ubiquitin-independent

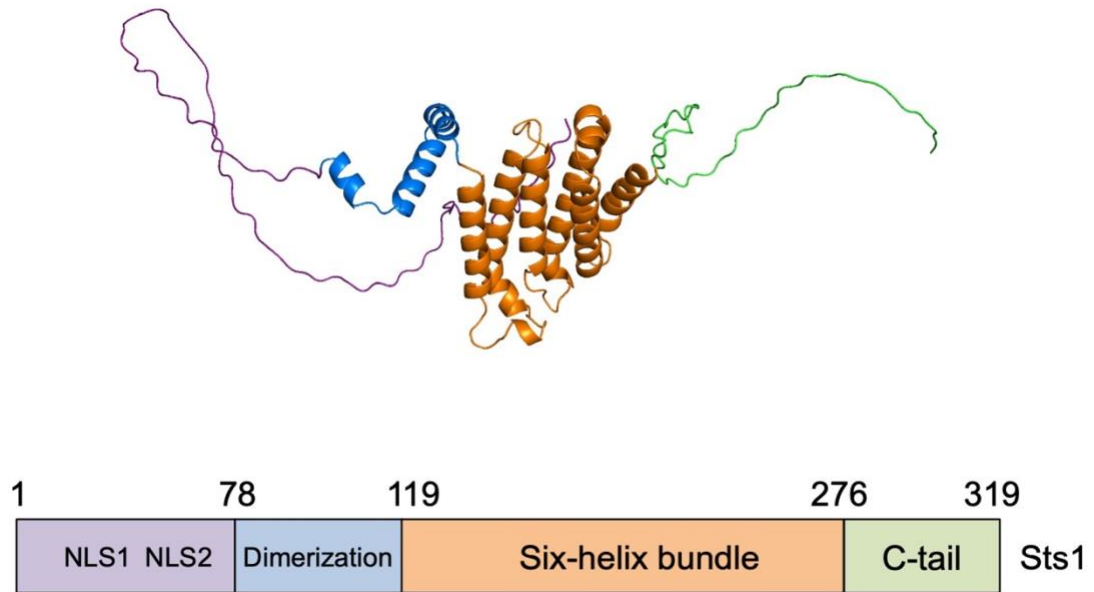


Figure 1.4: Predicted structure and domain architecture of Sts1.

The predicted structure of an Sts1 monomer generated using AlphaFold2. Sts1 is predicted to contain a non-canonical bipartite nuclear localization signal (“NLS1” and “NLS2”) within its unstructured N-terminus (purple). Sts1 is predicted to form a homodimer through its three-helix domain (blue) based on the published crystal structure of the homolog in *S. pombe* Cut8.

proteasomal degradation of Sts1 inside the nucleus upon disassembly of the karyopherin import complex. Finally, I will examine the conservation of Sts1 and the conclusions that can be drawn from its structural and functional counterparts in other species. My combined data suggest that Sts1 is an essential yeast protein that is responsible for the successful nuclear localization of fully assembled 26S proteasomes during exponential growth.

Chapter 2: Materials and Methods

2.1 *S. cerevisiae* strain construction and growth

A complete list of the yeast strains used in this study can be found in Appendix 1. Strains were created by a combination of mating followed by tetrad dissection, homologous recombination with PCR products, and plasmid transformation. All strains are based on the MHY500 WT background unless otherwise noted in Appendix 1. Since *Sts1* is an essential protein in *S. cerevisiae*, the endogenous allele typically remains unmodified and the various constructs of *Sts1* were expressed from plasmids as described in each assay. The viability assays are the sole exception, where I used a *sts1* Δ /pRS316-STSI strain.

Yeast cells were grown in rich yeast-peptone-dextrose (YPD) or minimal (SD) media (2% glucose in either media) typically at either room temperature, 30°C, or 37°C. Strains that were temperature sensitive were typically grown at either room temperature or 30°C and shifted to growth at 37°C for 1-2 hrs before assaying. With the exception of experiments performed under glucose starvation conditions (described below), all experiments using yeast in liquid culture were performed using exponentially growing yeast between OD₆₀₀ 0.8 and 1.2. Variations of yeast growth conditions are noted in the appropriate figure legends.

For glucose starvation experiments, yeast cells were grown overnight at 30°C in synthetic complete (SC) medium (0.67% yeast nitrogen base without amino acids, 0.5% casamino acids, 0.002% adenine, 0.004% tryptophan, 0.002% uracil, and 2% glucose) (Li et al., 2022). Cells were diluted to 0.2 OD₆₀₀ in fresh SC medium and grown to mid-exponential phase (OD₆₀₀ between 0.8 and 1.2). Cells were centrifuged (5000 rpm, 5 min), rinsed with sterile water, and resuspended in SC medium containing 0.025% glucose

(labeled as “Glucose Starvation” in figures) and cultured at 30°C for 48-72 hours, as indicated in the figure legends. For refeeding conditions, cells that were grown in SC medium containing 0.025% glucose were supplemented with 2% glucose and grown for 1 hr at 30°C before assaying.

2.2 Plasmid constructions

A complete list of the plasmids used in this study appears in Appendix 2. All plasmids used were constructed using standard molecular genetic techniques. The *STS1* allele was originally amplified from pGEX-2TK-Sts1, received from Kiran Madura’s lab (Chen et al., 2011; Smith and Johnson, 1988). The *CUT8*, *IMP1*, and *CUT15* alleles were originally amplified from *S. pombe* genomic DNA. The *AKIRIN2* allele was originally synthesized by GenScript and codon-optimized for expression in *S. cerevisiae* (de Almeida et al., 2021). All other plasmids were created using a combination of restriction enzyme- or PCR-based cloning and site-directed mutagenesis. Constructs were verified by DNA sequencing. Yeast genomic DNA or other plasmids already in the Hochstrasser Lab database served as templates for cloning.

2.3 Antibodies and immunoblotting

Immunoblotting was performed using the following primary antibodies: anti-GFP (JL8 antibody catalog no. 632380, Takara; 1:1000), anti-PGK (catalog no. 459250, Invitrogen; 1:20,000), anti-FLAG (catalog no. F3165, Sigma; 1:10,000), anti-Sts1 (Budenholzer et al., 2020; 1:5000), anti-Tetra-His (catalog no. 34670, Qiagen; 1:4000), anti-Rpn11 (Michael Glickman, 1:5000), anti-Pre6 (Dieter Wolf, 1:5000), anti-G6PDH

(catalog no. A9521, Sigma; 1:20,000), and anti-GST (catalog no. ab19256, Abcam; 1:10,000). Either donkey anti-rabbit IgG linked to horseradish peroxidase or sheep anti-mouse IgG linked to horseradish peroxidase (catalog no. NA934V and catalog no. NXA931V, GE Healthcare, respectively) was used as the secondary antibody. Proteins were visualized on film (catalog no. E3018, Thermo Fisher Scientific) or with a G-box (for quantification) using enhanced chemiluminescence (ECL).

2.4 Viability assay (plasmid shuffle) and plasmid curing

MHY9580 was made by Dr. Chris Hickey by knocking out one out of two wild type (WT) *STS1* alleles in the diploid yeast MHY606. The resultant heterozygous diploid was then transformed with *URA3*-marked pRS316-*STS1* plasmid, followed by sporulation and tetrad dissection. Spores that were capable of growth on hygromycin plates (200 pg/mL hygromycin) (*sts1Δ* is marked with the hygromycin resistance *hphMX4* gene) but that could not survive on plates containing 5'-fluororotic acid (5-FOA) (1 mg/mL), which causes loss of the pRS316-*STS1* plasmid, were identified as *sts1Δ*/pRS316-*STS1* segregants. These include MHY9579 and MHY9580.

Yeast with chromosomal knockouts of *STS1* were transformed with the appropriate plasmids. After selection, transformants were struck on plates containing 5-FOA at 1 mg/mL. Since the inclusion of 5-FOA is incompatible with expression of the *URA3* gene, this treatment allows us to selectively grow cells that had lost the original pRS316-*STS1* cover plasmid. Growth on 5-FOA plates indicates the gene on the introduced plasmid in question supports viability in the absence of WT *STS1*. Conversely, colonies that do not show growth on 5-FOA, must express an allele that cannot complement the *sts1Δ* knockout.

2.5 Serial dilution growth assay

Cells were grown overnight in YPD or SD media, diluted to 0.2 OD₆₀₀ equivalents per mL in sterile water and spotted across the plate in 6-fold serial dilutions. Depending on the number of strains being tested, either five or six dilutions were plated. Plates contained either rich or synthetic medium and were incubated at temperatures ranging from 25°C-37°C. Growth was observed for up to four days, as noted in each figure legend. Specific growth conditions are noted in the figure legends.

2.6 Protein expression level analysis

Yeast cells were grown overnight in 5 mL of the appropriate medium, diluted to 0.2 OD₆₀₀ in 20 mL of fresh medium, and grown to mid-exponential phase (OD₆₀₀ between 0.8-1.2). Cells were lysed using an NaOH/SDS boiling method (Kushnirov, 2000). Briefly, cells equivalent to 2.0 OD₆₀₀ units were harvested, centrifuged, and washed with sterile water. The cells were resuspended in 0.4 mL of 0.1 M NaOH, incubated at room temperature for 5 min, centrifuged, and resuspended in 100 µL of 1X Laemmli Loading Buffer (5X stock is 10% SDS, 0.04% Bromophenol blue, 600 mM DTT, 50% Glycerol, 300 mM Tris HCl, pH 6.8). Samples were heated at 95°C for 5 min and frozen at -80°C until use. Yeast proteins from 0.1 OD₆₀₀ units were resolved by sodium dodecyl sulfate-polyacrylamide gel electrophoresis (SDS-PAGE) followed by immunoblotting for the appropriate protein or affinity tags.

For analysis of protein levels during glucose starvation, cells were grown overnight in 5 mL of synthetic complete medium (SC) as noted above, diluted to 0.2 OD₆₀₀ in 20 mL of fresh SC complete medium, and grown to mid-exponential phase (OD₆₀₀ between 0.8

and 1.2). Cells were washed with sterile water and glucose starved by growing in SC medium containing 0.025% glucose for 72 hrs; recovery from starvation was done by supplementing the starved cells with 2% glucose and growing for an additional 7 hrs, as described above. Yeast cells were lysed and resuspended as above.

2.7 Protein purification

Recombinant glutathione S-transferase (GST), hexahistidine (6His), and maltose-binding protein (MBP) protein fusions were expressed and purified from Rosetta *E. coli* cells by their respective affinity tags using standard affinity purification methods (Budenholzer et al., 2020). In brief, typically 500 mL *E. coli* cultures were grown at 37°C for 5 hrs until OD₆₀₀ = 0.6 and induced with 0.4 μM IPTG at 16°C for 18 hrs. Bacterial cell extracts were typically produced by sonication or using the French press in the presence of proteasome inhibitors, followed by centrifugation. Typically, ~20 mL of cleared cell extract was applied to the appropriate resin for affinity-tag purifications. Columns were washed extensively following application of cell extracts and purified proteins eluted using buffers containing L-glutathione, imidazole, or maltose as appropriate. The homogeneity of eluted species was assessed by SDS-PAGE and Coomassie staining.

In the case of co-purified complexes comprising His-tagged and GST-tagged species, the individual plasmids were co-transformed into Rosetta *E. coli* cells (pET42b-based plasmids for His-tagged proteins and pGEX-6-P-1-based plasmids for GST-tagged proteins). The co-expressed complexes were grown and lysed as above and subsequently affinity purified using 6His-tag binding to TALON resin (Takara). Bound species were co-

eluted with imidazole-containing buffer as above, and the purity of the purified complexes was assessed by SDS-PAGE and Coomassie staining.

In the case of the Sts1-6His/GST-Srp1/Kap95 complex, the Sts1-6His and GST-Srp1 proteins were co-expressed and lysed by sonication, followed by centrifugation (as above). This clarified cell extract was combined with lysed and clarified *E. coli* cell extracts expressing untagged Kap95. The full complex was then purified using 6His-tag binding to TALON resin. Purity of the full complex was assessed by SDS-PAGE and Coomassie staining.

6His-Gsp1 bound to either GTP or GDP was purified according to the protocol outlined in Clarkson et al., 1996. Briefly, 6His-Gsp1 was expressed and purified from Rosetta *E. coli* cell extracts using Ni-NTA resin (Thermo Scientific) as above, and the eluted protein volume was divided for nucleotide loading. 6His-Gsp1 was loaded with 1 mM of GDP or GTP in the presence of 5 mM EDTA to ensure exchange of nucleotide. Nucleotide-loaded Gsp1 was then dialyzed overnight at 4°C and concentrated. The concentrated protein was then purified by gel filtration using a Superdex S200 column. Purity of the protein following gel filtration was assessed by SDS-PAGE and Coomassie staining.

26S proteasomes were affinity purified from yeast as described previously (Li et al., 2015). Briefly, yeast cells chromosomally tagged with *RPN11-3xFLAG* were grown in 2 L of rich medium (4% glucose) for 48 hrs. Harvested cells were lysed via production of cell powder in liquid nitrogen using a mortar and pestle in an ATP-containing lysis buffer. Cell powder was flash frozen in liquid nitrogen and smaller volumes of cell powder were thawed for each affinity purification. Typically, 20 mL of cell powder was thawed and

resuspended in an equivalent volume of ATP-containing lysis buffer. Cells were centrifuged and supernatant applied to FLAG resin for 2 hrs. 26S proteasomes were then affinity-purified using 3xFLAG peptide to produce roughly 1 μ M 26S proteasomes. The concentration and purification of proteasomes were evaluated by SDS-PAGE and Coomassie staining using a BSA standard curve. To purify proteasome subcomplexes, yeast expressing Rpn11-3xFLAG was used to purify the 19S regulatory particle, and yeast expressing Pre1-3xFLAG was used to purify the 20S core particle.

2.8 Binding assays and pull-down assays with purified proteins

Analytical binding assays with 26S proteasomes affinity purified from yeast were conducted according to previously described protocols using various recombinant Sts1 species (Budenholzer et al., 2020). Pull-down assays using the karyopherin proteins were conducted according to a previously described protocol with slight modifications (Hirano et al., 2017). Briefly, recombinant bait proteins (GST-Sts1 in Figure 4.3A or GST-Srp1 in Figure 4.3B) were immobilized on 20 μ L (packed volume) of glutathione (GSH) beads (equilibrated in binding buffer: PBS, 0.1% Tween-20, 0.2 mM DTT, fresh 0.2 mM PMSF). Bait proteins and resin were mixed and rotated at 4°C for 1 hr to bind the bait to the resin. Beads were centrifuged at room temperature (4000 rpm, 2 min), washed with 1 mL of binding buffer, and subsequently incubated with equal amounts of Srp1-6His and GST-cleaved Kap95 at 4°C for 2 hrs on a rotator. Beads were centrifuged as before, washed once with 1 mL of binding buffer, and subsequently incubated with four-fold excess of 6His-Gsp1 (compared to Srp1-6His and Kap95) bound to the nucleotide GTP or GDP, as indicated (“RanGTP” and “RanGDP,” respectively in figures). Beads were incubated with

these Gsp1 species at 4°C for 2 hrs on a rotator. Beads were then centrifuged as before and washed four times with 1 mL of binding buffer. Bound proteins were eluted from the GSH beads in 50 µL of 1X Laemmli sample buffer and analyzed by SDS-PAGE and Coomassie staining.

2.9 Degradation assays with purified proteins

Degradation of purified proteins *in vitro* by proteasomes was conducted according to previously described protocols with slight modifications (Budenholzer et al., 2020). Recombinant prey species (Sts1-6His, Sts1-6His/GST-Srp1, MBP-Sts1, GST-Sts1(116-276), or Sts1-6His/GST-Srp1/Kap95) were incubated in the presence or absence of 26S proteasomes purified from yeast (assay buffer conditions: 50 mM HEPES, pH 7.0, 150 mM NaCl, 10% glycerol, 6 mM MgCl₂, 5 mM ATP, 0.1 mg/ml BSA). Reactions comprised final concentrations of 600 nM 26S proteasomes and 1.2 µM prey species. Reactions were incubated at room temperature with 20 µL fractions removed at the indicated intervals. Where indicated, reaction mixtures were supplemented with two-fold molar excess 6His-Gsp1 (compared to prey species) bound to either GTP or GDP. Fractions were centrifuged at room temperature (10,000 rpm, 2 min), the supernatant was separated from any precipitated material and mixed with Laemmli sample buffer to stop the reaction. Fractions were placed on ice until the experiment was completed. Where indicated, a separate reaction of the prey species was tested in the absence of 26S proteasomes, or in the presence of 26S proteasomes that were pre-incubated for 10 min with 50 µM MG132 (Sigma Aldrich), a proteasome inhibitor, at room temperature. Supernatant fractions were resolved

by SDS-PAGE and immunoblotted for Sts1 via the anti-Sts1, anti-GST, or anti-His antibodies.

2.10 Live cell microscopy and nuclear/cytoplasmic signal quantification

Live cell microscopy and nuclear/cytoplasmic signal quantification were conducted according to established protocols with slight modifications (Budenholzer et al., 2020). Cells were grown overnight in synthetic media (where indicated) at the appropriate temperature (typically either room temperature of 30°C), diluted to 0.2 OD₆₀₀ and grown to mid-exponential phase (OD₆₀₀ between 0.8 and 1.2). Culture aliquots of 1 mL were centrifuged, and cells were typically resuspended in 50 µL of the appropriate synthetic media. Glass slides were spotted with 4 µL of cell suspension and cover slips sealed with nail polish. Cells were immediately imaged.

Imaging was performed on an Axioskop epifluorescence microscope (Carl Zeiss, Thornwood, NY) using a 100x objective lens (plan-Apochromat 100x/1.40 oil DIC) and an AxioCam MRm CCD camera (Carl Zeiss) with AxioVision software. All fluorescent images were captured using auto-exposure. After capture, the background was subtracted in ImageJ, followed by quantification (Schneider et al., 2012).

Quantification was performed using ImageJ (Schneider et al., 2012). The summed signal intensities in equal sized regions in the nucleus (N) and cytoplasm (C) of the same yeast cell were measured and the N/C ratio was determined using Microsoft Excel. Only cells with an identifiable nucleus (excluding cells that were clearly sick or dying or cells where the nucleus was not in the plane of focus) were counted. In all images where the

vacuole was visualized, this region was avoided when taking measurements of cytoplasmic signal intensity.

Every experiment was repeated with three independent liquid-growth cultures of each strain or three independent plasmid transformants per strain. At least 100 yeast cells were quantified from each replicate. The difference in ratio of the nuclear to cytoplasmic signals between different strains or conditions was analyzed for statistical significance in GraphPad Prism8 by unpaired t-test or two-way ANOVA (Figure 3.2C).

2.11 Cycloheximide-chase analysis

Protein degradation rates were determined by following a previously described protocol with slight modifications (Hickey and Hochstrasser, 2015). Cells were grown overnight at 30°C in 5 mL of synthetic medium and diluted to 0.2 OD₆₀₀ in 20 mL. Once they reached mid-exponential phase (OD₆₀₀ between 0.8 and 1.2), enough yeast cells were harvested for 2.5 OD₆₀₀ units per timepoint and resuspended in 7.5 mL medium and incubated for 5 minutes at 30°C. 1 mL was harvested from each sample, followed by addition of cycloheximide to a final concentration of 0.25 mg/mL. Subsequent 1 mL aliquots were harvested at various intervals. Each 1 mL sample was added to 950 µL of ice-cold stop solution (30 mM sodium azide in water), followed by washing, cell lysis and protein extraction via the NaOH/SDS heating method.

2.12 Anchor Away yeast protein degradation assays

For cycloheximide-chase analysis of Sts1-3xFLAG in the different Anchor Away strains, protein degradation rates were determined following previously described

protocols with slight modifications (Hickey and Hochstrasser, 2015; Tsuchiya et al., 2013). Cells were grown overnight at 30°C in 5 mL cultures in rich YPD medium and diluted to 0.2 OD₆₀₀ in 40 mL of fresh medium. After approximately four hours of growth at 30°C, cells were supplemented with 10 µg/mL or DMSO (vehicle control) or rapamycin to allow specific subcellular localization of proteasomes as noted in the figures. Once cells reached mid-exponential phase (OD₆₀₀ between 0.8 and 1.2) after roughly 6 hrs, 5 OD₆₀₀ equivalents per timepoint were collected by centrifugation and resuspended in 5 mL culture medium (at temperature) and incubated for 5 minutes at 30°C. 1 mL was harvested from each sample, followed immediately by addition of cycloheximide to each culture at a final concentration of 0.25 mg/mL. Subsequent 1 mL aliquots were harvested at various intervals, centrifuged (2 min, 10,000 rpm), and supernatant removed. Cell pellets were flash frozen in liquid nitrogen and stored at -80°C until use.

Cell pellets were thawed and resuspended in 325 µL of urea lysis buffer (50 mM Tris-HCl pH 7.5, 5 mM EDTA, 6M urea, 0.5% SDS, 500 µM PMSF, 100 µM MG132). Roughly 100 µL of acid-washed glass beads (Sigma-Aldrich) were added to each sample and cells were beaten using a bead beater for three cycles (1 min of bead beating, 2 min rest) at 4°C. The sample tubes were then punctured using a syringe and centrifuged at room temperature to separate the cell extracts from the glass beads (4000 rpm, 2 min). To immunoprecipitate Sts1-3xFLAG from cell extracts, 20 µL (packed volume) of anti-FLAG M2 affinity gel (Sigma Aldrich) was added to 1.5 mL of wash buffer (150 mM NaCl, 30 mM HEPES, pH 7.5, 5 mM EDTA, 0.2% Triton-X100, 0.1% SDS). 300 µL of each sample extracts added to the equilibrated anti-FLAG resin and rotated at 4°C for 2 hrs. Samples were then centrifuged at room temperature (4000 rpm, 2 min) and the resin pellets washed

three times with 1 mL of wash buffer. Bound proteins were eluted from the anti-FLAG resin by heating for 5 min at 95°C in 50 µL of 1X Laemmli sample buffer and analyzed by SDS-PAGE and immunoblotting with anti-Sts1 antibody. For quantification of cycloheximide-chase data, images digitally collected using a G-box system were processed using ImageJ. Quantifications represent the mean and standard deviation of three independent replicates.

For radioactive pulse-chase analysis, protein degradation rates were determined following previously described protocols with the addition of incubation in the presence of 10 µg/mL rapamycin or DMSO (as described above) (Hickey et al., 2018).

Chapter 3: Sts1 structural domains

Portions of this chapter were previously published in Budenholzer L, Breckel C, Hickey M, Hochstrasser M. (2020). The Sts1 nuclear import adaptor uses a non-canonical bipartite nuclear localization signal and is directly degraded by the proteasome. *Journal of Cell Science* **133**, jcs236158. I performed all experiments presented in this chapter except for those depicted in the following figures: Figures 3.1A, C, E (Lauren Budenholzer), Figure 3.2C (Lauren Budenholzer), Figure 3.3A (Chris Hickey and Jason Berk), and Figure 3.8B (conducted with Chris Hickey).

3.1 Introduction

Sts1 is a small essential protein in *S. cerevisiae* that has been previously associated with the nuclear import of proteasomes as well as other cellular pathways including proper chromosomal segregation during cell division and several ribosome-associated functions (Tabb et al., 2000; Liang et al., 1993; Houman and Holm, 1994; Amrani et al., 1996; Ha et al., 2014). Previous scholarship has demonstrated that Sts1 can suppress mutations in the yeast karyopherin- α protein Srp1, as well as interact with the proteasome lid subunit Rpn11 (Tabb et al., 2000; Chen et al., 2011). Sts1 can also bind to fully assembled 26S proteasomes in the presence of Srp1 and has been characterized as possessing a bipartite nuclear localization signal (Budenholzer et al., 2020). Though previous studies of Sts1 have indicated that it primarily resides in the cytoplasm of yeast, more recent work utilizing Sts1 overexpression have repeatedly shown that Sts1 likely localizes to the cell nucleus (Liang et al., 1993; Amrani et al., 1996; Tabb et al., 2000) This evidence has produced the hypothesis that Sts1 acts as a possible bridge between the karyopherin machinery (through

interaction with its NLS) and the proteasome to facilitate its nuclear import (Chen et al., 2011; Chen et al., 2014).

Though the structure of Sts1 has not been solved, the strong sequence similarity between Sts1 and its homolog in *S. pombe* fission yeast Cut8 have allowed inferences to be made about the possible structural features of Sts1. Cut8 has previously been characterized as a proteasome nuclear envelope tethering protein, binding to the proteasome via a poly-ubiquitin chain (Takeda and Yanagida, 2005). Based on x-ray crystallography data, Cut8 is primarily composed of α -helices and contains a disordered domain at its N-terminus. Additionally, the crystal structure of Cut8 indicates that it acts as a homodimer, linking two monomers through a central domain composed of three helices (Takeda et al., 2011). Studies into Cut8 identified that it likely interacts with the nuclear envelope by making hydrophobic contacts with cholesterol molecules embedded in the inner nuclear membrane; these interactions are proposed to occur within a large helical bundle that comprises the majority of the protein's defined structure (Takeda et al., 2011). Interestingly, the unstructured N-terminal region of Cut8 contains the predicted NLS sequence, though Cut8 has not been reported to interact with any karyopherin proteins in *S. pombe* (Tatebe and Yanagida, 2000).

Due to their high sequence conservation, secondary structure predictions of Sts1 have largely produced theoretical structures of Sts1 that approximate that of Cut8. Specifically, Sts1 is predicted to have unstructured domains at both its N- and C-terminus, as well as two distinct helical domains (Figure 3.1A) (Jumper et al., 2021; Varadi et al., 2022). Preliminary studies into Sts1 similarly identified an NLS sequence within its N-terminal domain, though this sequence was not originally characterized as a bipartite NLS

(Tabb et al., 2000). In these experiments, plasmid-expressed Sts1 mutants with either basic patch of the NLS deleted (NLS1 and NLS2 in Figure 3.1A) were tested for the restoration of growth in yeast deleted for the *STS1* allele. Though deletion of NLS2 allowed complementation of *sts1* Δ , deletion of NLS1 did not (Tabb et al., 2000); however, it is important to note that such drastic truncation mutants may not accurately represent endogenous Sts1 behavior. In summary, these and other data suggest that Sts1 likely binds to Srp1 in an NLS-dependent manner, directly binds to proteasomes, and may form a homodimer, as does Cut8 (Tabb et al., 2000; Chen et al., 2011; Takeda et al., 2011).

In this chapter, we clarify the role that Sts1 plays in proteasome nuclear import by first characterizing the various predicted structural domains of Sts1. We show that Sts1 contains a non-canonical bipartite nuclear localization signal in its N-terminus that is sufficient for nuclear accumulation and interaction with Srp1. Additionally, Sts1 likely homodimerizes through its three-helix domain, and this dimerization behavior may be important to the maintenance of a transport-competent complex with Srp1. We show that the Sts1 six-helix bundle is sufficient for interaction with the proteasome, and that the Sts1 C-terminal tail may contribute to regulating the interaction between Sts1 and the proteasome. These combined data suggest that Sts1 contains distinct structural domains that confer specific functions during proteasomal nuclear import.

3.2 Results

3.2.1 Sts1 contains a non-canonical bipartite NLS that is sufficient for recruitment of karyopherin- α

Previous evidence had indicated that Sts1 possesses a nuclear localization signal that likely mediates interaction with the yeast karyopherin- α protein Srp1; we thus focused

on the previously identified N-terminal basic patches that comprise the NLS to assess this hypothesis (Tabb et al., 2000). The Sts1 NLS sequence was not initially predicted to be a bipartite NLS owing to the unusually long linker sequence between two distinct basic patches composed of lysine and arginine (KQKRRYANEEQEEEEELPRNKNVMKY-GGVSKRR) (Figure 3.1A) (Kosugi et al., 2009). Traditional bipartite NLSs are characterized as possessing a linker sequence of 9-12 residues while the putative Sts1 linker is 24 residues long (Nakai et al., 1999; Cokol et al., 2000). Though the Sts1 sequence represented an unusual bipartite NLS, similar sequences have been noted in other nuclear proteins. In particular, the Ty1 integrase protein, a component of the *S. cerevisiae* Ty1 retrotransposon, contains a bipartite NLS with a 29-residue linker and has been denoted as a “non-canonical” bipartite NLS (Figure 3.1B). In studies of the Ty1 integrase, inactivation of either of the two NLS patches was sufficient to greatly reduce the nuclear accumulation of a double GFP-GFP tandem fusion protein, indicating that they contribute to a bipartite NLS as opposed to two independent NLS sequences (Hodel et al., 2006; Lange et al., 2010). We thus sought to similarly examine the Sts1 bipartite NLS to determine whether both basic regions are required for successful nuclear localization of Sts1.

Nuclear localization signals are composed of short patches of basic amino acids that contact the conserved Srp1 concave binding pocket (Conti et al., 1998). While previous reports had deleted the Sts1 NLS1 and NLS2 sequences, we instead introduced single point mutations in each of the two basic patches, R38D and R65D, to interrogate the putative NLS sequence with minimal disruption to the overall protein structure. These mutants allowed us to assess the bipartite nature of the NLS sequence, and the importance of nuclear localization to Sts1 function and cell viability (Figure 3.1A) (Tabb et al., 2000; Chen et al.,

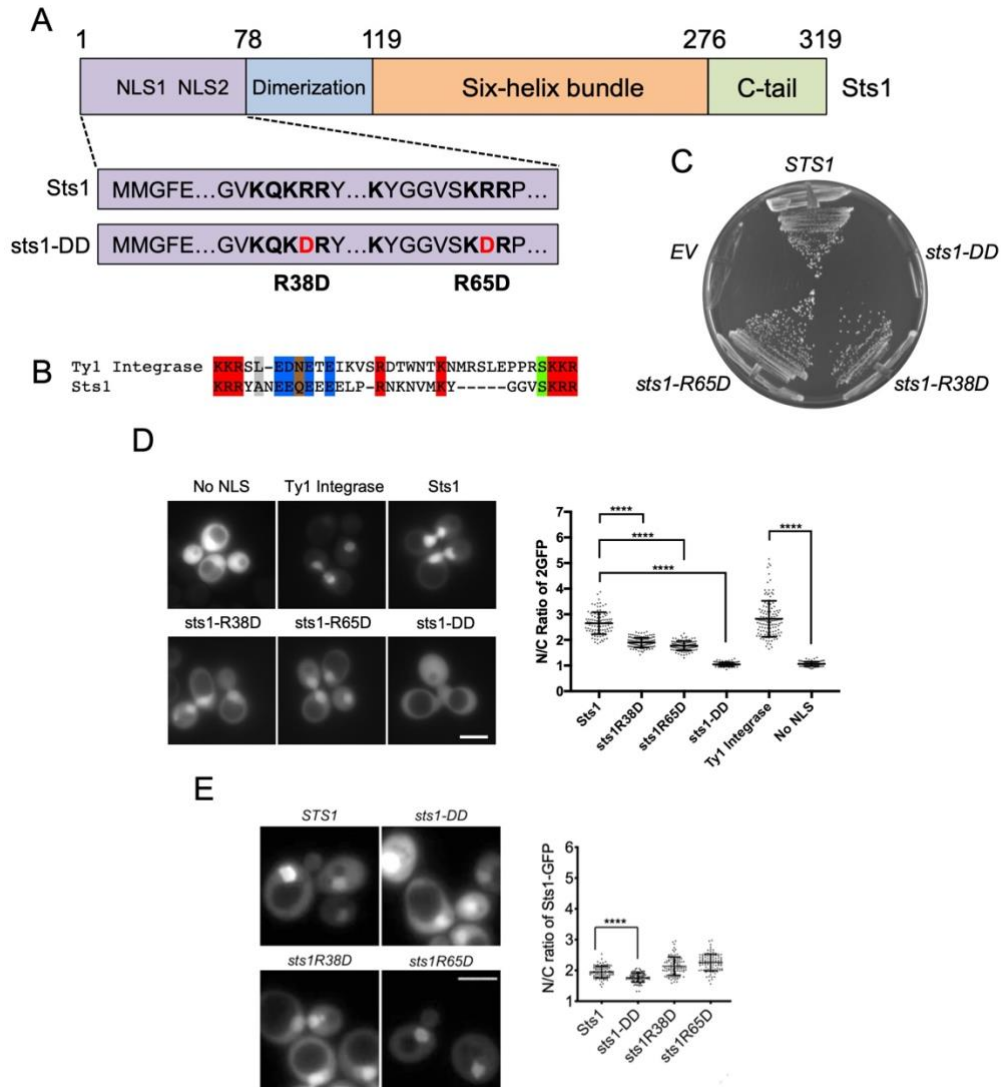


Figure 3.1: Sts1 contains a bipartite NLS.

(A) Predicted domain architecture of Sts1 (as in Figure 1.4). The suggested NLS elements are indicated in bold in the sequences shown below. The two point mutations that comprise the Sts1-DD mutant are highlighted in red. (B) Sequence alignment between the Sts1 bipartite NLS and the known bipartite NLS of the Ty1 integrase, both of which contain unusually long linker regions. The basic NLS patches are highlighted in red and acidic residues are highlighted in blue. (C) Yeast viability assay for Sts1 NLS mutants. Plasmids bearing the noted alleles were transformed into *sts1Δ* yeast bearing a wild-type (WT) *STS1* cover plasmid. Yeast were grown on 5-FOA media to evict the WT Sts1 cover plasmid. EV indicates empty vector. (D) The

Sts1 NLS is a bipartite sequence and mediates nuclear import. WT yeast transformed with plasmids expressing the indicated NLS sequences fused to a 2GFP reporter protein. Sts1 constructs expressed Sts1 residues 1–76 appended to the N-terminus of 2GFP. The NLS sequence from Ty1 integrase N-terminally tagged with 2GFP was used as a positive control for a bipartite NLS, and 2GFP without an NLS ('No NLS') was used as a negative control. Transformants were grown to mid-exponential phase at 30°C prior to fluorescence imaging. **(E)** The Sts1 bipartite NLS affects Sts1 localization. WT yeast transformed with plasmids expressing the indicated Sts1-GFP fusion alleles. The transformants were grown at room temperature prior to imaging by fluorescence microscopy in mid-exponential phase. For (D) and (E), a t-test was used to determine statistical significance of differences in localization (****p<0.0001). Three replicates of at least 100 cells were counted. Scale bar: 5 μ m.

2011). We expressed Sts1-R38D, Sts1-R65D, or the double mutant Sts1-R38D, R65D (hereafter referred to as Sts1-DD) proteins from plasmid-borne alleles bearing the natural *STSI* promoter transformed into yeast that had the chromosomal *STSI* gene deleted but also carried a wild-type (WT) *STSI* cover plasmid. We streaked these yeast transformants onto minimal media containing 5'-fluororotic acid (5-FOA) to determine if these mutants could complement *sts1Δ* and restore cell viability. We observed that while neither single point mutant showed significant growth defects compared to strains expressing wild-type Sts1, *sts1-DD* was inviable, indicating that these NLS sequences are redundant (Figure 3.1C). While these growth data would be consistent with independent activity of NLS1 and NLS2, it remained possible that the single point mutations only partially inactivated the bipartite NLS.

To determine whether the Sts1 NLS sequence(s) is sufficient for nuclear import, I utilized a double GFP-GFP (2GFP) fusion reporter protein to assess nuclear transport. The 2GFP motif is sufficiently large to prevent passive diffusion of the reporter protein through the NPC and on its own concentrated in the cytoplasm by fluorescence microscopy. I appended residues 1-76 of the disordered Sts1 N-terminus to the 2GFP reporter and introduced the R38D, R65D, and DD double mutations into this Sts1 fragment. The WT NLS sequence showed significant nuclear accumulation of the reporter construct compared to a control lacking an NLS, indicating the sufficiency of this N-terminal Sts1 fragment for nuclear transport (Figure 3.1D). Additionally, I observed partial enrichment of the 2GFP reporter in the cytoplasm when either single NLS mutation was introduced, whereas the DD double mutant showed severe reduction in nuclear signal. The strong cytoplasmic localization of the 2GFP reporter only after mutating both NLS sequences agrees with

observations of the bipartite Ty1 integrase NLS (Lange et al., 2010). These results suggest that Sts1 contains a non-canonical bipartite NLS and that the lethality of *sts1-DD* in our viability assay may be the result of disrupted Sts1 nuclear import.

We next sought to determine whether the bipartite NLS contributes to full-length Sts1 subcellular localization using fluorescence microscopy. We expressed the NLS point mutants fused to the GFP gene from the yeast *GPD* (*TDH3*) promoter in a plasmid and evaluated their localization in *sts1Δ* yeast. The WT Sts1-GFP protein showed strong nuclear localization and we observed little to no decrease in the nuclear to cytoplasmic ratio (N/C) of Sts1-GFP in either of the single mutants. However, Sts1-DD-GFP showed enrichment in the cytoplasm relative to WT Sts1-GFP, suggesting that inactivating both halves of the bipartite NLS is sufficient to disrupt Sts1 nuclear import (Figure 3.1E). It is important to note that since *sts1-DD* is insufficient for cell survival as the only Sts1 allele in yeast cells, these experiments were performed in the presence of the chromosomal WT *STS1* allele. It is possible that WT Sts1 may form a heterodimer (as suggested by our structure predictions) with Sts1-DD-GFP yielding a higher fraction of Sts1-DD-GFP in the nucleus than might be expected for the double mutant. These results suggest that the Sts1 NLS is important for nuclear localization of Sts1 and may be essential for cell survival.

Since our results indicated that Sts1 has a functional bipartite NLS, we next sought to determine whether Sts1 binds to Srp1, the yeast karyopherin- α protein, which is known to bind such sequences (Radu et al., 1995). As previous coimmunoprecipitation experiments have indicated that these species bind *in vivo*, we first co-expressed recombinant fusion constructs of both proteins from *E. coli* (Tabb et al., 2000). Using Sts1-6His and GST-Srp1 fusions, we could affinity purify either species by its affinity tag and

then determine if this was sufficient to pull down the other protein expressed in the same cells. The data in Figure 3.2A indicated that Sts1 and Srp1 form a complex *in vitro*. Importantly, binding of Sts1 and Srp1 appeared to be stoichiometric, consistent with a tight NLS-mediated interaction. If Srp1 interacts with Sts1 solely through its bipartite NLS, we would expect that the Sts1 N-terminus would be sufficient to bind Srp1 in solution. We therefore created a truncation mutant of Sts1 comprising only residues 1-116, which lacked the six-helix bundle and unstructured C-terminal tail. Pulldown analysis of co-expressed recombinant Sts1(1-116)-6His and GST-Srp1 showed that this N-terminal domain was sufficient for recruitment of Srp1 and that Srp1 still bound stoichiometrically (Figure 3.2A).

We next examined whether Srp1 binding requires the Sts1 NLS sequence itself. To test for an NLS-specific interaction, we utilized the Sts1-DD double NLS mutant that was previously observed to disrupt Sts1 subcellular localization. We theorized that the reduced nuclear localization of Sts1-DD reflected a reduced interaction with Srp1 *in vivo*. Copurification analysis of Sts1-DD-6His and GST-Srp1 based on purification via the hexahistidine tag did not yield detectable levels of GST-Srp1 (Figure 3.2B). These results indicate that disruption of the Sts1 bipartite NLS abolished interaction with Srp1. This paralleled our microscopy results with the 2GFP fusions wherein introducing both R38D and R65D mutations to the Sts1 N-terminal sequence completely blocked nuclear accumulation of the 2GFP fusion. We conclude that Sts1 contains a bipartite NLS that is both necessary and sufficient for binding Srp1 and that Srp1 binding is likely required for nuclear localization of Sts1.

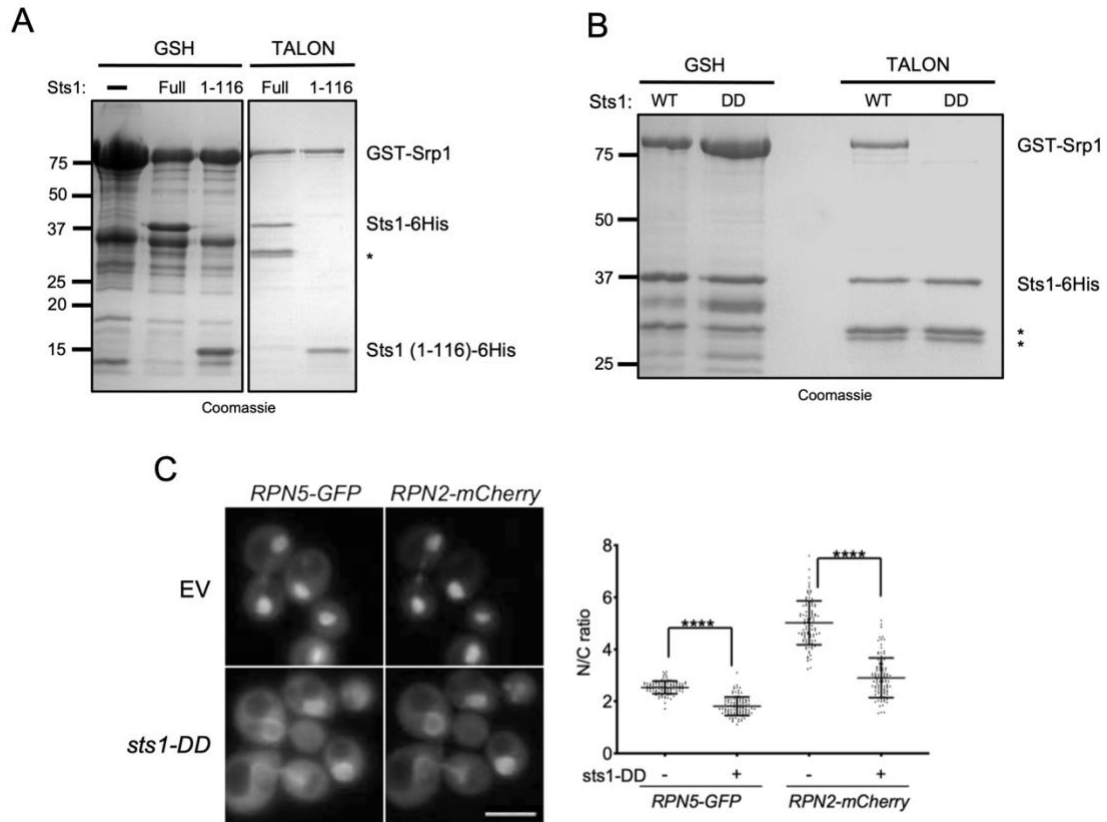


Figure 3.2: The Sts1 N-terminus is sufficient for Srp1 recruitment and nuclear localization of the proteasome.

(A) Srp1 binds to the Sts1 N-terminal domain. The indicated recombinant proteins were co-expressed in *E. coli*, and binding was determined based on co-purification from either GST-binding glutathione resin (GSH) or polyHis-binding TALON resin followed by SDS-PAGE and Coomassie staining. (B) Formation of the Sts1–Srp1 complex depends on the Sts1 bipartite NLS. The indicated recombinant proteins were co-purified as in (A). For (A) and (B), * indicates proteolytic fragments derived from Sts1–6His. (C) The Sts1-DD mutant affects proteasome localization *in vivo*. Yeast bearing chromosomal *RPN5-GFP* and *RPN2-mCherry* were transformed with an empty vector (EV) or plasmid expressing Sts1-DD-GFP (*STS1* background). Two-way ANOVA was used to determine statistical significance of differences (right panel) (****p<0.0001). Three replicates of at least 100 cells were counted. Scale bar: 5 μ m.

Previous studies of Sts1 indicated that it binds to the full 26S proteasome and might be responsible for proteasome nuclear import by virtue of its interaction with Srp1 (Ha et al., 2014; Chen et al., 2011). We therefore assessed whether the Sts1-DD NLS mutant would impact proteasome nuclear localization. We conducted fluorescence microscopy on yeast cells overproducing Sts1-DD under the control of the strong *GPD* promoter; the cells expressed the chromosomally encoded fusion proteins Rpn5-GFP (proteasome lid subunit) and Rpn2-mCherry (proteasome base subunit) for tracking proteasome localization. Expression of Sts1-DD substantially reduced relative nuclear levels of both subunits compared to WT Sts1, despite the presence of the chromosomal *STS1* allele (Figure 3.2C). These results indicate that the Sts1 NLS is integral to proper proteasome nuclear transport.

3.2.2 The Sts1 three-helix domain likely mediates homodimerization

The published crystal structure of Cut8, the Sts1 homolog in *S. pombe*, revealed a homodimer mediated by a three-helix domain downstream of its unstructured N-terminus (Takeda and Yanagida, 2005; Takeda et al., 2011). In this structure, α -helices from either Cut8 monomer form a coiled-coil interaction flanked by two oblique helical interactions, all of which are largely composed of hydrophobic interactions (Takeda et al., 2011). Importantly, Cut8 homodimerization could be disrupted by introducing mutations in residues identified in the dimer interface. Disruption of Cut8 homodimerization also greatly decreased the solubility of Cut8 in solution, indicating destabilization of the protein. Assessing the multimeric state of Cut8 dimerization mutants by size exclusion chromatography showed that the double mutant of L39E, I65E was sufficient to produce a peak shift consistent with Cut8 monomers. Additionally, expression of Cut8 dimerization

mutants could not rescue the temperature sensitive *cut8Δ* mutant, indicating that Cut8 homodimerization is important to its function (Takeda et al., 2011). Based on these data we hypothesized that Sts1 may similarly function as a homodimer and that dimerization may contribute to its function.

Our previous results indicated that Sts1 and Srp1 bind stoichiometrically, and we first examined this complex by size exclusion chromatography. We co-expressed the complex of Sts1-6His and GST-Srp1 in *E. coli* cells, first purifying the complex on a glutathione resin that binds the GST affinity tag. This complex was eluted from the resin using PreScission protease, cleaving the affinity tag from Srp1 so that the GST moieties would not homodimerize in the Sts1/Srp1 complex. The cleaved complex was subsequently purified using a 6His-binding TALON resin and fractionated by Superose-6 chromatography. In this analysis, the complex of Sts1 and Srp1 eluted at a volume suggesting a molecular weight of ~200-300 kDa (Figure 3.3A). This molecular weight range was consistent with a complex of two Sts1 monomers (combined mass of ~75 kDa) and two Srp1 monomers (combined mass of ~121 kDa). This 2:2 assembly suggested that Sts1 might form a homodimer that recruits an Srp1 monomer to each Sts1 NLS sequence.

Comparison of the Cut8 crystal structure and secondary structure predictions of Sts1 indicated that Sts1 likely contains a three-helix domain in residues 78-119 that mirrors the dimerization domain of Cut8 (Takeda et al., 2011; Jumper et al., 2021; Varadi et al., 2022). We therefore examined whether mutations in these helices would cause functional defects such as those observed in Cut8 mutants. Based on the coiled coil interactions that form the Cut8 homodimer, we identified the hydrophobic residues L80 and L95 as likely contributors to Sts1 homodimerization, though these were not exactly equivalent mutations

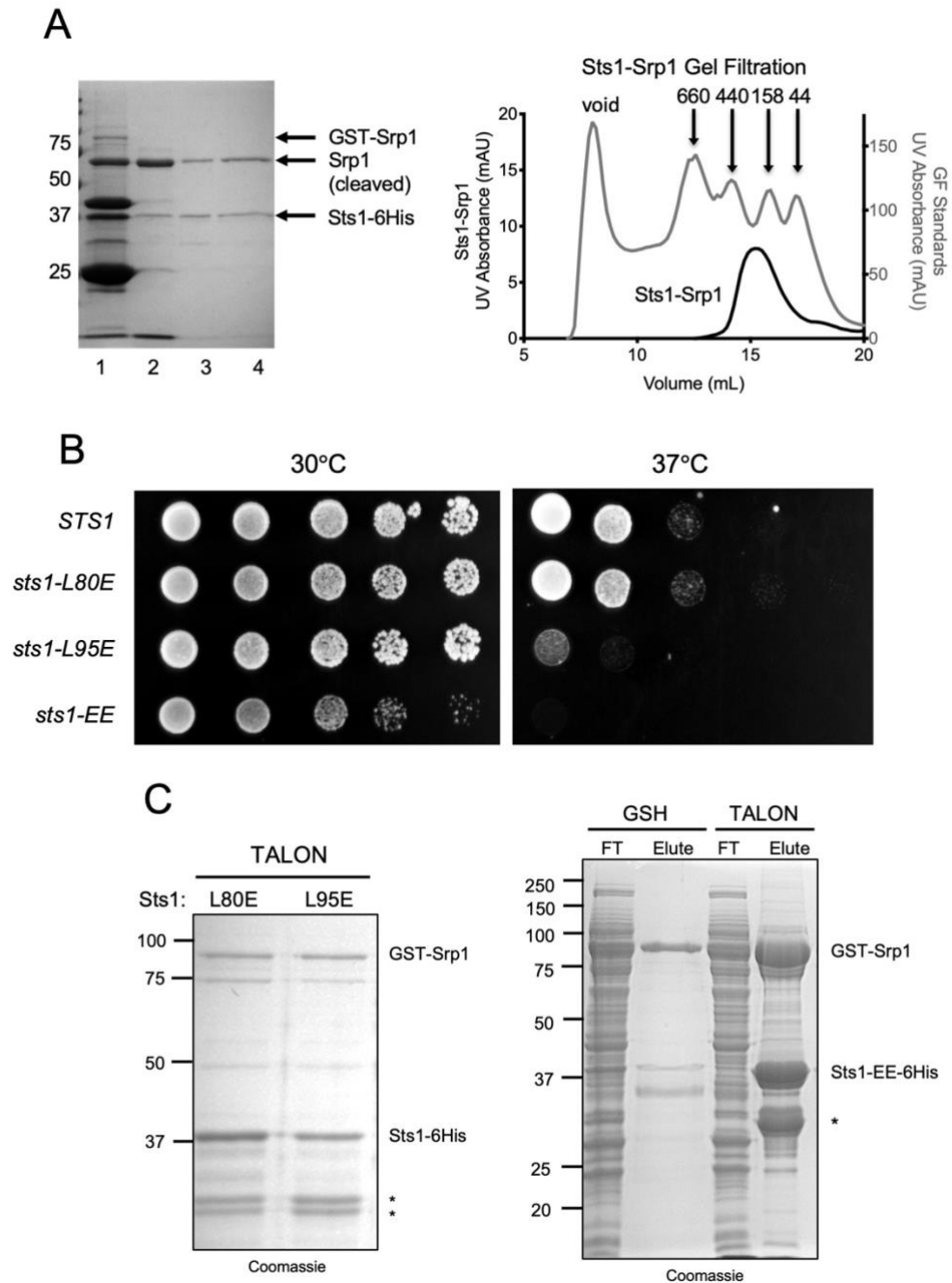


Figure 3.3: Sts1 likely forms a homodimer that is important to cell viability.

(A) The complex of Sts1/Srp1 forms a “dimer of dimers.” Recombinant GST-Srp1 and Sts1-6His were initially co-purified from *E. coli* with GSH resin (lane 1). This complex was treated with GST-PreScission Protease to elute the Srp1/Sts1-6His complex from the GSH beads by cleaving the GST tag (lane 2), and

further purified with TALON resin by the Sts1 polyhistidine tag (lane 3). The purified Sts1/Srp1 complex was analyzed by size exclusion chromatography using a Superose 6 column to determine the molecular weight and multimeric state of the complex (right panel). The gel filtration standards are shown in light grey and the Sts1/Srp1 complex is shown in black. **(B)** Dimerization mutants affect cell health. Plasmids bearing the noted *sts1* alleles were transformed into *sts1* Δ . Cells were grown for 3 days on minimal media following ejection of the WT *STS1* cover plasmid. **(C)** Sts1 dimerization mutants preserve Srp1 interaction. The indicated recombinant proteins were co-expressed in *E. coli*, and binding was determined based on co-purification from TALON resin or GSH resin followed by SDS-PAGE. * indicates proteolytic fragments derived from Sts1-6His.

to that of Cut8, and substituted them with glutamate residues either singly or together; the Sts1-L80E, L95E double mutant is referred to as Sts1-EE. We expressed each of these mutants as plasmid-encoded GFP fusion proteins in *sts1Δ* yeast and assessed viability by serial dilution growth assays at 30°C. Neither *sts1-L80E* nor *sts1-L95E* exhibited a growth defect but *sts1-EE* grew slower than WT (Figure 3.3B). At 37°C, *sts1-L95E* exhibited a considerable growth defect compared to *sts1-L80E* and WT yeast; *sts1-EE* was lethal at 37°C. These results suggested that the putative three-helix dimerization domain may be important to proper Sts1 function.

I next examined whether Sts1 dimerization mutants could retain interaction with Srp1. As noted previously, an Sts1 truncation mutant expressing residues 1-116 that includes the three-helix domain was sufficient for Srp1 binding. I introduced the L80E and L95E single point mutations as well as the double mutation into Sts1-6His and co-expressed these mutants in bacteria with GST-Srp1, as above. In co-purification experiments based on the Sts1 affinity tag, Srp1 remained bound to all three mutants and appeared to maintain a stoichiometric assembly (Figure 3.3C). These results are consistent with the Sts1 NLS sequence being sufficient for Srp1 interaction.

To examine whether the Sts1-EE double mutant resulted in disruption of Sts1 homodimerization, I co-purified the complex of recombinant Sts1-EE-6His and GST-Srp1 from *E. coli* and used Superdex S200 size exclusion chromatography to determine whether this mutant resulted in Sts1/Srp1 heterodimers. For comparison, the major peak for Sts1-6His/GST-Srp1 (verified by Coomassie staining the eluted fractions) eluted at a predicted size of ~270 kDa, consistent with a 2:2 assembly of Sts1 and Srp1 (Figure 3.4A, C). In contrast, Sts1-EE-6His/GST-Srp1 eluted as a major peak estimated at ~235 kDa, as well

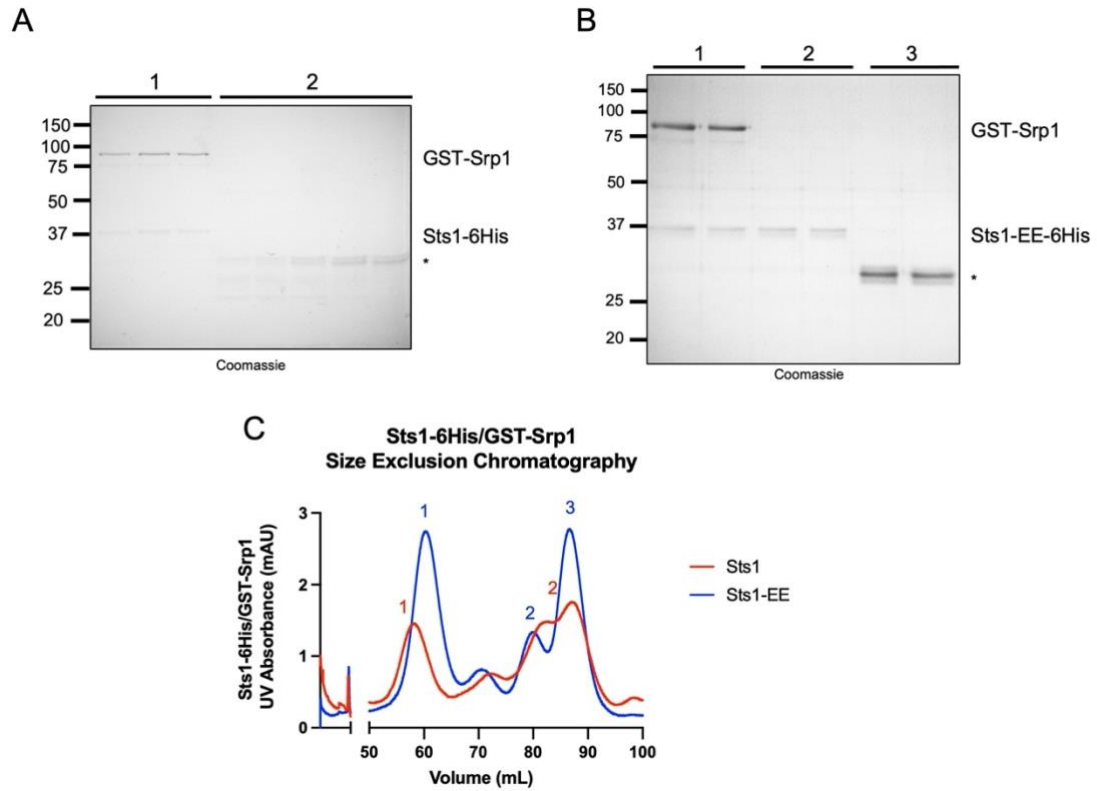


Figure 3.4: Sts1-EE is sufficient to disrupt the Sts1-Srp1 complex.

(A) Sts1 and Srp1 bind *in vitro*. Recombinant GST-Srp1 and Sts1-6His were previously co-purified from *E. coli* using TALON resin and subsequently purified by size exclusion chromatography. The eluted peaks from the chromatogram in (C) were analyzed by SDS-PAGE. (B) Sts1-EE produces Sts1 monomers. Recombinant GST-Srp1 and Sts1-EE-6His were co-purified and analyzed by size exclusion chromatography and the eluted peaks shown in (C) were analyzed by SDS-PAGE. For (A) and (B), * indicates proteolytic fragments derived from Sts1-6His. (C) Size exclusion chromatograms for the recombinant Sts1/Srp1 complexes described in (A) and (B). Size exclusion chromatography conducted using a Superdex S200 column.

as a minor peak of a ~45 kDa species. Analyzing fractions from these peaks by SDS-PAGE demonstrated that the major peak represents the Sts1-EE/Srp1 complex while the minor peak is consistent with Sts1-EE alone (Figure 3.4B, C). The approximate size of the major Sts1-EE/Srp1 peak is consistent with a 1:2 assembly of two Srp1 molecules attaching to a single Sts1 monomer. It is important to note that I was unable to cleave the GST tag from the Srp1 N-terminus in these experiments, and thus the GST moieties may be homodimerizing and artificially affecting the multimerization of the Sts1/Srp1 complex and the observed 1:2 assembly. Nonetheless, the appearance of a minor peak of free Sts1-EE indicates a change in the Sts1/Srp1 complex assembly. Overall, these data suggested that Sts1-EE retains interaction with Srp1 but yields free Sts1 monomers, possibly due to disruption of Sts1 homodimerization.

I next examined if mutations to the putative dimerization domain affected nuclear transport. I expressed Sts1-L80E, Sts1-L95E, and Sts1-EE as GFP fusion proteins under control of the *MET25* promoter as expression from this promoter approximates the levels observed for the endogenous protein. These fluorescently tagged proteins were expressed in *sts1Δ* yeast to determine the subcellular localization of Sts1 by fluorescence microscopy. At both 30°C and 37°C, Sts1-GFP appeared to be largely nuclear in each mutant (Figure 3.5). These data indicated that the putative dimerization domain mutants are still competent for nuclear transport. By contrast, the same yeast mutants expressing the chromosomal fusion protein Rpn2-mCherry showed considerable mislocalization of the proteasome to the cytoplasm. The N/C ratios of Rpn2-mCherry in *sts1-L80E* and *sts1-L95E* were slightly decreased compared to WT *STS1*, though *sts1-EE* showed a significant reduction in proteasome nuclear localization. These trends were more pronounced at 37°C wherein both

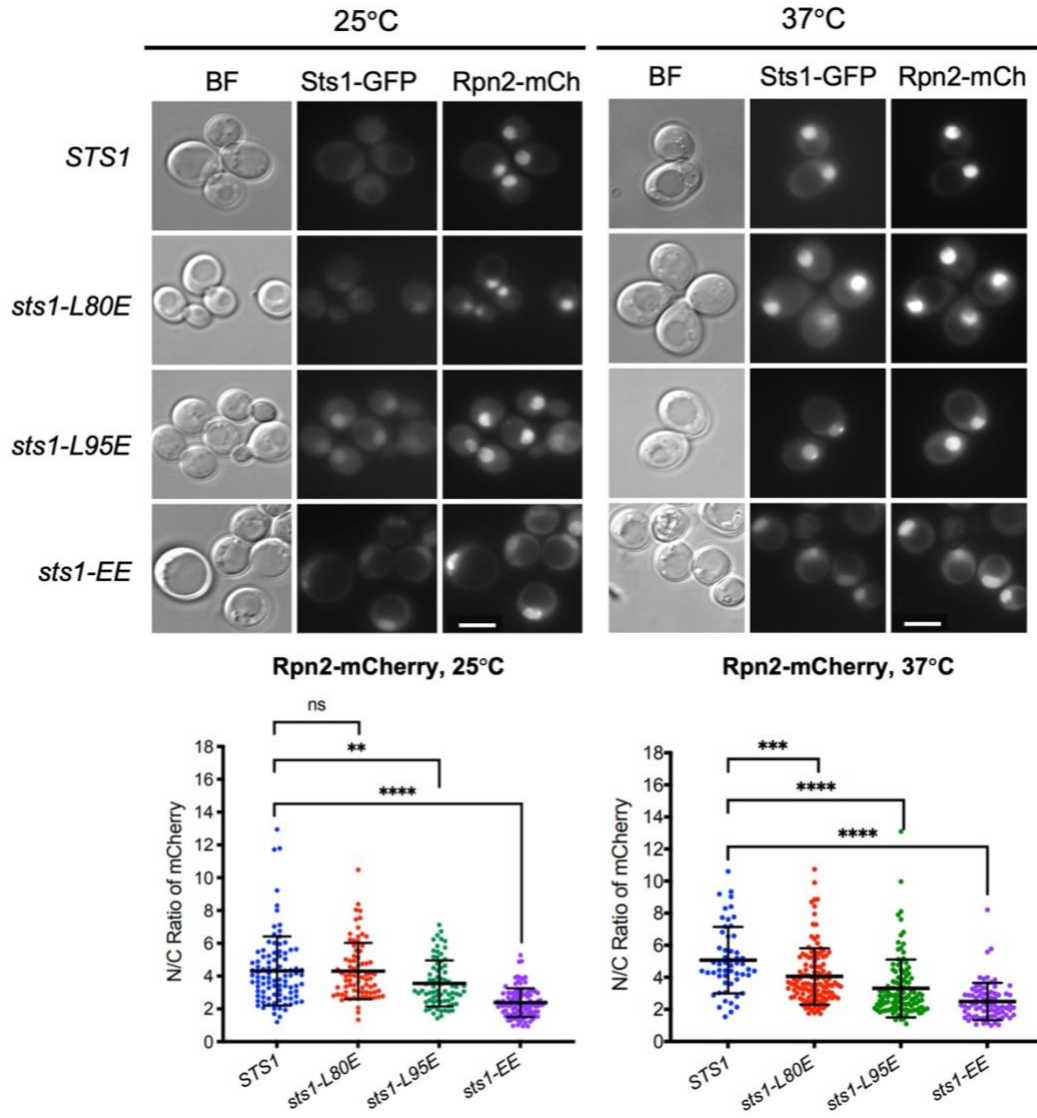


Figure 3.5: Sts1-EE affects proteasome localization *in vivo*.

Sts1 dimerization mutants disrupt proteasome nuclear localization. Yeast bearing *sts1* Δ and chromosomal *RPN2-mCherry* was transformed with the indicated *sts1* alleles. Transformants were grown to mid-exponential phase at 25°C prior to fluorescence imaging, and a population were shifted to 37°C for two hours. A t-test was used to determine statistical significance of differences in localization (**** $p < 0.0001$; *** $p < 0.001$; ** $p < 0.01$; ns indicates no significant difference). Three replicates of at least 100 cells were counted. Scale bar: 5 μ m.

the Sts1 single mutants as well as the double dimerization mutant exhibited statistically significant depletion of proteasomes in the cell nucleus (Figure 3.5). Examining the expression level of the proteasome in these mutants showed comparable levels between WT Sts1 and each dimerization mutant, indicating that reduced proteasome localization to the nucleus was not the result of differential proteasome expression (Figure 3.6). These data suggest that Sts1 likely forms a homodimer and that disruption of this assembly either affects the efficiency of proteasome nuclear import because of a failure to dimerize efficiently or because the three-helix bundle is necessary for proteasome binding.

3.2.3 The Sts1 six-helix bundle is sufficient for proteasome interaction

Sts1 has previously been noted to interact with the proteasome lid subunit Rpn11, as well as to bind to the fully assembled proteasome (Tabb et al., 2000; Chen et al., 2011; Ha et al., 2014). We therefore sought to validate this interaction with the proteasome and to identify the binding region within Sts1. To verify that Sts1 can interact with full proteasomes, I performed *in vitro* pull-down assays using 26S proteasomes affinity purified from yeast that expressed a FLAG-tagged Rpn11 subunit from the endogenous locus. Proteasomes were incubated with the bacterially purified recombinant GST-Sts1/Srp1-6His complex immobilized on glutathione beads. I analyzed proteasome recruitment by immunoblot and observed significant association of 26S proteasomes with this complex (Figure 3.7A). I next examined whether Sts1 interaction with the proteasome depends upon interaction with Srp1. To test this, I performed *in vitro* pull-downs of proteasomes with MBP-Sts1 or the double NLS mutant MBP-Sts1-DD immobilized onto amylose beads. Sts1 is often unstable in solution in the absence of Srp1 though the large MBP tag is sufficient to maintain Sts1 solubility. In this experiment, 26S proteasomes did not

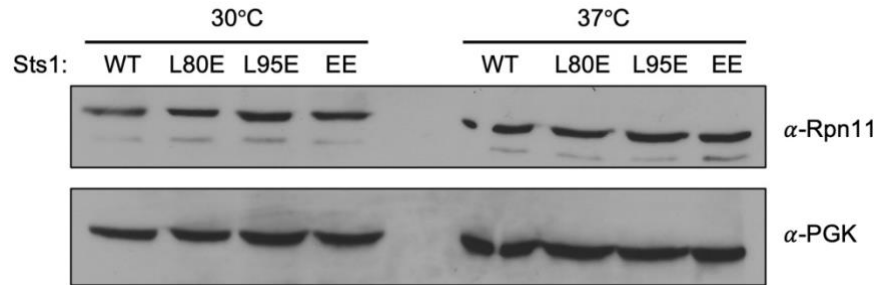


Figure 3.6: Sts1 dimerization mutants do not impact proteasome expression.

Sts1 dimerization mutants do not affect proteasome expression. Cell extracts from yeast transformed with the pRS415MET25-based plasmids bearing the indicated *sts1* alleles were separated by SDS-PAGE and immunoblotted with anti-Rpn11 and anti-PGK antibodies.

detectably bind to either MBP-Sts1 or MBP-Sts1-DD (Figure 3.7A). These results suggest that Srp1 is required for proteasome recruitment although it is possible that the MBP fusion blocked Sts1 binding. Srp1 by itself was also not tested for proteasome binding here.

Since Srp1 may be required for the proteasome to bind Sts1, we next examined whether the Srp1-binding Sts1 N-terminus is also sufficient for proteasome interaction. To test this, we utilized the Sts1 truncation mutant bearing only the N-terminus and dimerization domain, Sts1(1-116). As shown above, this segment was sufficient for Srp1 binding *in vitro*. We co-purified recombinant complexes of Sts1(1-116)-6His/GST-Srp1 and Sts1-6His/GST-Srp1 from bacterial extracts, bound them to glutathione beads, and then performed *in vitro* pull-down analysis of purified yeast 26S proteasomes. We could not detect any proteasome signal by immunoblotting with the complex of Sts1(1-116)/Srp1, whereas the full-length Sts1/Srp1 complex was still able to recruit 26S proteasomes (Figure 3.7B). These results suggest that, while Srp1 may be required for proteasome recruitment, Sts1 residues 1-116 are not sufficient for proteasome interaction and likely do not represent the proteasome binding site within Sts1.

The insufficiency of residues 1-116 for proteasome binding suggested that the proteasome interaction site(s) within Sts1 likely requires sequences downstream of the putative dimerization domain, in particular, the six-helix bundle and/or the unstructured C-terminal tail. To investigate this, I conducted *in vitro* pull-down assays of 26S proteasomes with immobilized recombinant GST-tagged Sts1 truncation mutants bearing only the six-helix bundle (residues 116-276) or the six-helix bundle together with the C-terminus (residues 116-319). Full-length GST-Sts1 and the complex of GST-Sts1/Srp1-6His were evaluated as well. The 26S proteasomes bound to both Sts1 truncation mutants *in vitro* at

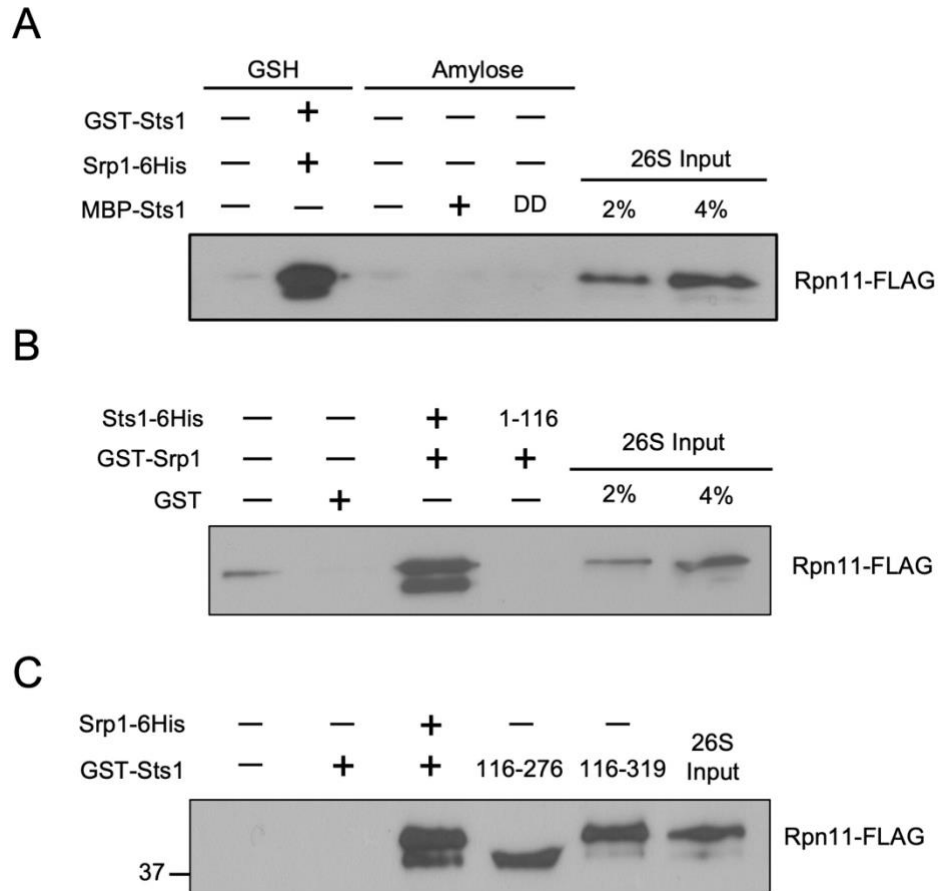


Figure 3.7: Srp1 is required for Sts1 to bind to the 26S proteasome within its six-helix bundle domain.

(A) Srp1 is required for Sts1 to bind to the 26S proteasome. Recombinant protein species as indicated were immobilized on either GST-binding glutathione resin (GSH) or maltose-binding amylose resin and incubated with 26S proteasomes purified from yeast to detect interactions. Negative controls were conducted with immobilized GST or maltose (lanes 1 and 3, respectively). (B) The N-terminal Sts1 domain is insufficient for proteasome interaction. The indicated recombinant species were immobilized on GSH resin and assessed for proteasome interaction, as in (A). (C) The Sts1 six-helix bundle is sufficient for 26S proteasome interaction. The indicated recombinant species were immobilized on GSH resin for proteasome interaction, as in (A). Note: the predicted molecular weight for GST-Sts1(116-276) is ~46 kDa and is likely to be overlapping with the upper band of the Rpn11-FLAG doublet. For (A-C), proteins from pull-downs were separated by SDS-PAGE and analyzed by anti-FLAG immunoblotting.

levels close to those seen with the full-length Sts1/Srp1 complex (Figure 3.7C). These data demonstrate that the Sts1 six-helix bundle is sufficient for binding proteasomes. Notably, full-length GST-Sts1 by itself was unable to bind to proteasomes *in vitro*, suggesting that the presence of Srp1 is not required for proteasome recruitment unless the N-terminal domains of Sts1 are present. Potentially, Srp1 binding to the N-terminal region of Sts1 reverses an autoinhibitory or unfolded Sts1 conformation that would otherwise block access of the six-helix bundle to its proteasome-binding site. Taken together, our results indicate that the Sts1 six-helix bundle domain is sufficient for proteasome recruitment but that bound Srp1 may be required for proteasome interaction to occur with full-length Sts1.

To test the potential impact of the Sts1 six-helix bundle on proteasome nuclear import *in vivo*, we introduced a single point mutation, C194Y, into the Sts1 six-helix bundle (also referred to as Sts1-2), which had been previously identified as a temperature-sensitive mutant that inhibits degradation of ubiquitylated proteins in yeast (Romero-Perez et al., 2007). We hypothesized that defects in this mutant might result from impaired proteasome interaction. We first purified a complex of recombinantly co-expressed Sts1-2-6His/GST-Srp1 from bacterial extracts using the hexahistidine tag on Sts1-2. The complex with Srp1 still forms in the Sts1-2 mutant (Figure 3.8A). This is consistent with our previous results suggesting that the Srp1 interaction is specific to the N-terminal NLS sequence.

I immobilized the purified Sts1-2-6His/GST-Srp1 and WT Sts1-6His/GST-Srp1 complexes on glutathione beads for *in vitro* pull-down analysis of 26S proteasomes purified from yeast. When these pull-downs were conducted at either 4°C or 25°C, no detectable difference in 26S proteasomes binding was seen between the mutant and WT Sts1/Srp1 complexes (Figure 3.8B). However, at 30°C the mutant Sts1-2/Srp1 complex

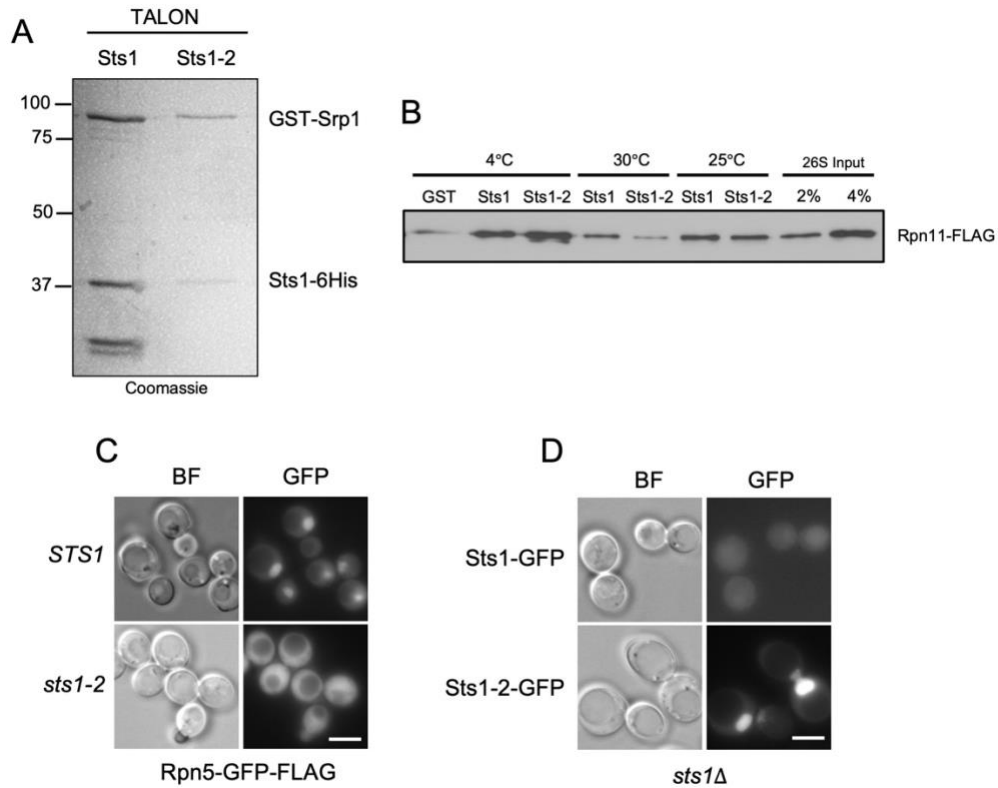


Figure 3.8: The six-helix bundle mutant *sts1-2* results in a proteasome interaction and localization defect.

(A) *Sts1-2* is able to recruit *Srp1*. Recombinant GST-*Srp1* was co-expressed in *E. coli* with either *Sts1-6His* or *Sts1-2-6His*, and binding was determined based on co-purification from TALON resin followed by SDS-PAGE and Coomassie staining. (B) *Sts1-2* results in a proteasome interaction defect. GST-*Srp1*/*Sts1-6His* (“*Sts1*”) or GST-*Srp1*/*Sts1-2-6His* (“*Sts1-2*”) were immobilized onto GSH beads. These complexes were incubated at the indicated temperatures with 26S proteasomes purified from yeast. Bound proteins were separated by SDS-PAGE and analyzed by anti-FLAG immunoblotting. (C) *sts1-2* results in proteasome cytoplasmic localization. *STS1* and *sts1-2* yeast were transformed with pRS316-*Rpn5*-GFP-FLAG (native promoter) and visualized by fluorescence microscopy. (D) *Sts1-2* is imported into the nucleus. *sts1Δ* yeast were transformed with pRS145MET25-based plasmids bearing GFP fusion proteins of either WT *Sts1* or *Sts1-2*. The WT *STS1* cover plasmid was evicted on 5-FOA media prior to analysis by fluorescence microscopy. WT *Sts1* accumulates *in vivo* at very low levels under the control of the *MET25* promoter. For (C) and (D), cells were grown to mid-exponential phase at 30°C. Scale bar: 5 μm.

exhibited a considerable reduction in proteasome interaction; this is consistent with the temperature-sensitivity of this mutant. This defect supports the hypothesis that Sts1 binds to the proteasome through its six-helix bundle region.

If Sts1-2 experiences reduced interaction with the proteasome and Sts1 is responsible for proteasome nuclear import, this binding defect should reduce proteasome accumulation in the nucleus *in vivo*. To test this hypothesis, I expressed the proteasome lid subunit Rpn5 as a GFP fusion protein on a low-copy plasmid under control of its native promoter and observed proteasome localization by fluorescence microscopy in WT *STSI* yeast or yeast bearing the chromosomal mutation *sts1-2*. At 30°C, the proteasome is strongly mislocalized to the cytoplasm in *sts1-2* cells, compared to nearly complete nuclear accumulation in WT cells (Figure 3.8C). This is consistent with our *in vitro* binding assays which indicated a reduced interaction between Sts1-2 and the proteasome at this temperature.

I similarly analyzed WT and mutant Sts1-2 localization by fluorescence microscopy. The proteins were expressed as GFP fusions from a plasmid where the genes were under the control of the *MET25* promoter in *sts1Δ* yeast. WT Sts1-GFP was difficult to visualize as it is very rapidly turned over (as will be discussed in Chapter 5), but the much more abundant Sts1-2-GFP fusion protein accumulated in the cell nucleus at 30°C, consistent with the intact NLS-Srp1 interaction (Figure 3.8D). Together, these data suggest that the effects on the ubiquitin-proteasome system observed in *sts1-2* yeast result from decreased proteasome recruitment and nuclear import.

It is important to note that these findings represent a clear divergence from reports about the proteasome-associated function of the Sts1 homolog Cut8. In *S. pombe*, Cut8 was

reported to act as an anchor protein, tethering the proteasome to the inner nuclear membrane, and it has not been reported to participate in nuclear import (Takeda and Yanagida, 2005; Takeda et al., 2011). Cut8 reportedly achieves this nuclear tethering through poly-ubiquitylation of its N-terminus by the E3 ligase Ubr1, facilitating Cut8-proteasome interaction in a ubiquitin-dependent manner. Importantly, the poly-ubiquitylated lysine residues of the Cut8 N-terminus are in a sequence that could be an NLS (KKRK), although Cut8 has not been shown to interact with karyopherin- α (Takeda and Yanagida, 2005). Additionally, while Cut8 contains a six-helix bundle domain, this domain was identified as being responsible for cholesterol-mediated binding of Cut8 to the inner nuclear membrane (Takeda et al., 2011). Our results suggest that Sts1 binds to the proteasome and mediates its nuclear enrichment by a substantially different mechanism compared to the mechanism proposed for Cut8, as will be discussed in Chapter 6.

3.2.4 The Sts1 C-terminus may regulate proteasome interaction

Having assigned distinct functions to all of the predicted Sts1 domains except the disordered C-terminal region, we next examined the Sts1 C-terminal tail. In secondary and tertiary structure predictions this domain is noted to be disordered and does not possess consensus motifs (Jumper et al., 2021; Varadi et al., 2022). To assess the contribution of the C-terminal tail, we first expressed an Sts1 truncation mutant (leaving residues 1-276) lacking the C-terminal tail as a GFP-fusion; the fusion gene was expressed from the *MET25* promoter on a plasmid in *sts1* Δ yeast, and the ability of this mutant to rescue yeast growth was assessed. Sts1(1-276)-GFP showed no growth defect compared to WT Sts1-GFP, even at higher temperature (Figure 3.9A). Additionally, determining the relative levels of this mutant *in vivo*, we observed that Sts1(1-276)-GFP was expressed at comparable levels to

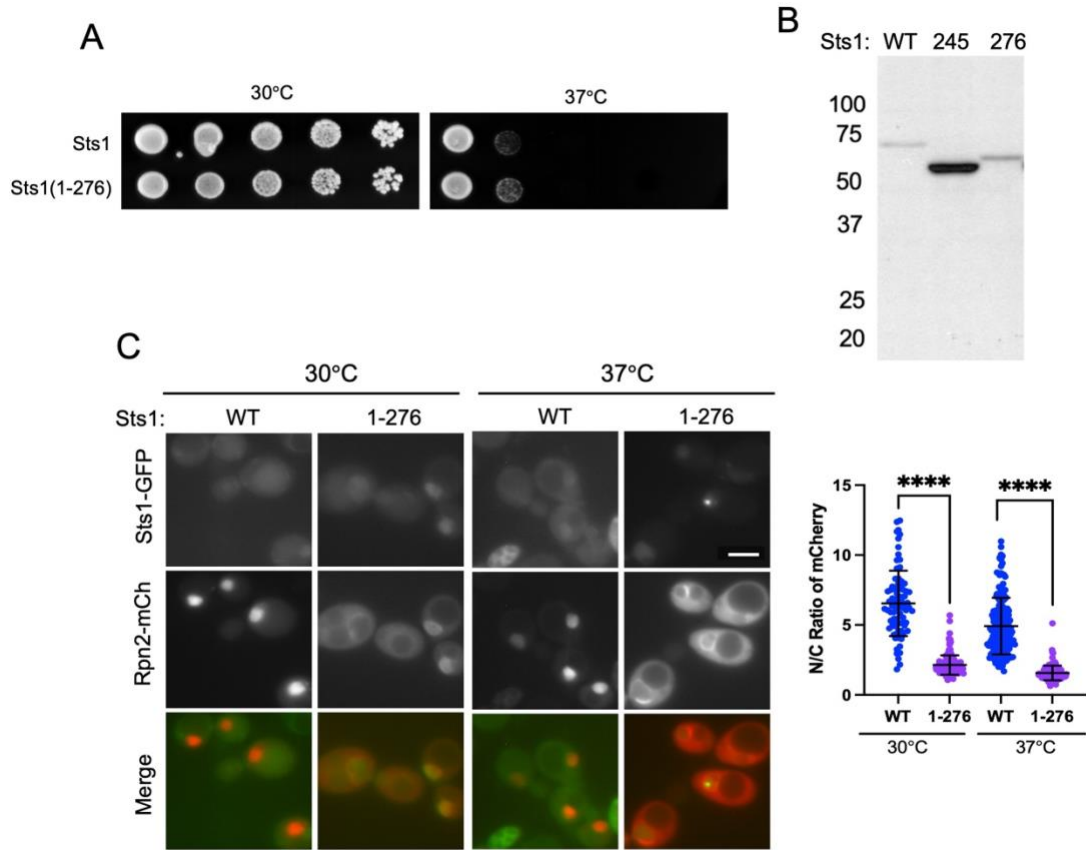


Figure 3.9: Sts1(1-276) rescues *sts1Δ* but results in cytoplasmic proteasome localization.

(A) Sts1(1-276) is sufficient to rescue *sts1Δ*. Yeast bearing *sts1Δ* were transformed with plasmids bearing GFP fusion proteins of either WT Sts1 or Sts1(1-276). The WT *STS1* cover plasmid was evicted on 5-FOA media prior to analysis. Cells were grown on minimal media for three days. (B) Sts1(1-276) is expressed at levels comparable to WT Sts1. *sts1Δ* yeast was transformed with plasmids bearing GFP fusion proteins of WT Sts1, Sts1(1-245) (“245”), or Sts1(1-276) (“276”). Cell extracts from these transformants were separated by SDS-PAGE and immunoblotted with anti-GFP to assess Sts1 levels. (C) Sts1(1-276) results in cytoplasmic localization of the proteasome. Yeast bearing *sts1Δ* and chromosomal *RPN2-mCherry* was transformed with the indicated *sts1* alleles as GFP fusion proteins. Transformants were grown to mid-exponential phase at 30°C prior to fluorescence imaging, and a population were shifted to 37°C for two hours. A t-test was used to determine statistical significance of differences in localization (**** $p < 0.0001$). Three replicates of at least 100 cells were counted. Scale bar: 5 μ m.

that of WT Sts1-GFP. In contrast, a more severe truncation mutant that lacks the C-terminal tail as well as the final two helices in the Sts1 six-helix bundle (leaving residues 1-245) was non-functional at 37°C and strongly stabilized *in vivo* compared to WT Sts1 (Figure 3.9B) (Budenholzer et al., 2020). These results indicated that the deletion of the disordered C-terminal tail is not detrimental to cell health.

If the C-terminal tail is not functionally relevant to Sts1-mediated nuclear import, we hypothesized that we would not observe a defect in proteasome nuclear transport *in vivo*. Therefore, I expressed Sts1-GFP and Sts1(1-276)-GFP on plasmids under the control of the *MET25* promoter in yeast that were chromosomally deleted for *STSI* and also expressed Rpn2-mCherry from the native locus. Imaging these cells by fluorescence microscopy, I observed that at both 30°C and 37°C, the accumulation of Rpn2-mCherry in the nucleus appeared to be severely reduced in many cells (Figure 3.9C). This was surprising as our previous assays did not suggest any functional difference between Sts1 and Sts1(1-276). However, Sts1(1-276)-GFP still appeared enriched in the nucleus, though the signal was quite weak. At high temperature, Sts1(1-276)-GFP often formed what appeared to be nuclear foci, possibly suggesting that Sts1(1-276) aggregates in the cell nucleus. This further suggested that Sts1 undergoes nuclear import in spite of defects associated with proteasome binding or nuclear transport.

In previous *in vitro* pull-down assays, I showed that the Sts1 six-helix bundle by itself was able to recruit the 26S proteasome (Figure 3.7C). This suggests that the apparent proteasome import defect is not due to its failure to bind Sts1(1-276). These data, while preliminary, suggest that this domain is not dispensable and may contribute to proteasome import, perhaps as a regulator of proteasome interaction.

3.3 Discussion

The structure of Sts1 has not yet been solved experimentally and much remains to be determined about how it functions in yeast. However, the results presented here contribute to a deeper understanding of the possible structural domains in Sts1 and the role that each domain plays in Sts1 function. We have assigned preliminary structural features to Sts1 based on homology to the *S. pombe* protein Cut8 as well as robust 3D structure predictions (Takeda et al., 2011; Jumper et al., 2021; Varadi et al., 2022). From my analyses, Sts1 contains an unstructured N-terminus bearing a bipartite NLS sequence, likely forms a homodimer through interactions within a central three-helix domain, directly binds to fully assembled 26S proteasomes via its six-helix bundle domain, and possesses an unstructured C-terminal tail that is not essential but may contribute to regulation of the interaction with the proteasome.

We have corroborated the existing characterization of Sts1 as an NLS-containing protein and have further shown that this is a bipartite sequence by analyzing the contribution of each basic amino acid patch *in vivo*. Mutating a single arginine residue in each basic patch of the bipartite NLS (Sts1-DD) is sufficient to severely impact proteasome nuclear accumulation *in vivo*, suggesting that Sts1 contributes to proteasome nuclear import (Figure 3.2C). We have also shown that Sts1 interacts with Srp1 *in vitro* in an NLS-dependent manner as Sts1-DD is insufficient for Srp1 binding (Figure 3.2B). Disrupting the NLS-based interaction between Sts1 and Srp1 is deleterious, as the yeast expressing only Sts1-DD are inviable (Figure 3.1C). This suggests that successful Sts1 nuclear import by Srp1, and possibly also successful proteasome nuclear import, is essential for viability.

Our experiments have also shown that Sts1 probably binds to Srp1 in a “dimer-of-dimers” configuration as a result of Sts1 homodimerization. Much like its *S. pombe* counterpart Cut8, Sts1 possesses a helical domain that appears to have a coiled-coil interaction with the same domain of another monomer. This Sts1 homodimer may allow for separate Srp1 subunits to be recruited to each Sts1 bipartite NLS sequence, assembling in a 2:2 complex. We examined Sts1 homodimerization by making two point mutations in the predicted hydrophobic binding interfaces, Sts1-EE. Sts1 dimerization mutants, including Sts1-EE, were still sufficient for Srp1 binding *in vitro*, supporting our hypothesis that Srp1 interaction is confined to the NLS sequence (Figure 3.3C). Analyzing the complex of Sts1-EE/Srp1 by size exclusion chromatography suggested that Sts1-EE may disrupt Sts1 homodimerization (Figure 3.4B, C). The Sts1-EE mutant was also non-functional at high temperature and produced a significant reduction in proteasome nuclear localization, though Sts1 itself remained nuclear by fluorescence microscopy (Figure 3.5). These results suggest that Sts1 homodimerization likely impacts proteasome nuclear transport. A possible explanation for the importance of Sts1 homodimerization is the significant size of the proteasome as a nuclear import cargo. Recent studies have indicated that larger cargo proteins likely require increasing numbers of NLS sequences for effective nuclear import (Paci et al., 2020); it is thus possible that Sts1 homodimerization contributes a second NLS sequence for additional karyopherin recruitment to a single proteasome and increases 26S proteasome import efficiency.

We have also shown that the Sts1 six-helix bundle domain is sufficient for binding to the 26S proteasome. We conducted *in vitro* pull-down assays using different mutants of Sts1 in the presence of purified yeast 26S proteasomes to identify a minimal proteasome

binding domain. In these experiments we observed that Sts1 residues 116-276 were sufficient to bind 26S proteasomes in solution; however, association of full-length Sts1 with the proteasome required Srp1 (Figure 3.7). Introduction of a single point mutation into the six-helix bundle (Sts1-2) reduced proteasome binding, and proteasomes were strongly enriched in the cytoplasm compared to their nuclear accumulation in WT cells (Figure 3.8B, C). These results suggested that while the Sts1 six-helix bundle domain is sufficient for proteasome interaction, Srp1 may be required to interact with Sts1 prior to proteasome recruitment.

Together, these results suggest that the distinct Sts1 structural domains might each contribute unique functions to facilitate proteasome nuclear import. One possible explanation of these connected functions is that full-length Sts1 in the cytoplasm may exist in a homodimeric state that is unable to bind to the proteasome, possibly due to auto-inhibition by the N- or C-termini. Upon Srp1 binding to the N-terminal NLS sequence, the Sts1 six-helix bundle domain may be accessed by the proteasome, forming a transport complex where the Sts1 homodimer serves as an adaptor between the proteasome and Srp1 for classical nuclear import. The C-terminal tail may modulate proteasome binding; thus, its deletion leads to a proteasome localization defect, but the intact NLS and six-helix bundle permit nuclear import to wild-type levels. Our analysis supports models in which Sts1 has a central role in proteasome nuclear import in yeast, and we therefore next endeavored to probe the contribution of the karyopherin proteins and RanGTPase cycle in Sts1-mediated proteasome nuclear import (Ha et al., 2014; Chen et al., 2011).

Chapter 4: Sts1 mediates proteasome nuclear transport

Portions of this chapter were previously published in Budenholzer L, Breckel C, Hickey M, Hochstrasser M. (2020). The Sts1 nuclear import adaptor uses a non-canonical bipartite nuclear localization signal and is directly degraded by the proteasome. *Journal of Cell Science* **133**, jcs236158. Portions of this chapter are included in a manuscript currently in preparation: Breckel CA, Johnson Z, Hochstrasser M. (2023). 26S proteasomes are transported into the nucleus by karyopherins and the adaptor protein Sts1 in a single turnover mechanism.

4.1 Introduction

The nucleus is responsible for housing the genetic material; a membrane-enclosed organelle, the nuclear envelope is arrayed with pores that permit the movement of various factors between the nucleus and cytoplasm (Gall 1964). The complex NPC architecture ensures that larger species moving between the nuclear and cytoplasmic compartments must be selectively carried via an active transport pathway. Active transport through the NPC primarily occurs via dedicated nuclear transport receptors.

Nuclear transport receptors (NTRs) generally refer to two distinct families of proteins known as the karyopherin- α and karyopherin- β proteins. Karyopherin- α proteins are a class of import receptors composed of multiple HEAT repeat domains and an importin- β binding domain (IBB). Known in budding yeast as Srp1 or Kap60, karyopherin- α recognizes nuclear localization signals in cargo proteins in the cytoplasm to initiate their entry into the cell nucleus (Enenkel et al., 1995; Conti et al., 1998; Conti and Kuriyan, 2000). Importantly, karyopherin- α proteins form a heterodimer with karyopherin- β proteins (yeast Kap95) through their IBB domain. Karyopherin- β receptors form transient

interactions with the hydrophobic nucleoporin channel, guiding the cargo-containing complex through the NPC (Enenkel et al., 1995). Directional movement across the nuclear membrane is regulated by a gradient of the small GTPase Ran (yeast Gsp1) (Moore et al., 1998; Chook et al., 2011). In the cytoplasm, Ran is bound mostly to GDP as a result of GTP hydrolysis by Ran that is stimulated by the cytoplasmic RanGTPase activating protein (GAP, called Rna1 in yeast) (Hopper et al., 1990). In the cell nucleus, Ran is primarily bound to the nucleotide GTP through the action of the guanine nucleotide exchange factor (GEF, known in yeast as Prp20) (Kunzler et al., 2000). RanGTP in the nucleus interacts with the cargo-bound karyopherin- α/β heterodimer and initiates the release of cargo proteins inside the nucleus and export of the RanGTP-bound karyopherin proteins to the cytoplasm (Lee et al., 2005; Kobe 1999; Matsuura and Stewart, 2004; Nachury and Weis 1999; Stewart 2007; Gorlich et al., 1996).

In yeast as well as in many mammalian cells, proteasomes concentrate in the nucleus, though the mechanism of nuclear accumulation remains poorly understood. Subunits of the proteasome base and core particle contain nuclear localization signals, indicating that they may be imported separately from the proteasome holoenzyme (Lehmann et al., 2002; Tanaka et al., 1990); however, the proteasome lid does not contain any known NLS sequences (Isono et al., 2007). If proteasomes are imported as subcomplexes and assembled in the nucleus following import, the lid nuclear localization *in vivo* likely results from interaction with an NLS adaptor protein or through piggybacking on other proteasome subcomplexes. Whether proteasomes are imported as the fully assembled holoenzyme or separately as individual subcomplexes, these proteasome units are too large to pass through the NPC unassisted. The yeast proteasome holoenzyme

measures approximately 15 nm in diameter and 45 nm in length, compared to the 26 nm diameter of the NPC interior, though NPC dilation leads to variable pore size (Forster et al., 2013; Wendler and Enenkel, 2019; Dworetzky and Feldherr, 1988; Felderr et al., 1998; Strambio-de-Castillia and Rout, 2002). These observations imply the involvement of the karyopherin import pathway and an NLS-dependent active transport mechanism.

As discussed in Chapter 3, the yeast protein Sts1 has previously been identified as a candidate for mediating nuclear import of proteasomes. Early studies suggested that Sts1 possibly binds to the proteasome lid subunit Rpn11 and thus may serve specifically as an import adaptor for the lid subcomplex that lacks an NLS sequence (Tabb et al., 2000). In our earlier study, we confirmed that Sts1 undergoes nuclear transport in a karyopherin-dependent pathway by virtue of its bipartite NLS (Budenholzer et al., 2020). Additionally, we demonstrated that a complex of Sts1 and Srp1 is sufficient to interact with the 26S proteasome holoenzyme, supporting this theory of Sts1-mediated proteasome transport. Here we show that Sts1 and Srp1 form a ternary complex with the yeast karyopherin- β protein that is selectively disrupted by the nuclear protein RanGTP. Sts1 preferentially binds to the 26S proteasome over its subcomplexes, and proper proteasome nuclear entry relies upon karyopherin-mediated transport and the Ran cycle. Finally, we demonstrate that Sts1 does not contribute to reimport of proteasomes from cytoplasmic granules formed during quiescence, suggesting that the Sts1-based import mechanism is specific to exponentially growing yeast. These data together indicate that Sts1 facilitates 26S proteasome nuclear import in a karyopherin-dependent manner.

4.2 Results

4.2.1 Sts1 preferentially binds to 26S proteasomes

Previous studies have indicated that Sts1 can bind fully assembled proteasomes and may specifically interact with the proteasome lid subunit Rpn11 (Tabb et al., 2000; Chen et al., 2011; Ha et al., 2014). In agreement with this, our early results indicated that a complex of Sts1 and Srp1 is sufficient to bind to the fully assembled 26S proteasome *in vitro* (Figure 3.6). However, since the lid is the only proteasome subcomplex that lacks a nuclear localization signal, it was possible that Sts1 is responsible for lid import only, and our *in vitro* binding assays were simply demonstrating a lid-specific interaction in the context of the available 26S proteasome. We therefore investigated if Sts1 is responsible for nuclear transport of specific proteasome subcomplexes.

To examine the specificity of Sts1, we performed *in vitro* pull-down assays using the Sts1-6His/GST-Srp1 co-purified from *E. coli* extracts. This complex was immobilized on glutathione beads and incubated with different proteasome complexes purified from yeast: the 20S core particle, 19S regulatory particle, and 26S proteasome. To ensure that Sts1 does not bind to an unknown proteasome-associated factor that may co-purify from yeast with 26S proteasomes, we also tested a species of 26S proteasome that was reconstituted from purified CP and RP species incubated in the presence of ATP to reassociate the subcomplexes. In our experiments, the individual RP and CP subcomplexes did not detectably bind to the Sts1/Srp1 complex; however, both purified 26S proteasomes and reconstituted RP-CP bound to the complex (Figure 4.1A). In contrast, performing the same binding assay using only GST-Srp1 showed very weak association with RP, CP, and reconstituted RP-CP, though we did not observe association with purified 26S proteasomes

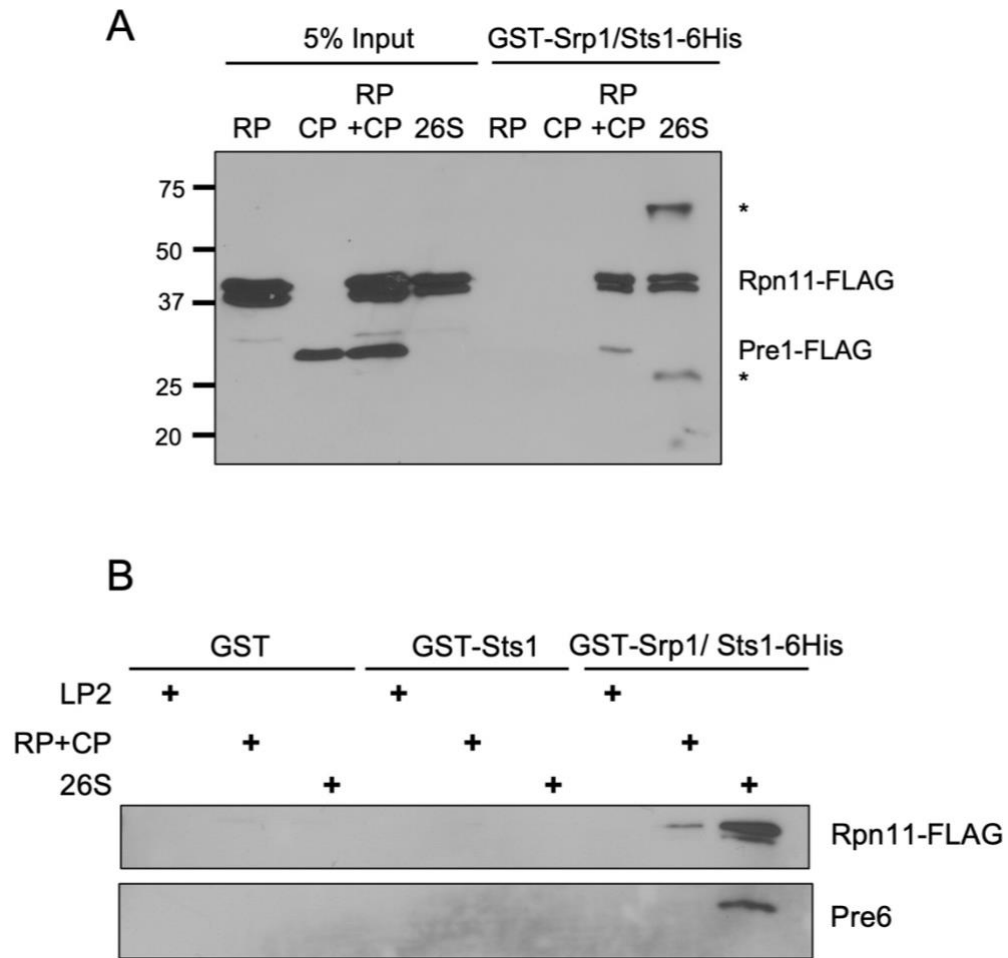


Figure 4.1: Sts1 preferentially binds to 26S proteasomes.

(A) Sts1 preferentially binds to the 26S proteasome. Recombinant Sts1-6His/GST-Srp1 was immobilized on GSH resin and incubated with purified CP, RP, 26S proteasome, or 26S proteasomes reconstituted from RP and CP ('RP+CP') to detect interactions. All input complexes were isolated from yeast using anti-FLAG affinity purifications. Proteins from the GSH pull-downs were examined by anti-FLAG immunoblotting. * indicates non-specific cross-reactive species. (B) Sts1 does not bind to the lid assembly intermediate LP2. The indicated recombinant species were immobilized and incubated with purified LP2, RP+CP, or 26S proteasome as in (A). Proteins from the pull-downs were analyzed by anti-FLAG and anti-Pre6 immunoblotting.

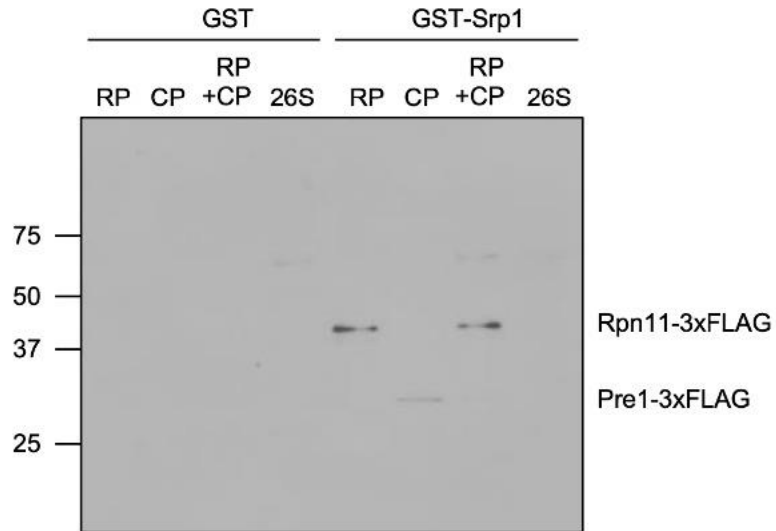


Figure 4.2: Srp1 can weakly bind purified RP and CP *in vitro*.

Recombinant GST-Srp1 was immobilized on glutathione (GSH) resin and incubated with purified CP, RP, 26S proteasomes, or 26S proteasomes reconstituted from RP and CP ('RP+CP') to detect interactions. All input complexes were isolated from yeast using anti-FLAG affinity purifications. Proteins from the GSH pull-downs were examined by anti-FLAG immunoblotting.

(Figure 4.2). These interactions were significantly weaker than those observed for the Sts1/Srp1 complex and could possibly be the result of association of Srp1 with exposed NLS sequences in the CP and RP base. To determine if Sts1 binds to the lid outside of the 26S proteasome, we similarly assayed interaction with the lid assembly intermediate LP2, consisting of Rpn3, Rpn5-9, and Rpn11 (Tomko and Hochstrasser, 2011; Budenholzer et al., 2017). In these experiments, we did not observe any detectable interaction with either the Sts1/Srp1 complex or Sts1 alone (Figure 4.1B). Though previous studies implied an association between Sts1 and Rpn11, possible Sts1 interaction with the proteasome lid appears specific to the fully assembled 26S proteasome. However, the specific proteasome subunit or site for Sts1 interaction is not yet clear. We conclude that the Sts1/Srp1 transport complex exhibits a strong preference for 26S proteasomes and likely facilitates transport of the fully assembled complex.

4.2.2 Sts1 binds the karyopherin- α/β heterodimer and is disrupted by RanGTP

In classical cNLS-containing cargo, karyopherin- α and karyopherin- β form a heterodimer that is responsible for ferrying nuclear-targeted proteins through the nuclear pore complex. The concave binding pocket of karyopherin- α binds to the basic amino acids of NLS sequences, and recruits karyopherin- β to facilitate movement across the nuclear envelope (Kalderon et al., 1984; Leung et al., 2003; Conti et al., 1998; Cingolani et al., 1999). Karyopherin- β transiently interacts with the Phe-Gly repeats of the nucleoporin proteins that span the NPC interior, allowing it to move through the NPC with karyopherin- α and the NLS cargo in tow (Bayliss et al., 2000; Enenkel et al., 1995; Lott et al., 2010; Ribbeck and Gorlich, 2002). Though association between Sts1 and the karyopherin- α

protein Srp1 has been observed for many years, I next wanted to confirm the likely participation of karyopherin- β in yeast proteasome nuclear transport.

The contribution of karyopherin- β to proteasome nuclear import would most likely occur through formation of the classical karyopherin- α/β heterodimer at the Sts1 NLS sequence. The yeast SUMO protease Ulp1, like Sts1, possesses a long bipartite NLS and was recently found by *in vitro* binding assays to form a complex with the karyopherin- α/β heterodimer that is selectively disassembled by RanGTP (yeast Gsp1) (Hirano et al., 2017). To investigate the possibility of a similar ternary complex forming with Sts1, I utilized *in vitro* pull-down assays with full-length recombinant GST-Sts1 bound to a glutathione resin. Both recombinant Srp1-6His and untagged Kap95 bound to immobilized GST-Sts1, indicating the formation of a ternary complex most likely assembling at the Sts1 NLS sequence (Figure 4.3A, lane 2). Furthermore, the relative amounts of GST-Sts1, Srp1-6His, and Kap95 in this assembly appear to be stoichiometric, consistent with our previous size-exclusion chromatography data suggesting that Sts1 and Srp1 together assemble in a 2:2 conformation. To verify that Kap95 binds to Srp1 and not Sts1, I repeated this *in vitro* pull-down assay utilizing recombinant GST-Srp1 as the bait species. GST-Srp1 was sufficient to recruit Kap95, consistent with previous observations of their specific interaction behavior (Figure 4.3B, lane 3) (Enenkel et al., 1995). Additionally, a ternary complex was observed to assemble when GST-Srp1 was incubated in the presence of Kap95 and the recombinant truncation mutant Sts1(1-116)-6His (Figure 4.3B, lane 4). This indicated that the formation of the Sts1/Srp1/Kap95 ternary complex does not require the C-terminal domains of Sts1. It is thus likely that each Srp1 subunit binds to an available NLS sequence in the Sts1 dimer, and each subsequently recruits a Kap95 subunit at its individual IBB

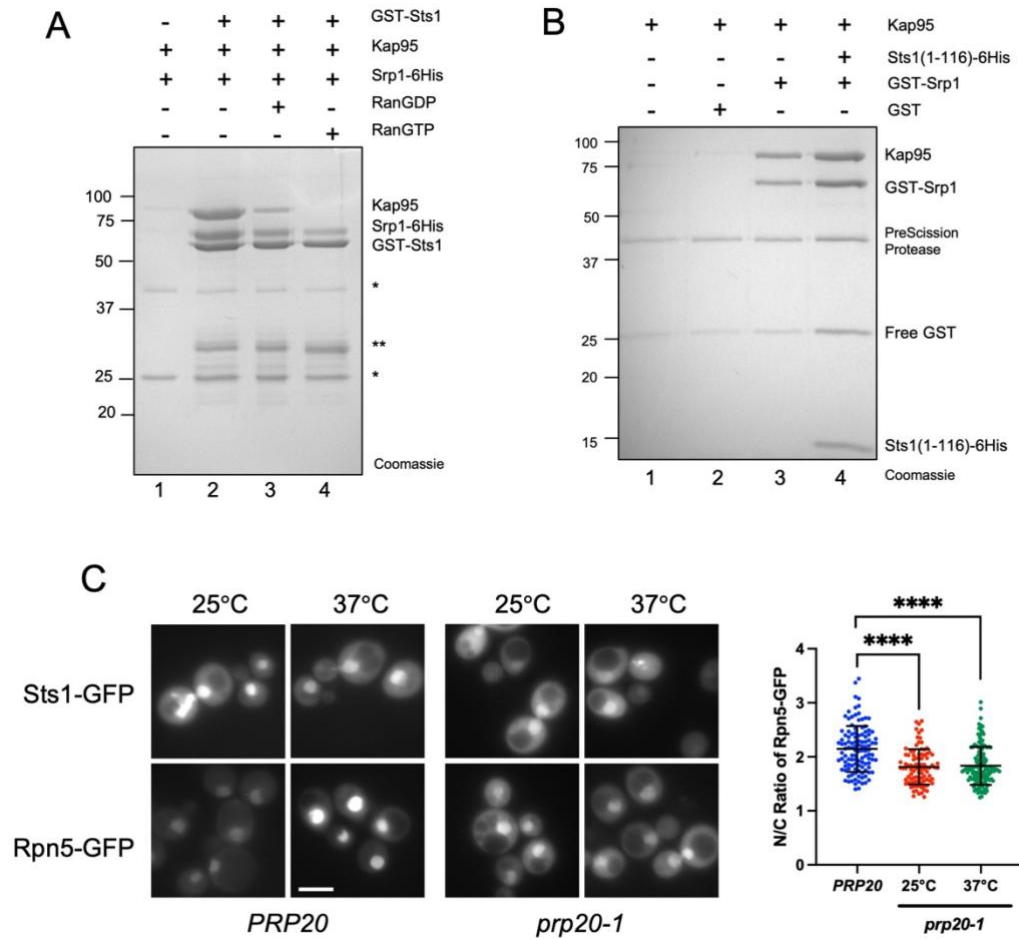


Figure 4.3: Sts1 forms a transport-competent complex with Srp1 and Kap95 that is disrupted by RanGTP.

(A) The Sts1/Srp1/Kap95 ternary complex is disrupted by RanGTP but not RanGDP. Recombinant GST-Sts1 was immobilized onto GSH resin and incubated with Srp1-6His and Kap95 (lanes 2-4). Protein complexes were subsequently incubated with RanGDP or RanGTP (lanes 3 and 4, respectively), and bound proteins were analyzed by SDS-PAGE. * indicates proteolytic fragments derived from Kap95 and ** indicates proteolytic fragments derived from GST-Sts1. (B) The Sts1 NLS is sufficient to recruit both Srp1 and Kap95 in a classical NLS and IBB-dependent manner. Recombinant GST-Srp1 was immobilized onto GSH resin and incubated with the indicated species (lanes 3 and 4). Bound proteins were eluted from the GSH resin by cleavage of the GST-Srp1 affinity tag using GST-PreScission Protease. The eluted species were analyzed by SDS-PAGE. (C) Disruption of the yeast RanGEF Prp20 results in a proteasome localization defect. Yeast expressing *prp20-1* were transformed with pRS415MET25-Sts1-GFP or pRS316-Rpn5-GFP-

FLAG in the presence of a wild-type *PRP20* cover plasmid (left images, *PRP20*), or following ejection of the WT cover plasmid on 5-FOA (right images, *prp20-1*). Transformants were grown to mid-exponential phase at 25°C prior to fluorescence imaging, and a population were shifted to 37°C for two hours. A t-test was used to determine statistical significance of differences in localization (**** $p < 0.0001$). Three replicates of at least 100 cells were counted. Scale bar: 5 μm .

domain (Lott et al., 2010). The recruitment of both Srp1 and Kap95 is consistent with our hypothesis that Sts1-mediated nuclear transport of proteasomes occurs in a karyopherin- α/β -dependent manner.

I next examined whether the Sts1/Srp1/Kap95 ternary complex could be disrupted by RanGTP. In the nucleus, RanGTP displaces NLS-containing cargo from the Srp1 binding pocket and triggers the release of the karyopherin proteins for cytoplasmic recycling (Kobe, 1999; Nachury and Weis, 1999; Matsuura and Stewart, 2004; Lee et al., 2005). If Sts1 participates in nuclear transport with the karyopherin- α/β heterodimer, we would expect similar release of the heterodimer from the Sts1 NLS in the presence of RanGTP. Following assembly of the recombinant GST-Sts1/Srp1-6His/Kap95 ternary complex on a glutathione resin, I incubated the resin with bacterially purified RanGTP or RanGDP. The full ternary complex remained intact upon exposure to RanGDP, while incubation with RanGTP triggered complete removal of Kap95 but not Srp1 from the complex (Figure 4.3A). Maintenance of the ternary complex in the presence of RanGDP and the persistence of the NLS-Srp1 interaction is consistent with what has previously been observed for Ulp1 (Hirano et al., 2017). In those experiments, Srp1 was only removed from the Ulp1 NLS upon the concerted action of RanGTP and Exportin-2 (yeast Cse1). Unfortunately, I was unable to successfully purify Cse1 from bacterial extracts to examine its contribution to the disassembly of the Sts1/Srp1/Kap95 complex. Together these data suggest that the Sts1/Srp1/Kap95 complex may stably form in the cytoplasm for recruitment of proteasome cargo followed by disassembly in the nucleus through the action of RanGTP after successful transport through the NPC.

Though I had observed that RanGTP is sufficient to impact the Sts1-karyopherin- α/β complex *in vitro*, I next investigated the effect of the Ran cycle *in vivo*. As noted, RanGTP is concentrated in the nucleus, while RanGDP is primarily found in the cytoplasm (Wendler and Enenkel, 2019). RanGTP is maintained in the cell nucleus through the action of the RanGEF, known as Prp20 in yeast. GEF proteins mediate the exchange of GDP for GTP on their cognate small GTPase (Moore 1998; Gorlich and Kutay, 1999; Atkinson et al., 1995; Aebi et al., 1990). This function contrasts with that of the cytoplasmic RanGAP, which stimulates Ran GTPase activity to convert Ran to its GDP-bound form (Becker et al., 1995; Bischoff et al., 1995). If disassembly of the Sts1/Srp1/Kap95 complex is required for proteasome trafficking, I should be able to see proteasome localization defects in cells where the Ran cycle was perturbed. For this, I expressed the fusion protein Rpn5-GFP-FLAG from a plasmid under the control of its native promoter in a temperature-sensitive mutant of the yeast RanGEF *prp20-1* (Vijayraghavan et al., 1989; Fleishmann et al., 1991). Rpn5-GFP was slightly enriched in the cytoplasm compared to WT yeast at permissive temperature (25°C) as well as after shifting to restrictive temperature for one hour (37°C) (Figure 4.3C). In comparison, expressing WT Sts1-GFP under the control of the yeast *GPD* promoter in *prp20-1* yeast did not appear to result in a reduction in Sts1 nuclear localization. One possible explanation for this result is that *prp20-1* disrupts recycling of the karyopherin proteins, causing a reduction in the rate of proteasome import. These results may indicate that the accumulation of RanGDP in the cell nucleus due to dysfunctional Prp20 does not affect Sts1 nuclear import but does adversely affect proteasome nuclear import.

4.2.3 The karyopherin complex can import proteasome-free Sts1

Our results thus far have indicated that proteasome nuclear import depends upon an interaction with Sts1 and the karyopherin- α/β heterodimer. Additionally, the formation of this ternary complex appears to be specific to the cytoplasm because RanGDP predominates there and this form of the GTPase cannot remove the karyopherin proteins from Sts1. Our previous results have shown that the ternary complex of Sts1/Srp1/Kap95 can form *in vitro* and that Sts1 is insufficient for binding to the proteasome in the absence of Srp1. One unanswered question is whether Sts1 normally binds the karyopherin- α/β heterodimer prior to recruitment of the proteasome. In my analysis of Sts1 mutants such as Sts1-2, I observed that Sts1 can accumulate in the nucleus even when the proteasome is largely excluded. I therefore hypothesized that the Sts1 transport complex assembles prior to proteasome recruitment and that the Sts1 adaptor could be transported to the nucleus in the absence of its proteasome cargo.

I utilized the Anchor Away system to selectively sequester the proteasome to different cellular compartments and determine whether Sts1 can undergo nuclear import in the absence of bound proteasomes. (Haruki et al., 2008; Fan et al., 2011; Tsuchiya et al., 2013). The Anchor Away system employed here uses yeast that are chromosomally tagged with *RPN11-FRB-GFP*. Additionally, the plasma membrane protein Pma1, large ribosomal subunit Rpl13A, and histone H2B were each chromosomally fused to an FKBP12 protein domain. In the presence of rapamycin, FRB-tagged proteasomes form a complex with the FKBP12-tagged anchor proteins, forcing the proteasome to be tethered to the plasma membrane, ribosome, or chromatin within the nucleus (Figure 4.4). I examined whether a population of Sts1 is bound to sequestered proteasomes in the cytoplasm by expressing the

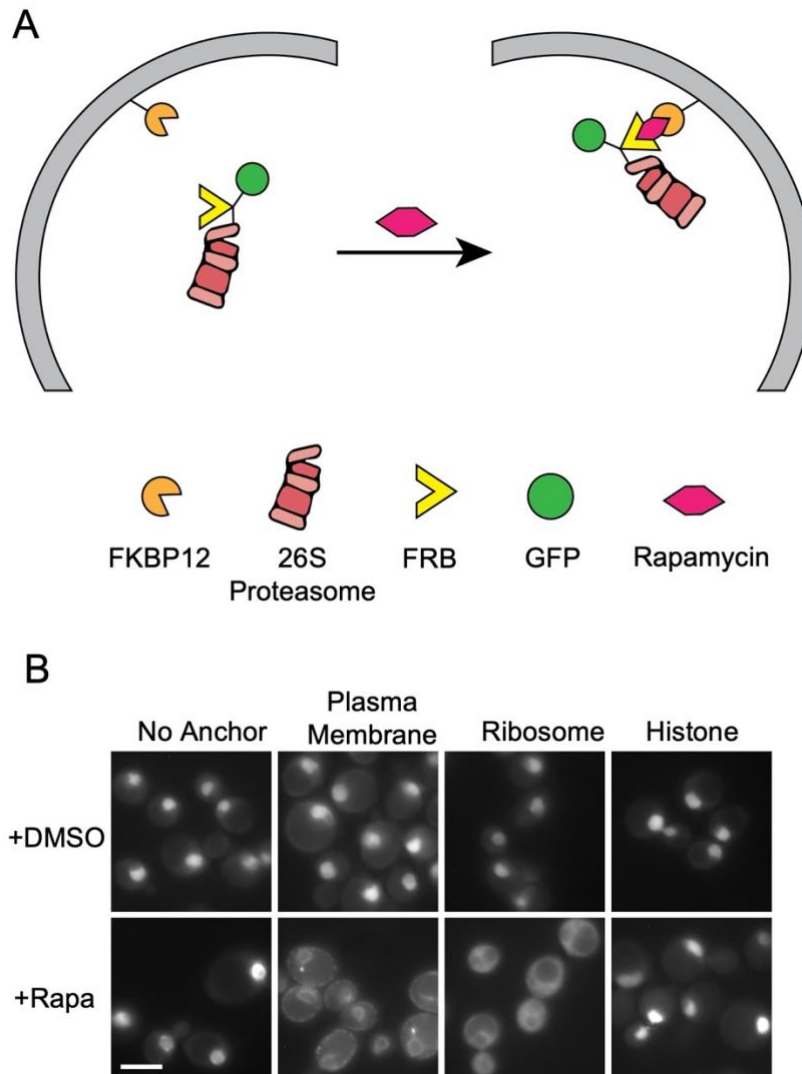


Figure 4.4: The Anchor Away system sequesters proteasomes to various cellular compartments.

(A) Schematic of the Anchor Away system. The proteasome subunit Rpn11 is chromosomally tagged with FRB and GFP (*RPN11-FRB-GFP*) and properly localizes to the cell nucleus in the absence of rapamycin. An anchor protein is tagged with the FKBP12 protein such that in the presence of rapamycin a ternary complex will form between Anchor-FKBP12, rapamycin, and Rpn11-FRB-GFP. This will tether the fully assembled proteasome to the site of the anchor protein. (B) Representative examples of proteasomes sequestered to different cellular compartments in the Anchor Away system. Cells grown and treated with either DMSO or rapamycin for 2 hrs at 30 °C and visualized by fluorescence microscopy (Rpn11-GFP). Scale bar indicates 5 μm .

Sts1-mCherry fusion protein from the *MET25* promoter in the various Anchor Away yeast strains. If Sts1 cannot be transported to the cell nucleus without binding to the proteasome, I would expect to see co-localization of Sts1-mCherry with the sequestered proteasome populations.

In each Anchor Away strain, both Rpn11-GFP and Sts1-mCherry localized to the cell nucleus upon control treatment with the DMSO vehicle, indicating unobstructed Sts1-mediated nuclear import. However, when proteasomes were sequestered to the plasma membrane or ribosome by rapamycin treatment, I observed that Sts1-mCherry still predominantly localized to the nucleus despite proteasomal exclusion (Figure 4.5). These results indicate that karyopherin-mediated import of Sts1 can occur in the absence of proteasome cargo; this is consistent with classical nuclear import behavior, as the Sts1 NLS is likely available and would retain its interactions with Srp1. This also indicates that recruitment of karyopherin proteins in the cytoplasm can occur prior to proteasome binding, consistent with the inability of GST-Sts1 to pull down 26S proteasomes in the absence of Srp1 *in vitro*. As suggested earlier, it is possible that Sts1 exists in a conformation that is unable to bind to the proteasome prior to recruitment of the karyopherins; upon formation of the karyopherin- α/β transport complex, Sts1 will facilitate the nuclear entry of proteasome targets, but only if it encounters a free proteasome. When proteasomes are unable to undergo transport—such as under Anchor Away tethering conditions—the Sts1/Srp1/Kap95 complex simply enters the nucleus without the proteasome cargo. It remains to be seen what conditions or cellular locations trigger Sts1 recruitment of the 26S proteasome for transport, but we conclude here that Sts1 nuclear import does not depend upon proteasome availability.

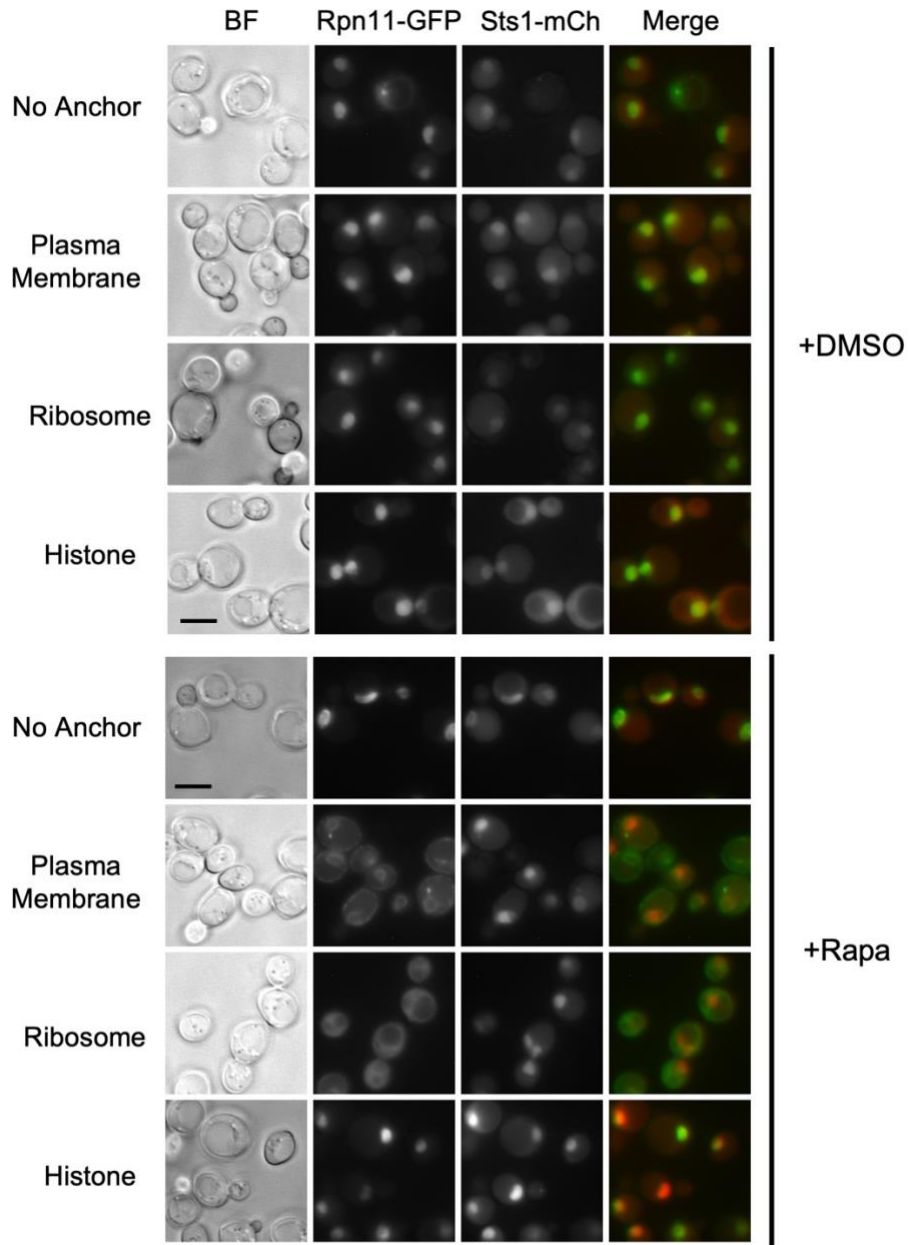


Figure 4.5: Sts1 can undergo nuclear import without bound proteasomes.

Using the Anchor Away system, the proteasome was sequestered to the indicated cellular compartments after 3 hours rapamycin treatment (“+Rapa,” no sequestration control indicated by “+DMSO”). Proteasomes were visualized by chromosomally expressed Rpn11-GFP. Cells were also transformed with pRS415MET25-Sts1-mCherry-FLAG to visualize Sts1 co-localization. Cells were grown to mid-exponential phase at 30°C prior to fluorescence imaging. Scale bar: 5 μ m.

4.2.4 Sts1 does not contribute to proteasome reimport from PSGs

The role of Sts1 in karyopherin-mediated proteasome nuclear import in exponentially growing cells led me to investigate if Sts1 has a similar role in the reimport of proteasomes from proteasome storage granules (PSGs). In budding yeast, proteasomes undergo relocation from the nucleus to the cytoplasm under glucose-limiting conditions such as during stationary phase to form PSGs (Laporte et al., 2008; Li and Hochstrasser, 2021). PSGs persist in the cytoplasm until the reintroduction of glucose causes their dissipation and the rapid reimport of proteasomes into the cell nucleus (Laporte et al., 2008; Peters et al., 2006). Interestingly, PSGs almost exclusively contain proteasomes and their subcomplexes, though ubiquitin and the reimport factor Blm10 have both been identified in PSGs (Enenkel 2018; Weberuss et al., 2013).

I first examined if Sts1 localizes to PSGs under glucose starvation by expressing the WT Sts1-GFP fusion protein on a plasmid bearing the strong *GPD* promoter in a yeast strain chromosomally tagged with *RPN2-mCherry* and assessed the localization of Sts1-GFP after two days of glucose starvation, as well as after one hour of glucose refeeding. In exponential growth phase, Sts1-GFP strongly accumulates in the cell nucleus, colocalizing with Rpn2-mCherry. However, under glucose starvation I observed no Sts1-GFP signal colocalizing with Rpn2-mCherry in cytoplasmic PSG foci (Figure 4.6A). This suggests that Sts1 is not found in PSGs during periods of nutrient deprivation. After adding glucose to the media, I found that Rpn2-mCherry strongly accumulated in the nucleus again—consistent with PSG dissipation—while Sts1-GFP was absent from the nucleus. I hypothesized that the lack of Sts1 in PSGs or other cellular compartments during glucose starvation may result from Sts1 expression being downregulated and thus examined the

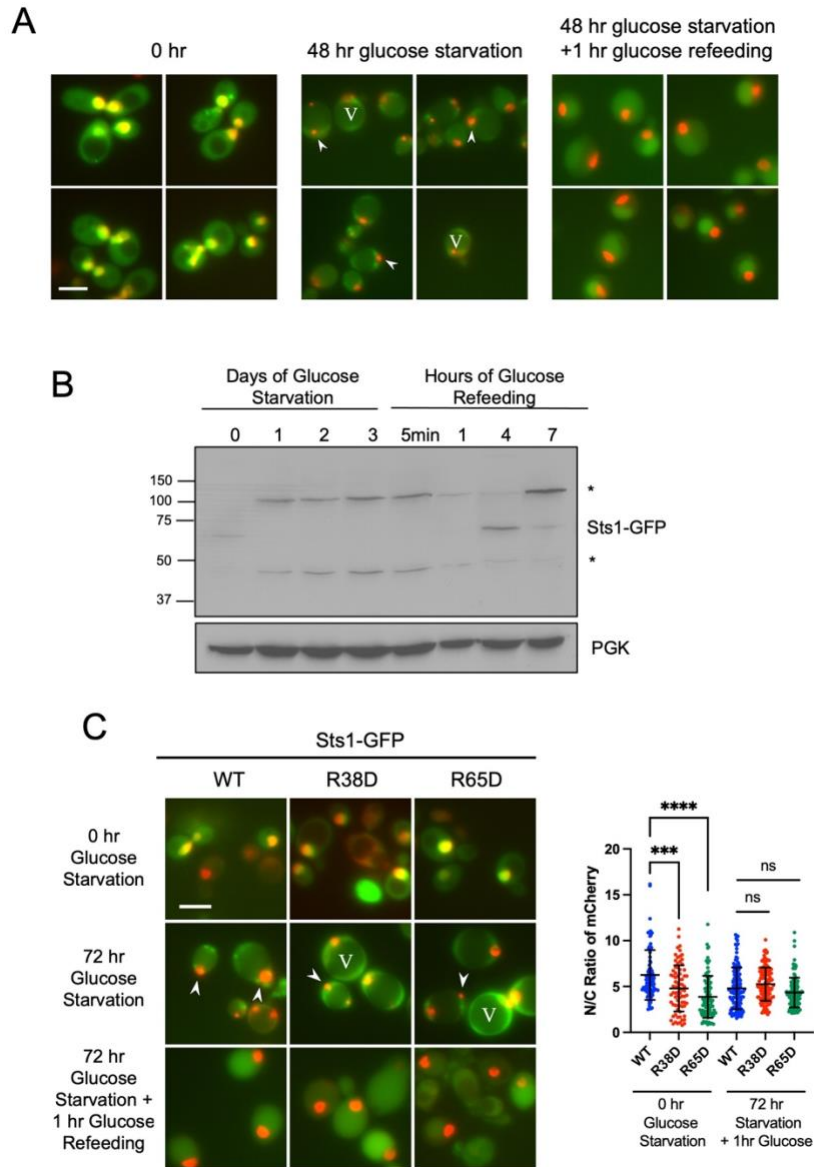


Figure 4.6: Sts1 does not contribute to the reimport of proteasomes from PSGs.

(A) Sts1 does not localize to PSGs upon glucose starvation and is not found in cell nuclei following reimport of proteasomes from PSGs. Yeast bearing *sts1Δ* and chromosomal *RPN2-mCherry* were transformed with plasmid pRS415-GPD-Sts1-GFP for fluorescence microscopy. Cells grown in rich media at 30°C and imaged (0 hr of glucose starvation). Cells harvested and subsequently grown in low-glucose media (0.025% glucose) for two days and imaged (48 hrs glucose starvation), then supplemented with 2% glucose and imaged after 1 hr of glucose treatment (48 hrs glucose starvation + 1 hr glucose refeeding). (B) Sts1 is not expressed upon

glucose starvation and is also not expressed for several hours after glucose refeeding. Yeast as described in (A) were grown in rich media and transferred to low-glucose media for three days. Samples taken every 24 hrs and at the indicated timepoints after glucose refeeding. Cell extracts from the indicated timepoints were separated by SDS-PAGE and analyzed by anti-Sts1 and anti-PGK immunoblotting. * indicates non-specific cross-reactive bands. (C) Import-defective Sts1 mutants do not exhibit a proteasome localization defect following reimport of proteasomes from PSGs. Yeast as described in (A) were transformed with plasmids bearing the indicated Sts1-GFP alleles for fluorescence microscopy. Cells were grown in rich media, transferred to low-glucose media, and supplemented with glucose as in (A). A t-test was used to determine the statistical significance of differences in localization (****p<0.0001, ns indicates no significant difference). Three replicates of at least 100 cells were counted. For (A) and (C) Scale bars indicate 5 μ m, arrowheads indicate PSGs, and “V” indicates cell vacuole.

steady-state levels of Sts1-GFP during starvation and refeeding. I observed that Sts1-GFP is not expressed during glucose starvation, nor for several hours after glucose reintroduction (Figure 4.6B). This was striking as proteasomes reenter the nucleus in a matter of minutes following glucose supplement (Laporte et al., 2008). This observation suggested that Sts1 is not involved in the reimport of proteasomes from PSGs.

To further test this hypothesis, I utilized two single point mutations in the Sts1 NLS sequence, R38D and R65D (previously discussed in Chapter 3), that exhibit reduced nuclear localization of both Sts1 and the proteasome. I similarly expressed these mutants as GFP fusion proteins from plasmids in *RPN2-mCherry* yeast and analyzed the ratio of proteasomes in the nucleus and cytoplasm (N/C ratio). During exponential growth, proteasome nuclear accumulation was severely impaired in both Sts1 mutants (Figure 4.6C). When cells were deprived of glucose, proteasomes were still able to form PSGs in the NLS mutants, and like WT Sts1, neither Sts1 mutant colocalized to proteasome foci. When the starved cells were supplemented with glucose, the N/C ratio of proteasomes appeared similar among WT Sts1 and the NLS mutant strains (Figure 4.6C). If Sts1 participates in proteasome reentry to the nucleus from PSGs, one would expect the proteasome nuclear import defects of Sts1-R38D and Sts1-R65D to similarly persist after glucose refeeding. However, neither mutant showed any defect in nuclear accumulation of proteasomes, consistent with a repression of Sts1 expression during nutrient deprivation and immediately following glucose exposure.

Though I did not observe Sts1-GFP signal in PSGs during glucose starvation conditions, I often observed cytoplasmic puncta in the GFP fluorescence channel that seemed to accumulate in the vacuole following glucose refeeding (Figure 4.7A). I

investigated this Sts1-GFP behavior in yeast bearing *cue5* Δ or *atg8* Δ mutations, to assess if this focus formation is regulated by autophagy. The puncta persisted in both autophagy mutants, suggesting that their formation is unrelated to autophagy during glucose starvation (Figure 4.7B). Importantly, I also imaged yeast bearing no fluorescently tagged recombinant proteins, and still observed puncta in the GFP channel after three days of glucose starvation (Figure 4.7B). I conclude that these foci do not represent Sts1-GFP, consistent with my analysis of Sts1-GFP levels during glucose starvation and following refeeding. Taken together, these data suggest that Sts1 does not localize to PSGs nor does it contribute to reimport of proteasomes from PSGs upon cellular exit from quiescence.

4.3 Discussion

Nuclear accumulation of proteasomes is generally conserved across eukaryotes, though the necessity for proteasomes in the nucleus is not well understood (Wilkinson et al., 1998; Wojick et al. 2003; Pack et al., 2014; Albert et al., 2017). The importance of the UPS in DNA replication and repair, as well as the abundance of nuclear substrates, likely contribute to the predominance of proteasomes in the nucleus (Ulrich and Walden, 2010; McCann and Tansey, 2014). The evidence presented here indicate that yeast proteasome nuclear accumulation results from import of fully assembled 26S proteasomes. We further demonstrate that 26S proteasome nuclear import is facilitated by Sts1 through cooperation with the karyopherin- α/β heterodimer and the RanGTP cycle.

As discussed in Chapter 3, binding of the yeast karyopherin- α protein Srp1 to Sts1 requires exposure of the Sts1 N-terminal NLS sequence. In the experiments presented here, we examined whether Sts1-mediated nuclear import of proteasomes is specific to

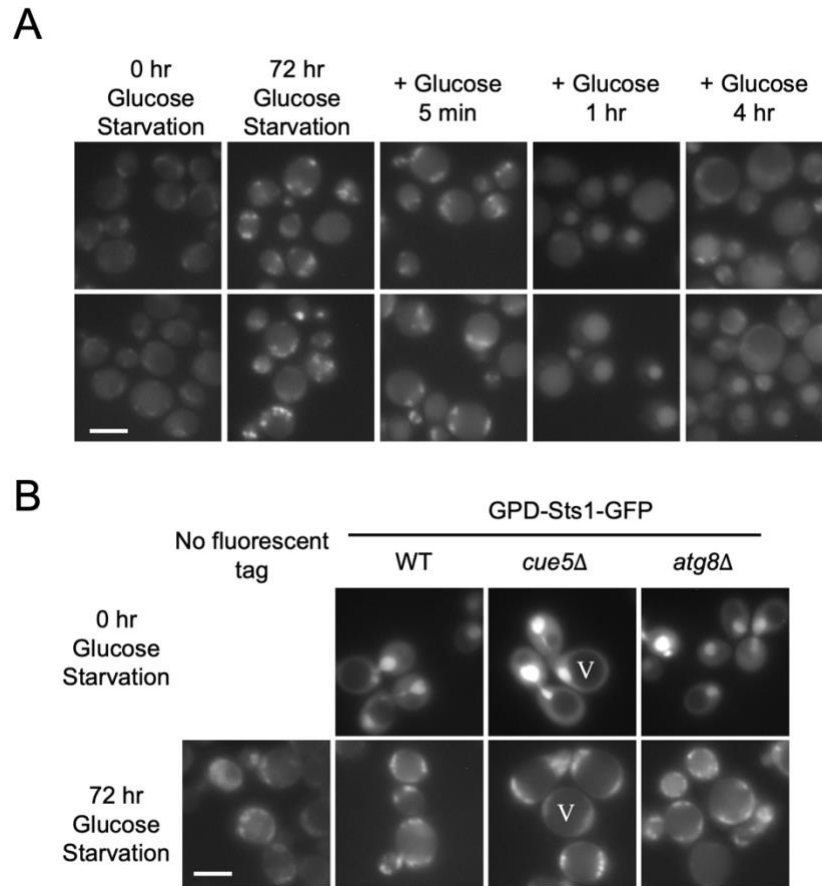


Figure 4.7: Cytoplasmic foci observed during glucose starvation do not contain Sts1-GFP.

(A) Cytoplasmic puncta are observed during glucose starvation that appear to localize to the vacuole upon glucose refeeding. Yeast as in Figure 4.6 were grown in rich media and transferred to low-glucose media for three days and imaged by fluorescence microscopy. (B) The cytoplasmic puncta observed under glucose starvation are not Sts1-GFP and are unrelated to autophagy. Yeast bearing no fluorescent label and the indicated strains transformed with plasmid pRS415-GPD-Sts1-GFP were grown in rich media and transferred to low-glucose media as in Figure 4.6 for three days and imaged by fluorescence microscopy. “V” indicates cell vacuole. Scale bar indicates 5 μ m.

subcomplexes of the proteasome. Importantly, Sts1 was reported to bind to the lid subunit Rpn11, although some studies suggested that interaction with the fully assembled 26S proteasome also occurs (Tabb et al., 2000; Chen et al., 2011; Ha et al., 2014). As the RP lid is the only proteasome subcomplex that does not contain an identified NLS sequence, we investigated whether Sts1 is a specific “NLS donor” for such subcomplexes that otherwise may not be imported outside of the fully assembled proteasome (Wendler and Enenkel, 2019; Isono et al., 2007). We observed *in vitro* that Sts1 specifically binds to the fully assembled 26S proteasome when in complex with Srp1, though there is no detectable interaction with the proteasome subcomplexes LP2, CP, or RP (Figure 4.1). Additionally, while several subcomplexes contain NLS sequences, GST-Srp1 alone was insufficient to pull down the 26S proteasome *in vitro*, though it showed slight association with free RP and CP, likely due to available NLS sequences (Figure 4.2) (Enenkel, 2014; Lehmann et al., 2002; Tanaka et al., 1990; Wendler et al., 2004). While the possibility remains that proteasome subcomplexes may be imported to the nucleus, the essential Sts1-mediated import pathway appears specific to the fully assembled proteasome.

The ability of Sts1 to bind to karyopherin- α and impact the nuclear accumulation of the proteasome implied the subsequent involvement of the karyopherin- β protein, yeast Kap95. To verify that proteasome nuclear import occurs in a classical karyopherin-mediated pathway, I assayed for the ability of Kap95 to interact with the Sts1/Srp1 complex. *In vitro* pull-down assays demonstrated formation of a ternary complex composed of Sts1/Srp1/Kap95. Additionally, this ternary complex could form even when only the Sts1 N-terminal domains (residues 1-116) were present (Figure 4.3). These results indicate that Kap95 and Srp1 likely form a canonical α/β heterodimer and interact with

Sts1 in an NLS-dependent manner. Additionally, the formation of the Sts1/Srp1/Kap95 complex *in vitro* suggests that Sts1 NLS recognition by Srp1 and subsequent recruitment of Kap95 to the Srp1 IBB domain can occur in the absence of the proteasome; this implies that karyopherin-binding to Sts1 occurs prior to proteasome-recruitment.

To address this question, I used the Anchor Away system and demonstrated that Sts1 can accumulate in the nucleus even when the proteasome is tethered to the plasma membrane or ribosomes in the cytoplasm (Figure 4.5); this indicates that Sts1 is able to undergo nuclear import via the Srp1/Kap95 heterodimer without bound cargo and supports the hypothesis that Sts1 may bind to the karyopherin heterodimer prior to interaction with the proteasome.

If Sts1-mediated nuclear import of proteasomes occurs via the karyopherin pathway, we hypothesized that the assembly of the karyopherin proteins might be influenced by the Ran cycle (Moore et al., 1998; Chook et al., 2011). RanGTP in the nucleus is responsible for the disassembly of the karyopherin- α/β heterodimer in classical NLS-dependent nuclear import, and we thus examined the dependence of Sts1/Srp1/Kap95 upon the nucleotide state of Ran. Emulating previous experiments performed on the NLS sequence of the SUMO protease Ulp1, I conducted *in vitro* pull-down assays using the immobilized Sts1/Srp1/Kap95 complex in the presence of RanGDP or RanGTP (Hirano et al., 2017). I observed that this ternary complex is selectively disrupted by the addition of RanGTP but not its hydrolyzed form RanGDP (Figure 4.3A). This is consistent with nucleus-specific disassembly of the karyopherin- α/β heterodimer following completion of nuclear import. Importantly, RanGTP alone was sufficient to remove Kap95 but not Srp1 from the ternary complex. It is possible that the Sts1 bipartite NLS creates a particularly

strong interaction that may not be disassembled by RanGTP alone; previous work had indicated a requirement for Exportin-2 in this process as well, and *in vivo* experiments have implicated the nucleoporin Nup2 in import complex disassembly (Hirano et al., 2017; Matsuura et al., 2003). These results suggest that Sts1 facilitates proteasome nuclear import in a karyopherin-dependent pathway and that a late step of import relies upon RanGTP in the nucleus.

A potentially surprising finding of this study is that Sts1 is not involved in the reimport of proteasomes from PSGs after exit from quiescence. Proteasome-associated factors such as Blm10 and ubiquitin have been identified as PSG components (Weberuss et al., 2013; Enenkel 2018), but we did not observe similar localization of Sts1 to PSGs. Additionally, though proteasomes successfully reentered the cell nucleus upon glucose addition, we did not observe Sts1 re-accumulation in the nucleus, indicating dissociation from this reimport process (Figure 4.6A). In fact, under the conditions tested, Sts1 was not detectable during glucose starvation and for several hours after glucose refeeding (Figure 4.6B). This confirms the absence of Sts1 from PSGs and from the cell nucleus after glucose refeeding. As I will discuss in Chapter 5, proteasome nuclear transport by Sts1 appears to terminate with the degradation of Sts1, likely necessitating repeated rounds of Sts1 translation, import, and degradation and thus may not be suitably efficient for proteasome reimport following PSG dissipation. Though we have not determined whether Sts1 is able to shuttle back to the cytoplasm, as do the nuclear transport receptors, our analysis suggests a model featuring its immediate proteolysis following import. As protein synthesis is the most energetically expensive process in the cell, and the high demand for nuclear proteasomes is immediate, an Sts1-independent reimport mechanism appears to be

necessary when cells are in the early stages of recovery from prolonged nutrient deprivation (Kafri et al., 2016). After energy levels recover and protein translational capacity is restored, cells may switch to an Sts1-dependent process. Importantly, though we observed Sts1 levels returning to steady state after several hours of glucose recovery, we have not identified the conditions or factors responsible for switching to this Sts1-catalyzed import mechanism.

Previous studies of Sts1 had proposed that its primary function is to serve as a nuclear import adaptor protein to facilitate the nuclear import of the proteasome. The results presented here deepen our understanding of the role that Sts1 plays in this process. We have shown that Sts1 dysfunction disrupts proper proteasome nuclear localization and determined that this import mechanism is mediated by recruitment of the karyopherin- α/β heterodimer. Additionally, the small GTPase Ran appears to impact this process, as nuclear RanGTP but not cytoplasmic RanGDP was sufficient to disrupt the assembled Sts1/Srp1/Kap95 import complex. Furthermore, the RanGEF mutant *prp20-1* exhibited proteasome mislocalization *in vivo* suggesting that RanGTP may influence the function of Sts1 or the karyopherin proteins.

Chapter 5: Sts1 is degraded by the proteasome following completion of nuclear import

Portions of this chapter are included in a manuscript currently in preparation: Breckel CA, Johnson Z, Hochstrasser M. (2023). 26S proteasomes are transported into the nucleus by karyopherins and the adaptor protein Sts1 in a single turnover mechanism. Portions of this chapter are also included in the published manuscript: Budenholzer L, Breckel C, Hickey M, Hochstrasser M. (2020). The Sts1 nuclear import adaptor uses a non-canonical bipartite nuclear localization signal and is directly degraded by the proteasome. *Journal of Cell Science* **133**, jcs236158. I performed all experiments presented in this chapter except for those depicted in the following figures: Figure 5.1A-C and Figure 5.2B (Chris Hickey).

5.1 Introduction

Proteostasis is an important facet of maintaining cell health and relies upon a balance between the synthesis of necessary proteins and the degradation of unnecessary and potentially toxic ones. The UPS is one of the major pathways for the targeted degradation of cellular proteins. The vast majority of proteasome substrates are degraded in a ubiquitin-dependent manner as a result of an enzyme cascade that mediates the recognition and ubiquitylation of target proteins. Ubiquitylation is initiated by the formation of a high-energy bond between free ubiquitin and a ubiquitin-activating enzyme (E1) (Finley et al., 2012). The thioester-linked ubiquitin is then transferred to a ubiquitin-conjugating enzyme (E2) thiol. Protein substrates are recognized for degradation by the presence of unique characteristics or degrons that are recognized and bound by ubiquitin ligases (E3 enzymes). The ubiquitin ligase, in concert with the E2-Ub conjugate, mediates ubiquitylation of its bound substrate at an available lysine residue (Deshaies and Joazeiro,

2009; Fredrickson and Gardner, 2012). For certain E3s, the ubiquitin is first transferred from the E2 to a cysteine side chain of the E3 and only then ligated to the substrate. In yeast, there exists one ubiquitin-activating enzyme (Uba1), 11 ubiquitin-conjugating enzymes, and roughly 100 ubiquitin ligases with distinct but often overlapping specificity (Hochstrasser 1996; Finley et al., 2012).

Poly-ubiquitin chains are recognized by the proteasome regulatory particle (RP) as a means of targeting substrates for proteasomal degradation. However, a growing number of proteasome substrates have been identified as ubiquitin-independent degradation targets. While the mechanism by which ubiquitin-independent degradation is carried out is not generally well-characterized, several common features of ubiquitin-independent substrates have emerged from known examples. Specifically, many targets of proteasomal degradation by this pathway are intrinsically disordered or otherwise contain distinct unstructured domains and possess a means of associating with the proteasome outside of ubiquitylation (Erales and Coffin, 2014). These characteristics theoretically allow for the substrate to encounter the 26S proteasome unassisted and subsequently initiate their own degradation through engagement of their unstructured domains by the RP ATPase ring (Jariel-Encontre et al., 2008; Yu et al., 2016). In some studies, it has also been demonstrated that intrinsically disordered proteins can be degraded by the 20S core particle (CP) *in vitro*, likely due to the unstructured nature of such substrates making the unfolding capability of the regulatory particle superfluous (Baugh et al., 2009; Suskiewicz et al., 2011).

In our analyses, we have thus far learned that Sts1 can bind to the 26S proteasome directly. Though it has been suggested that Sts1 binds to the RP, particularly Rpn11, the specific site(s) of interaction in the intact proteasome has not been determined (Tabb et al.,

2000). While we observed no interaction of Sts1 with the CP, its ability to bind to the fully assembled 26S proteasome *in vitro* suggests that Sts1 may represent a proteasome substrate that undergoes ubiquitin-independent degradation. This hypothesis is further supported by predicted structures of Sts1 that indicate both its N-terminus and C-terminus are unstructured (Jumper et al., 2021; Varadi et al., 2022). Importantly, although its homolog Cut8 shares the unstructured domains predicted for Sts1, Cut8 may not interact with the proteasome directly; Cut8 association is prompted by poly-ubiquitin chain attachment to its N-terminal domain by the E3 ligases Ubr1 and Rhp18 (Rad18 in *S. cerevisiae*) (Takeda and Yanagida, 2005). Cut8 is a very short-lived protein, and this rapid turnover may be linked to its polyubiquitylation. With these ideas in mind, we turned our analysis to determining whether the interaction between Sts1 and the proteasome causes Sts1 to become a ubiquitin-independent degradation substrate, as well as the possible significance of such behavior.

We have shown that Sts1 forms a ternary complex with the karyopherin- α/β heterodimer, and that this assembly is disrupted by the addition of RanGTP which is at high concentration in the nucleus. This raises the question of the fate of Sts1 following the successful deposition of the 26S proteasome in the nucleus. Here we show that Sts1 is a bona fide ubiquitin-independent proteasome substrate and that its proteolysis is linked to its nuclear transport function. Though Sts1 can be degraded by the proteasome *in vitro*, Sts1 proteolysis is blocked when the unstructured N-terminus is not made available to the proteasome. In particular, Sts1 degradation is inhibited when the karyopherin- α/β heterodimer remains bound to its N-terminus as is expected when it is in the cytoplasm, and Sts1 degradation is likely initiated by the addition of RanGTP and disassembly of the

transport complex in the nucleus. The results presented here demonstrate that Sts1 acts as a karyopherin-assisted proteasome nuclear transport factor in a unidirectional mechanism that terminates with its degradation in the cell nucleus.

5.2 Results

5.2.1 Sts1 undergoes proteasomal ubiquitin-independent degradation

Previous analyses into Sts1 stability conducted by cycloheximide-chase and radioactive pulse-chase analysis have indicated that Sts1 is a very short-lived protein with a half-life of ~5 minutes (Budenholzer et al., 2020). To assess whether this rapid turnover occurs in a ubiquitin-independent manner, we first assessed the dependence of Sts1 degradation on ubiquitin conjugation. We conducted cycloheximide-chase analysis on yeast expressing a temperature-sensitive ubiquitin-activating enzyme mutant, *uba1-204*, and assayed for the stability of endogenous Sts1. Despite the inability of the cell to ubiquitylate protein substrates, we observed that Sts1 degradation was unaffected even at high temperature, suggesting that Sts1 proteolysis occurs in the absence of ubiquitin attachment (Figure 5.1A). A known ubiquitin-dependent substrate, *Deg1*-FLAG-Ura3, was completely stabilized under the same conditions (Figure 5.1B). Results described earlier demonstrated binding of Sts1 and the full 26S proteasome, but we had not directly shown that Sts1 degradation *in vivo* required the full RP-CP complex. To determine this, we conducted cycloheximide-chase analysis of Sts1 degradation in yeast bearing the temperature-sensitive RP mutant *cim3-1* allele (Ghislain et al., 1993). Endogenous Sts1 was strongly stabilized at restrictive temperature as compared to wild-type cells (Figure 5.1C). Stabilization in this mutant indicates Sts1 degradation depends on the full 26S

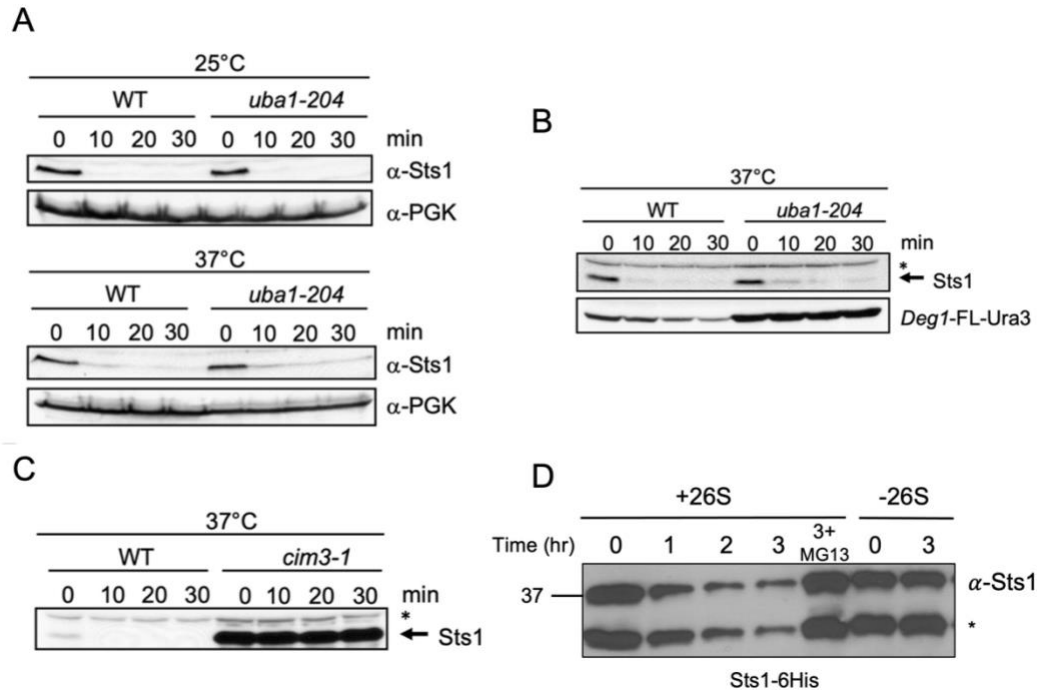


Figure 5.1: Sts1 is a ubiquitin-independent proteasome substrate.

(A) Sts1 is a ubiquitin-independent substrate. Cycloheximide-chase analysis to determine the degradation rates of endogenous Sts1 in the indicated strains at both the permissive (25°C) and restrictive (37°C) temperatures for the *uba1-204* strain. Immunoblot for PGK serves as a loading control. (B) *uba1-204* stabilizes ubiquitin-dependent substrates. Cycloheximide-chase analysis of endogenous Sts1 and plasmid-expressed *Deg1-FLAG-Ura3* in the indicated strains at the restrictive temperature (37°C) for the *uba1-204* strain. A cross-reactive band in the immunoblot for Sts1, indicated by an asterisk, shows unchanging levels of a protein that is not degraded over the 30 min chase. (C) Sts1 degradation depends on the 19S RP. Cycloheximide-chase analysis of endogenous Sts1 in the indicated strains at the restrictive temperature (37°C) for the *cim3-1* strain. (D) Sts1 ubiquitin-independent degradation can be reconstituted *in vitro*. *In vitro* degradation of purified recombinant Sts1-6His by 26S proteasomes purified from yeast. For ‘3+MG’ sample, proteasomes were treated with 50 μM MG132 inhibitor for 10 min prior to addition of Sts1-6His. Degradation was measured at room temperature. * indicates an Sts1 fragment that is often generated during purification from *E. coli* when Sts1 is not co-expressed with Srp1 (see Figure 3.2). This fragment is also a substrate for the proteasome *in vitro*.

proteasome, and altogether, our results indicate that Sts1 is a ubiquitin-independent substrate of the 26S proteasome *in vivo*.

If Sts1 degradation occurs in a ubiquitin-independent manner, we should be able to reconstitute this behavior *in vitro* using purified components. I conducted *in vitro* degradation assays using purified recombinant Sts1-6His and purified yeast 26S proteasomes incubated together for several hours in the presence of ATP. With no other components present, I observed that Sts1 levels decreased over the three-hour experimental time-course, consistent with continued proteolysis (Figure 5.1D). In comparison, Sts1 levels were not depleted over the course of three hours in the absence of the 26S proteasome, indicating that the observed reduction in Sts1 levels was not the result of some intrinsic instability in solution. Importantly, Sts1 degradation was blocked when the proteasome was inhibited by the addition of the proteasome inhibitor MG132, confirming that Sts1 degradation is specific to the proteasome. Though Sts1 proteasomal degradation *in vitro* appears to occur at a much slower rate, it is possible that this is due to a reduced rate of interaction with the proteasome due to lack of agitation or association with the karyopherin proteins. Taken together, these results support the view that Sts1 is a ubiquitin-independent substrate of the 26S proteasome.

5.2.2 Availability of the N-terminus is required for Sts1 degradation

Ubiquitin-independent degradation often requires RP subunits to bind to the substrate directly to facilitate unfolding and entry into the CP core. Additionally, a common feature of ubiquitin-independent degradation substrates is the availability of disordered domains that can be engaged by the CP while the substrate is still bound to the RP (Erales and Coffino, 2014; Yu et al., 2016). As with other ubiquitin-independent substrates, Sts1

directly binds to the proteasome and possesses unstructured domains at both its N- and C-termini. However, Srp1 specifically interacts with the disordered N-terminus of Sts1, and we thus investigated whether its presence might affect the ubiquitin-independent proteolysis of Sts1. I conducted an *in vitro* ubiquitin-independent degradation assay as before using the co-purified complex of Sts1-6His/GST-Srp1 in the presence of the 26S proteasome. In this experiment, I did not observe a decrease in Sts1 levels after several hours, and the overall level of Sts1 remained comparable to the control reaction that lacked 26S proteasomes (Figure 5.2A). This suggested that bound Srp1 blocks Sts1 degradation *in vitro*, possibly indicating a dependence upon the Sts1 N-terminus. In agreement with these data, we observed by cycloheximide-chase analysis of yeast cells that endogenous Sts1-6xGly-3xFLAG levels were strongly stabilized when Srp1 was overexpressed from a plasmid (Figure 5.2B). We speculate that excess Srp1 may have bound most of the endogenous Sts1 pool, blocking its degradation. It is possible that Srp1 overexpression may have had indirect effects *in vivo* that influenced Sts1 stability, rather than a direct association, but our combined results suggest that Srp1 inhibits Sts1 degradation.

Based on our findings that Srp1 inhibits Sts1 degradation, I next investigated whether the ubiquitin-independent proteasome-mediated degradation of Sts1 is related to its intrinsically disordered N-terminal domain. We hypothesized that the karyopherin-free disordered Sts1 N-terminus likely initiates proteasomal degradation when Sts1 is bound to the RP, and that appending a bulky protein domain to the N-terminus would phenocopy the Srp1-induced inhibition of proteolysis *in vitro*. Purified recombinant MBP-Sts1 mixed with yeast 26S proteasomes was not degraded, suggesting that protection of the disordered N-terminus by the MBP fusion is sufficient to block Sts1 degradation (Figure 5.2C). It is

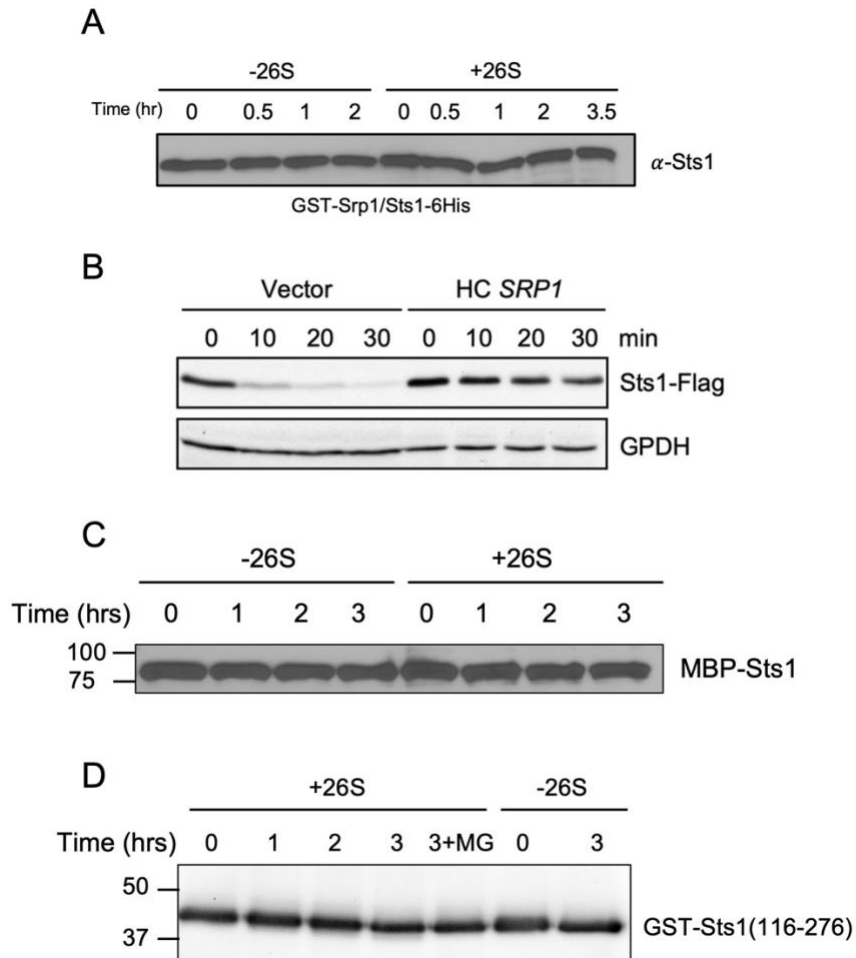


Figure 5.2: The free Sts1 N-terminus is required for its ubiquitin-independent degradation.

(A) Sts1 *in vitro* degradation is blocked in the presence of GST-Srp1. *In vitro* degradation (as in Figure 5.1D) of purified recombinant Sts1-6His pre-bound to GST-Srp1 by 26S proteasomes purified from yeast. Degradation was measured at room temperature. Sts1 levels analyzed by anti-Sts1 immunoblotting. (B) Sts1 is stabilized *in vivo* when Srp1 is overexpressed. Cycloheximide-chase analysis of FLAG-tagged Sts1 in WT cells carrying either an empty high-copy (HC) vector or the same plasmid with *SRP1*. GPDH served as a loading control. Threefold less protein was loaded for the latter extracts to achieve roughly equal Sts1-FLAG levels for the zero-minute samples. The endogenous *STS1* locus was 3'-tagged with 6xGly-3xFLAG. (C) Sts1 *in vitro* degradation is blocked by a bulky N-terminal fusion protein. *In vitro* degradation as in (A) of purified recombinant MBP-Sts1 by 26S proteasomes purified from yeast. Degradation was measured at room

temperature. Sts1 levels analyzed by anti-Sts1 immunoblotting. **(D)** Sts1 *in vitro* degradation is blocked when its unstructured N-terminus is deleted. *In vitro* degradation as in (A) of purified recombinant GST-Sts1(116-276), expressing only the Sts1 six-helix domain. For '3+MG' sample, proteasomes were treated with 50 μ M MG132 inhibitor for 10 min prior to addition of GST-Sts1(116-276). Sts1 levels analyzed by anti-GST immunoblotting.

also possible that such large tags as MBP and GST may somehow block Sts1 interaction with the proteasome, though we previously observed that GST-Sts1 in complex with Srp1-6His is still able to bind the proteasome *in vitro*.

I also tested whether degradation was abrogated by deletion of the unstructured N-terminus. I repeated the *in vitro* ubiquitin-independent degradation assay using GST-Sts1(116-276), a truncation mutant that comprises only the six-helix bundle domain. This construct was similarly stable in solution and was not degraded in the presence of 26S proteasomes (Figure 5.2D). Though the six-helix bundle can interact with the proteasome, Sts1 proteolysis appears to depend upon the availability of an unstructured domain to be taken up by the CP and initiate degradation. As the GST-Sts1(116-276) truncation mutant is likely to be folded, it is unlikely that such degradation would be able to proceed in a ubiquitin-independent manner. Thus, our data implies that Sts1 directly binds to the proteasome within its six-helix bundle domain, but that Sts1 ubiquitin-independent degradation requires the availability of its N-terminus.

5.2.3 Sts1 degradation is initiated by RanGTP

In Chapter 4 we observed that RanGTP is sufficient to disrupt the ternary complex formed between Sts1 and the karyopherin- α/β heterodimer in solution. Additionally, the obstruction of Sts1 proteolysis by Srp1 *in vitro* suggested that Sts1 degradation may be dependent upon the disassembly of the Sts1/Srp1 complex. We hypothesized that the removal of Kap95 and Srp1 by a RanGTP-dependent pathway in the nucleus after successful import of 26S proteasomes would leave Sts1 bound to the proteasome RP with its disordered N-terminus available for proteolytic initiation. To test this hypothesis, I

attempted to reconstitute this initiation event *in vitro* using purified components. I pre-bound purified Sts1-6His/GST-Srp1/Kap95 and analyzed the amount of Sts1 remaining in the presence of 26S proteasomes and RanGTP. As I had observed previously, in the absence of RanGTP there is no detectable degradation of Sts1-6His, likely due to the stability of the Sts1/Srp1/Kap95 complex in solution. However, addition of RanGTP to the reaction after three hours was sufficient to trigger degradation of Sts1-6His (Figure 5.3A). This degradation was proteasome-dependent, as no Sts1 proteolysis was observed in the presence of the proteasome inhibitor MG132 even after six hours of incubation with proteasomes. While *in vitro* pull-down assays indicated that Sts1-Srp1 binding appeared to remain stable in the presence of RanGTP (Figure 4.3A), we suggest that association may be altered in a way that allows degradation initiation, for example, by partial release of the bipartite NLS from Srp1.

To further ensure that degradation of Sts1 in solution was not the result of decreased solubility in the presence of RanGTP, I also tested the stability of Sts1 in complex with the karyopherin- α/β heterodimer after several hours of incubation with either RanGTP or RanGDP but in the absence of the proteasome. No Sts1 degradation was observed, indicating that RanGTP does not affect Sts1 stability and that the reduction in Sts1 levels observed previously are due to proteasomal degradation (Figure 5.3B). These data suggest that the ternary complex formed between Sts1 and the karyopherin proteins is specifically disrupted by RanGTP and precedes the direct proteasomal degradation of Sts1.

It is important to note that while I had observed that incubation of the Sts1/Srp1/Kap95 complex with RanGDP was not sufficient to initiate the removal of Kap95 *in vitro*, I observed Sts1 degradation *in vitro* when RanGDP was utilized in the

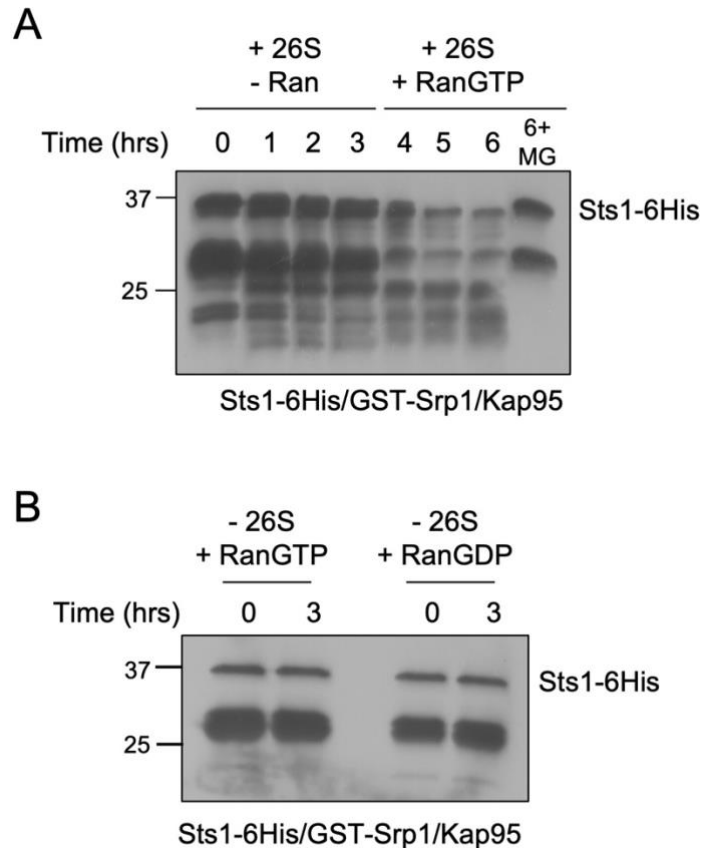


Figure 5.3: Sts1 ubiquitin-independent degradation is initiated by RanGTP.

(A) Degradation of Sts1 is initiated when RanGTP removes karyopherin proteins from the Sts1 N-terminus. *In vitro* degradation assay (as in Figure 5.1D) using the purified complex of recombinant Sts1-6His/GST-Srp1/Kap95 incubated with 26S proteasomes purified from yeast. After 3 hrs, purified RanGTP was added to the reaction mixture and incubated for an additional three hours (4-6 hours, '+RanGTP'). For '6+MG' samples, proteasomes were incubated with 50 μ M MG132 proteasome inhibitor for 10 min prior to addition of Sts1 species. Sts1 levels examined by anti-Sts1 immunoblotting. Lower bands represent Sts1 breakdown products that are proteasome-dependent substrates (most likely residues 116-319). (B) Neither RanGTP nor RanGDP causes Sts1 instability in the absence of proteasomes. *In vitro* degradation as in (A) using the purified complex of Sts1-6His/GST-Srp1/Kap95 in the presence of purified RanGTP and RanGDP, respectively. Sts1 levels analyzed by anti-His immunoblotting.

preceding ubiquitin-independent degradation assay (Figure 5.4A). In fact, Sts1 proteolysis occurred *in vitro* even when Ran was incubated with the non-hydrolysable GTP analog GTP- γ -S (Figure 5.4B). Ran binds to GTP and GDP with picomolar affinity, and some studies suggest that it is likely able to bind any nucleotide tri-phosphate (de Boor et al., 2015; Schwoebel et al., 1998). In support of this fact, I observed that Sts1 degradation also proceeds when Ran is purified in the presence of ATP instead of GTP (Figure 5.4B). These results suggest that the exogenous ATP present in these degradation reaction mixtures to support proteasome processivity *in vitro* may be displacing GDP from purified Ran. If ATP has a similarly high affinity for Ran, it is possible that ATP is being hydrolyzed and initiating Sts1 degradation behavior in the same mechanism as has been observed for RanGTP. Nonetheless, these results demonstrate that *in vitro*, proteasomal degradation of Sts1 occurs in a RanGTPase-dependent manner.

5.2.4 Sts1 degradation only occurs in the cell nucleus

Though I could not demonstrate that Sts1 proteolysis is blocked in the presence of RanGDP *in vitro*, I was encouraged by the previous pull-down data indicating the stability of the Sts1/Srp1/Kap95 ternary complex in the presence of RanGDP (Figure 4.3A). Based on this experiment, we hypothesized that Sts1 degradation would not be triggered in the cytoplasm despite Sts1 recruitment of 26S proteasomes due to the low RanGTP levels. The initiation of Sts1 degradation by RanGTP *in vitro* also suggested this degradation might be nuclear compartment-specific. To determine if Sts1 degradation occurs preferentially in the nucleus, I first examined whether Sts1 accumulates in the nucleus when it is not degraded. Using yeast bearing the temperature-sensitive *cim3-1* RP mutation, I expressed

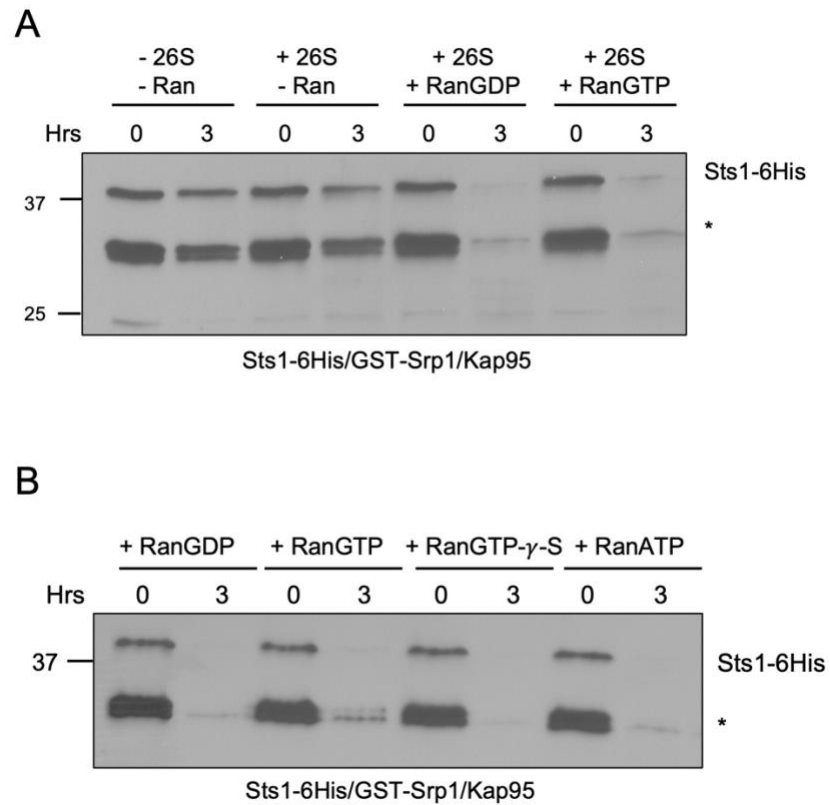


Figure 5.4: Ran may bind and hydrolyze ATP.

(A) Degradation of Sts1 *in vitro* is observed upon RanGDP treatment. *In vitro* degradation assay as in Fig. 5.3 using the purified complex of recombinant Sts1-6His/GST-Srp1/Kap95 incubated with 26S proteasomes purified from yeast, RanGTP, or RanGDP, as indicated. (B) Ran can bind various nucleotides and may hydrolyze ATP. *In vitro* degradation assay as in (A) using 26S proteasomes purified from yeast and Ran bound to the various indicated tri-phosphate nucleotides. For (A) and (B), reactions conducted at room temperature. Sts1 levels analyzed by anti-Sts1 immunoblotting. * indicates proteolytic fragments derived from Sts1-6His.

an Sts1-GFP fusion protein on a plasmid under the yeast *GPD* promoter and confirmed that Sts1 localization in the nucleus persists in *cim3-1* cells at restrictive temperature (Figure 5.5A) (Ghislain et al., 1993). This suggests that Sts1 continues to transport proteasomes to the nucleus but will accumulate there if proteasomes are inactive.

To determine whether Sts1 degradation relies on the presence of proteasomes in the nucleus, I again utilized the Anchor Away technique to sequester proteasomes in different cellular compartments (Haruki et al., 2008; Fan et al., 2011; Tsuchiya et al., 2013). In the presence of rapamycin, proteasomes were tethered to the plasma membrane, ribosome, or chromatin via histone H2B (Figure 4.4). I conducted cycloheximide-chase analysis of chromosomally expressed Sts1-3xFLAG in each sequestration condition. Due to the low concentration of Sts1, I first concentrated the protein by immunoprecipitation via its FLAG affinity tag from large amounts of cell extract. Thus, I was able to compare the degradation rates of endogenous Sts1 *in vivo* when proteasomes were localized to or specifically excluded from the nucleus. In the absence of rapamycin (DMSO control treatment), I observed that endogenous Sts1 was rapidly degraded, exhibiting a half-life of ~5 minutes. Rapamycin treatment dramatically stabilized Sts1 levels when proteasomes were anchored at the plasma membrane or ribosome, implying that Sts1 cannot be degraded in the cytoplasm (Figure 5.5B). When proteasomes were anchored to histones, Sts1 degradation continued, albeit not quite to the extent of the “no anchor” control condition. It is possible that tethering proteasomes to histones and chromatin may slightly constrain proteasome function or reduce the rate at which they encounter free Sts1. By radioactive pulse-chase analysis and immunoprecipitation of endogenous Sts1 under the Anchor Away tethering conditions, the same trends seen by cycloheximide-chase analysis were documented

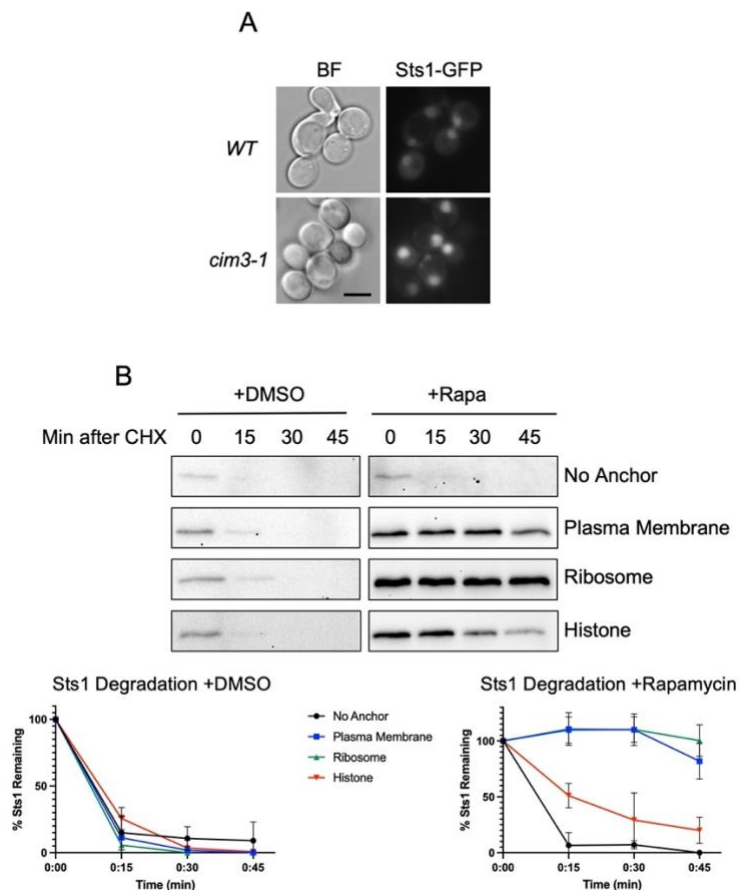


Figure 5.5: Sts1 proteasomal degradation occurs in the nucleus following nuclear import.

(A) Sts1 accumulates in the cell nucleus when proteasomes are catalytically inactive. Catalytically inactive proteasome mutant *cim3-1* yeast expressing the plasmid pRS415-GPD-Sts1-GFP were visualized by fluorescence microscopy at 37°C. Scale bar indicates 5 μ m. (B) Sts1 degradation occurs when proteasomes are sequestered inside the nucleus but not when sequestered to the plasma membrane or ribosome. Using the Anchor Away yeast system, 26S proteasomes are anchored to the plasma membrane, ribosome, or histones. Cycloheximide-chase analysis was performed to determine the degradation rates of Sts1-3xFLAG in the presence (+Rapa) or absence (+DMSO) of proteasome sequestration. Cells were grown at 30°C, treated with rapamycin or DMSO for 2 hrs, and cycloheximide added to block further protein synthesis. FLAG immunoprecipitation was performed on cell extracts collected at each timepoint to enrich for Sts1-3xFLAG, anti-Sts1 used for immunoblotting. Bottom panels: quantification of cycloheximide-chase data in the presence (right) or absence (left) of proteasome sequestration.

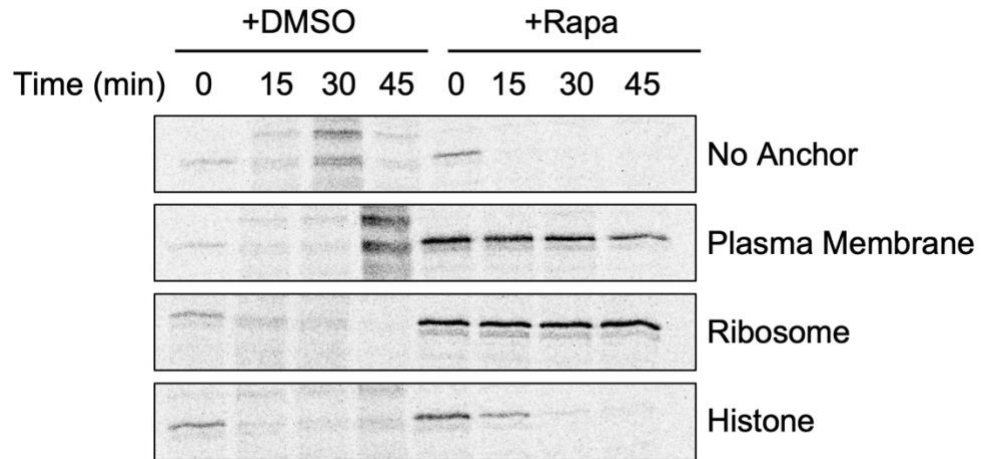


Figure 5.6: Sts1 degradation in the nucleus but not the cytoplasm is observed by radioactive pulse-chase.

Yeast cells were grown and treated with either DMSO or rapamycin as in Figure 5.5B. Radioactive pulse-chase analysis was performed and anti-Sts1 immunoprecipitation performed on cell extracts collected at each timepoint to enrich radio-labeled Sts1 for phosphorimaging.

(Figure 5.6). We conclude from these results that Sts1 degradation occurs preferentially in the nucleus, potentially only after proteasomes have been delivered there by the Sts1/Srp1/Kap95 complex and after nuclear RanGTP triggers removal of the karyopherins from Sts1.

5.3 Discussion

Proteasomal degradation is one of the primary paths by which eukaryotic cells maintain protein homeostasis. For the vast majority of proteasome substrates, degradation is preceded by the attachment of the small protein ubiquitin to the target protein. (Hochstrasser 1996; Varshavsky 2012). Ubiquitin-mediated binding to the proteasome permits unfolding of the target protein by the ATPase ring in the RP base and subsequent proteolysis within the core particle interior. Substrate ubiquitylation represents an important part of the UPS and the diverse features of proteasome targets that are recognized by the various ubiquitin ligases contribute to the efficiency and regulatory flexibility of this degradation pathway (Gödderz et al., 2011; Xie and Varshavsky, 2001; Ha et al., 2012).

Despite the predominance of ubiquitylation in proteasome-mediated degradation, several target proteins undergo proteasome-mediated degradation in a ubiquitin-independent manner. Such substrates interact with the proteasome directly or via regulatory factors other than the RP and possess significant unstructured domains (Erales and Coffino, 2014; Yu et al., 2016). While the mechanisms of ubiquitin-independent degradation are not generally well understood, it is thought that direct substrate binding to the proteasome allows the substrate's disordered regions to engage the CP to begin degradation, bypassing the need for RP-mediated substrate unfolding (Yu et al., 2016). The prevalence of disordered domains within ubiquitin-independent degradation substrates has also led to the

discovery that ubiquitin-independent degradation can occur via the 26S proteasome or the 20S CP alone. Ubiquitin-independent degradation by the CP may have first occurred in species that lacked a ubiquitin-conjugation system, as in bacteria (Sharp and Li, 1987; Valas and Bourne, 2008). A well-studied example of ubiquitin-independent degradation is the yeast transcription factor Rpn4. Able to undergo both ubiquitin-dependent and ubiquitin-independent degradation, Rpn4 degradation appears to be linked to its ability to interact with the proteasome RP via its unstructured N-terminus (Ju and Xie, 2004; Ju and Xie, 2006). The different means of proteolytic targeting of Rpn4 may be related to its integral role in proteasome gene transcription.

We previously showed that Sts1 has a half-life of only ~5 minutes in yeast and that it binds to the proteasome directly (Budenholzer et al., 2020). We suspected that the proteasome-Sts1 interaction needed for proteasome nuclear import may lead to ubiquitin-independent Sts1 degradation. Indeed, we found that not only is Sts1 a substrate of the 26S proteasome *in vivo*, but it is also a ubiquitin-independent substrate (Figure 5.1). Ubiquitin-independent degradation of Sts1 was confirmed by our *in vitro* assays which indicated that Sts1 proteolysis requires only 26S proteasomes in the presence of ATP. Additionally, we learned that Sts1 proteolysis *in vitro* was blocked when Sts1 was pre-bound to Srp1, and that overexpression of Srp1 *in vivo* was sufficient to stabilize endogenous Sts1 levels (Figure 5.2). These results suggested that Sts1 degradation relies upon the absence of the karyopherin heterodimer from its N-terminus, consistent with previous reports that ubiquitin-independent substrates utilize an accessible disordered domain to initiate their degradation. In the case of Sts1, Srp1 binding to the disordered Sts1 N-terminus may

simultaneously serve to initiate nuclear transport as well as prevent premature Sts1 degradation prior to completion of proteasome nuclear import.

We examined whether Sts1 relies upon the availability of its unstructured N-terminal domain to initiate degradation. Blocking the N-terminus by fusion with bulky protein tags or removing the disordered N-terminus both prevented proteasome-mediated proteolysis of Sts1 *in vitro*, consistent with our analysis of Srp1 interaction (Figure 5.2). Deletion of both the Sts1 unstructured termini was also sufficient to block *in vitro* proteasome-mediated degradation. These experiments suggest that Sts1 ubiquitin-independent degradation is initiated by access to its free N-terminal domain. This analysis raises the question of how Sts1 degradation can be initiated *in vitro* despite our results in Chapter 3 suggesting that full-length Sts1 cannot bind to the proteasome in the absence of Srp1. A possible explanation for this apparent inconsistency could be that the disordered N-terminal domain of Sts1 initially blocks proteasome binding by the Sts1 six-helix bundle unless Srp1 is bound to the bipartite NLS. Once the six-helix bundle-proteasome interaction has formed, the free N-terminal domain, after karyopherin displacement by RanGTP in the nucleus, can serve as a proteolysis initiator with the proteasome to which it is bound.

The ability of Srp1 to obstruct Sts1 degradation raises the question about the temporal nature of the NLS interaction. If proteolysis depends upon the removal of Srp1 from the Sts1 N-terminus, we speculated that the dependence upon RanGTP to mediate this disassembly might similarly impact Sts1 degradation. Our *in vitro* analysis of the purified Sts1/Srp1/Kap95 complex showed that Sts1 is stable for several hours until the addition of RanGTP disrupts this assembly (Figure 5.3A). As RanGTP represents the

nuclear form of Ran, we speculated that Sts1 degradation might be linked to the completion of proteasome nuclear import and thus specifically occurs in the cell nucleus. To examine this possibility, we utilized the Anchor Away system and conducted cycloheximide-chase analysis of Sts1 levels when proteasomes were concentrated in different cellular compartments. We observed that Sts1 degradation is stabilized when proteasomes are excluded from the nucleus, suggesting that Sts1 degradation follows the RanGTP-mediated dissociation of Kap95 and Srp1 from the Sts1 NLS (Figure 5.5B).

Taken together, our results suggest a model of Sts1-mediated nuclear import and degradation that is inextricably linked to the nuclear import machinery. In proliferating cells, karyopherin- α recognizes the Sts1 bipartite NLS in the cytoplasm and recruits karyopherin- β . This may trigger a conformational change in Sts1 that allows for binding to the 26S proteasome for karyopherin-mediated nuclear import. Once inside the nucleus, binding of RanGTP to karyopherin- β is sufficient to disrupt the import complex, ultimately freeing the Sts1 N-terminus and allowing it to initiate ubiquitin-independent proteasomal degradation *in cis*. A fuller discussion of this model and descriptive figure will be presented in Chapter 7.

Chapter 6: Structural and functional conservation of Sts1

I performed all experiments presented in this chapter except for those depicted in Figures 6.1B and 6.3B (Gabriel Romero-Ruiz).

6.1 Introduction

STSI is an essential gene in *S. cerevisiae*. Many studies have suggested that the role of Sts1 lies in nuclear localization of the proteasome, and the preservation of this function appears to be important to maintenance of cell health (Tabb et al., 2000; Romero-Perez et al., 2007; Chen et al., 2011). Nuclear localization of proteasomes is evolutionarily conserved as many species exhibit proteasomes concentrated in the nucleus itself or at the nuclear periphery (Pack et al., 2014; Chowdury and Enenkel, 2015; Laporte et al., 2008; Albert et al., 2017). It remains an open question whether facilitated proteasome nuclear transport is mechanistically similar across different eukaryotic species. In particular, the closed mitosis of yeast compared to open mitosis in mammals represents a significant divergence that potentially impacts the respective need for proteasome import in these organisms. However, though species that undergo open mitosis may be able to engulf proteasomes upon nuclear reformation, such organisms likely still require a post-mitotic mechanism of facilitated proteasome import, especially in cell types that do not undergo mitosis or do so infrequently (Wendler and Enenkel, 2019).

Early studies identified Cut8 as a likely ortholog of Sts1 in the fission yeast *Schizosaccharomyces pombe* due to its high sequence similarity to Sts1 (Tatebe and Yanagida, 2000). Just as Sts1 has been implicated in proteasome nuclear import, Cut8 has been identified as a proteasome tethering protein, anchoring the proteasome to the inner

nuclear membrane (Chen et al., 2011; Chen et al., 2014; Takeda and Yanagida, 2005; Takeda et al., 2011). Composed mostly of α -helices and unstructured domains, Cut8 appears to form a homodimer and interacts with membrane cholesterol molecules via a CRAC-like consensus sequence (Takeda and Yangida, 2011; Expand, 2006). The unstructured N-terminal region of Cut8 contains several lysine residues that have been characterized as ubiquitylation sites resulting from the action of the ubiquitin-conjugating enzyme Rhp6 (*S. cerevisiae* Rad6/Ubc2) and the ubiquitin ligases Ubr1 and Rhp18 (Rad18 in *S. cerevisiae*); this N-terminal poly-ubiquitin chain mediates Cut8 interaction with the proteasome, securing it to the nuclear membrane (Takeda and Yanagida, 2005). Despite evidence associating Cut8 with proteasome nuclear accumulation, no studies have suggested that Cut8 participates in an import mechanism, as does Sts1, despite structure predictions of Sts1 indicating a conserved fold architecture (Jumper et al., 2021; Varadi et al., 2022).

Though Cut8 represents a close structural homolog of Sts1, no mammalian factor has been identified that belongs to the Cut8 superfamily. However, the mammalian protein AKIRIN2 was recently identified as a proteasome nuclear import factor with considerable mechanistic similarities to those we have proposed for Sts1. Cryo-electron microscopy experiments indicated that AKIRIN2 forms a homodimer and is likely a largely α -helical protein; additionally, AKIRIN2 contains a putative bipartite nuclear localization signal. As we have observed with Sts1, AKIRIN2 simultaneously binds to the mammalian karyopherin- α protein IPO9 and to the proteasome (de Almeida et al., 2021). Although AKIRIN2 can recruit the fully assembled 26S proteasome, at least in its singly capped form, structural studies indicate that it specifically binds to the CP via a conserved C-

terminal motif. This binding overlaps with the CP interface that interacts with the RP, unlike Cut8 which appears to bind the proteasome RP through a poly-ubiquitin chain. Importantly, AKIRIN2 is degraded by the proteasome, a process that is potentially linked to its nuclear transport function, as is the case for Sts1 and Cut8 (de Almeida et al., 2021; Takeda and Yanagida, 2005). The de Almeida et al. study demonstrates that AKIRIN2 represents a transport factor specifically for fully assembled proteasomes that has not previously been identified in vertebrates. Its mechanism of mediating proteasome import has strong analogies to that of Sts1, despite the structural and evolutionary dissimilarities.

The many structural and functional overlaps that exist between Sts1, Cut8, and AKIRIN2 prompted us to study the conservation of proteasome import factors in different species and specifically how these factors might relate to one another. Here, we show that expression of neither Cut8 nor AKIRIN2 was sufficient to rescue loss of *STSI* function in *S. cerevisiae* under the conditions tested. Though Cut8 is chiefly regarded as a proteasome nuclear tethering factor, I show that it is capable of binding to karyopherin- α proteins *in vitro*, including those from *S. pombe* and *S. cerevisiae*, possibly suggesting a more complex mechanism for Cut8 action than had previously been identified. Interestingly, Cut8-like and AKIRIN2-like proteins have been identified in various species, and sometimes co-exist in the same species (our observations). Ultimately, our results indicate that disparate factors have evolved across eukaryotes to achieve the same pivotal goal of proteasome nuclear accumulation.

6.2 Results and Discussion

6.2.1 Cut8 and AKIRIN2 do not complement an *STSI* deletion

The conservation of nuclear proteasomes across eukaryotes suggests that their nuclear localization mechanisms may have conserved features as well. Though Sts1 has long been associated with its fission yeast counterpart Cut8, it is only very recently that a similar pathway for the nuclear transport of proteasomes involving AKIRIN2 was identified in mammalian cells (de Almeida et al., 2021). To assess potential functional relationships between Sts1 and its putative counterparts in other species, we first investigated if Cut8 and AKIRIN2 could complement the deletion of *STS1* in budding yeast. As Sts1 is an essential protein, complementation by Cut8 or AKIRIN2 would be predicted to rescue the growth of *sts1*Δ cells. We expressed each protein sequence from a *MET25* promoter on plasmids that were transformed into *sts1*Δ yeast carrying WT *STS1* on a *URA3* cover plasmid. Growth of cells was then assessed on media containing 5-FOA, which causes the eviction of the cover plasmid. This allowed us to evaluate the ability of each protein to rescue the lethality of *sts1*Δ. At both 30°C and 37°C, no growth of yeast carrying the Cut8 or AKIRIN2 plasmids was observed (Figure 6.1A). This suggested that neither factor is capable of complementing the function of Sts1 *in vivo*, although expression of the respective proteins could not be verified.

In a reciprocal experiment, we expressed Sts1, Cut8, and AKIRIN2 under the control of a thiamine-repressible promoter in *S. pombe* yeast bearing a chromosomal deletion of *cut8*. While Cut8 is not essential in fission yeast, its deletion is lethal at high temperature. In agreement with our *S. cerevisiae* complementation assay, we observed that Sts1 and AKIRIN2 are similarly insufficient to overcome the temperature-sensitive growth defect in *cut8*Δ (Figure 6.1B). Despite their potential similarities, these results suggest that Sts1, Cut8, and AKIRIN2 are not interchangeable.

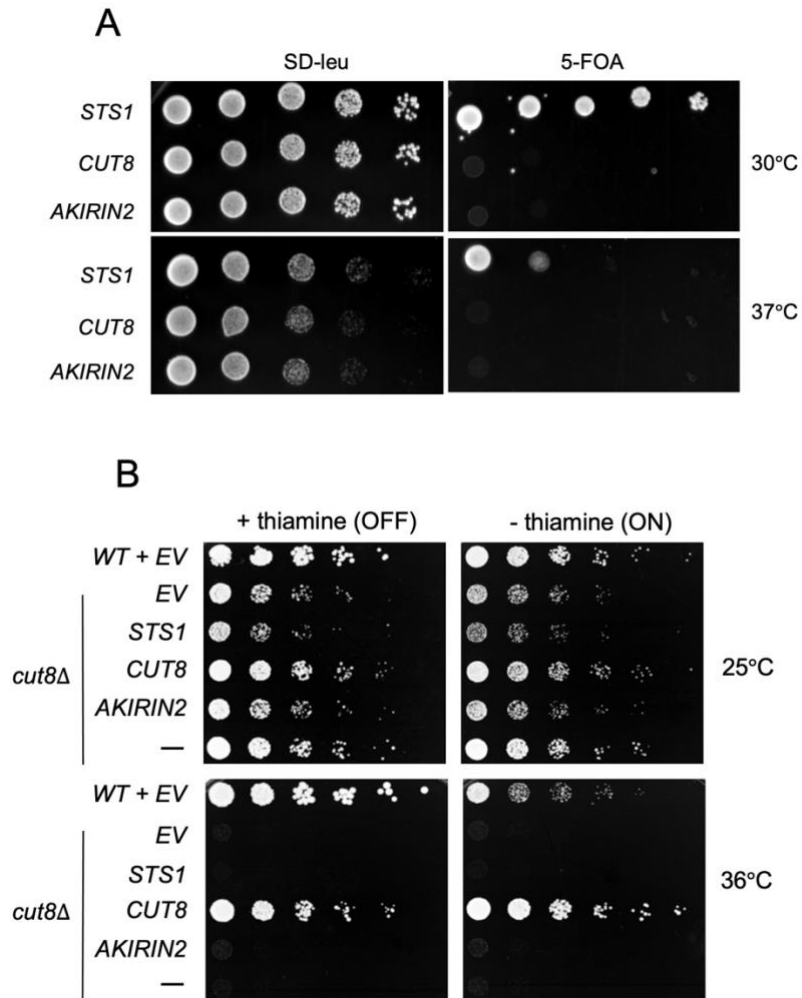


Figure 6.1: Sts1 and its homologs do not complement each other *in vivo*.

(A) Cut8 and AKIRIN2 cannot rescue *sts1*Δ mutation. *S. cerevisiae* yeast (MHY9580) bearing the chromosomal deletion of *sts1* (with a pRS316-*STS1* cover plasmid) was transformed with pRS14MET25-based plasmids with the indicated alleles. Cells were spotted onto 5-FOA media to eject the cover plasmid and assess cell viability in the presence of Sts1 homologs. Cells were grown at the indicated temperatures for three days. (B) Sts1 and AKIRIN2 cannot rescue the temperature-sensitive *cut8*Δ mutation. *S. pombe* bearing the chromosomal deletion of *cut8* was transformed with thiamine-repressible plasmids (pREP41-based) with the indicated alleles. Cells were spotted onto media lacking thiamine to induce protein expression and assess cell viability in the presence of Cut8 homologs. Cells were grown at the indicated temperatures for three days. “EV” indicates empty vector control.

To explore other potential similarities between Sts1 and Cut8, I expressed them as GFP fusion proteins under the control of the *MET25* promoter on plasmids in *S. cerevisiae*. At both 30°C and 37°C, I observed that Cut8-GFP was significantly overexpressed compared to Sts1-GFP, suggestive of increased stability or expression (Figure 6.2). To understand whether this expression impacts proteasome localization, I visualized these proteins *in vivo* by fluorescence microscopy in yeast expressing chromosomally tagged Rpn2-mCherry. These experiments were performed in yeast deleted for the *STS1* gene and bearing a WT *STS1* cover plasmid. Cut8-GFP mainly localized to the cytoplasm with a second population appearing to localize to the nucleus, in contrast to Sts1-GFP which is strongly nuclear. Interestingly, Rpn2-mCherry appeared primarily nuclear in cells expressing Cut8-GFP, though there was a statistically significant reduction in the N/C ratio versus Sts1-GFP expression, particularly at 37°C (Figure 6.3A). It is likely that nuclear accumulation is the result of the presence of WT Sts1, but these data suggest that high levels of Cut8 may interfere with host proteasome nuclear import. In a reciprocal experiment, we also expressed Sts1, Cut8, and AKIRIN2 in *cut8Δ* yeast and observed the impact on chromosomally expressed Rpn11-GFP. Neither Sts1 nor AKIRIN2 expression reversed the severe defect in proteasome nuclear accumulation, with localization of Rpn11-GFP being similar to *cut8Δ* alone (Figure 6.3B). In the case of Sts1, it is unlikely that Sts1 undergoes ubiquitylation in *S. pombe* and may simply be unable to bind the proteasome in this species. Taken together, these results suggest that Sts1 and Cut8 likely cannot accomplish their respective functions in the reciprocal species.

Cut8 undergoes ubiquitylation via the E3 ligase Ubr1, and this ubiquitylation is likely responsible for its interaction with the proteasome RP during 26S proteasome

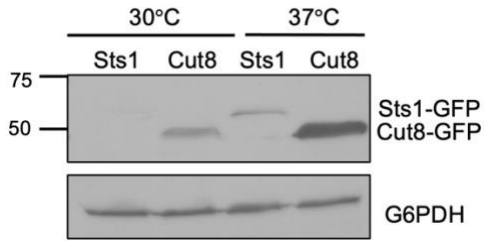


Figure 6.2: Cut8 is more stable compared to Sts1 in *S. cerevisiae*.

Cell extracts from *sts1Δ* yeast transformed with the pRS415MET25-based plasmids expressing Sts1 and Cut8 as GFP fusion proteins (in the presence of WT *STS1* cover plasmid) were separated by SDS-PAGE and immunoblotted with anti-GFP (top) and anti-G6PDH antibodies.

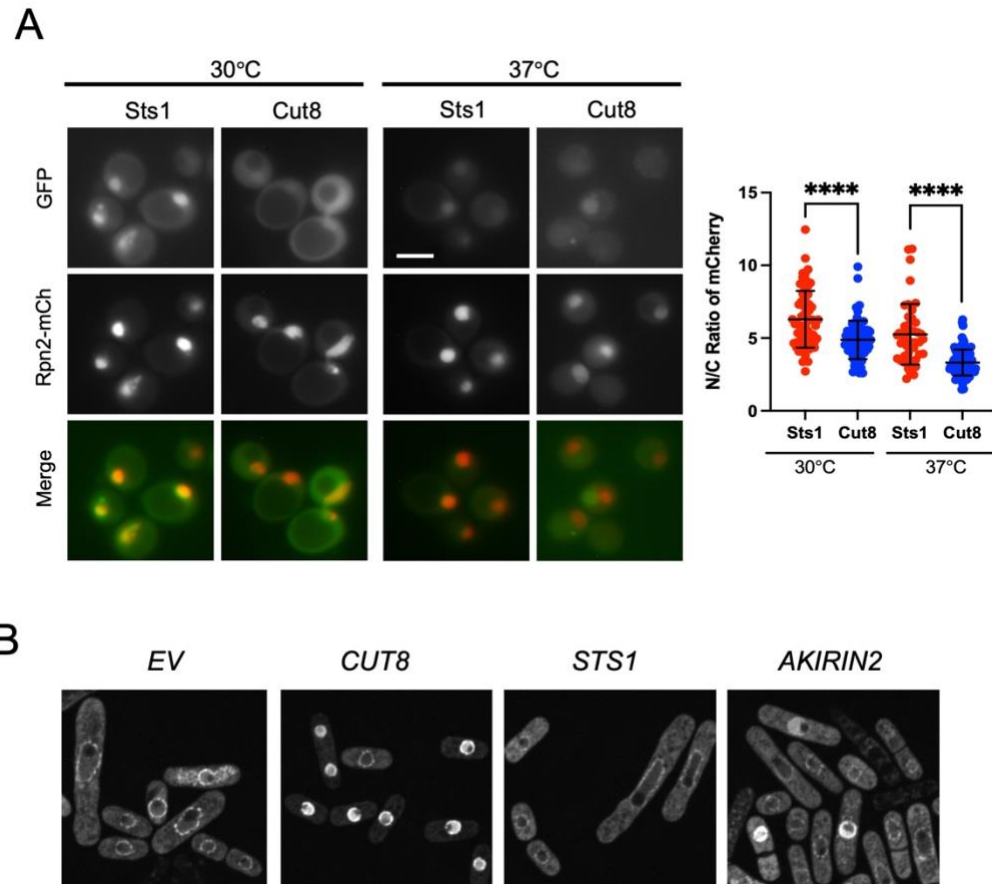


Figure 6.3: Sts1 and Cut8 are unable to achieve proteasome nuclear accumulation in their reciprocal species.

(A) Cut8 expression in *S. cerevisiae* results in a reduction in nuclear proteasomes. *S. cerevisiae* deleted for *sts1* (in the presence of a WT *STS1* cover plasmid) and chromosomally expressing Rpn2-mCherry were transformed with plasmids expressing Sts1 or Cut8 as GFP fusion proteins. Transformants were grown to mid-exponential phase at 30°C prior to fluorescence imaging, and a population were shifted to 37°C for two hours. A t-test was used to determine statistical significance of differences in localization (**** $p < 0.0001$). Three replicates of at least 100 cells were counted. Scale bar: 5 μ m. (B) Proteasomes do not accumulate in the nucleus of *S. pombe* during Sts1 or AKIRIN2 expression. *S. pombe* bearing *cut8* Δ were transformed with pREP41-based plasmids expressing the indicated alleles. Cells grown at 25°C prior to fluorescence imaging (Rpn11-GFP).

tethering to the inner nuclear membrane (INM); this modification appears responsible for rapid proteasome-dependent turnover of Cut8 as well (Takeda and Yanagida, 2005; Takeda et al., 2011). We investigated whether Cut8 is also a ubiquitin-dependent proteasome substrate in *S. cerevisiae* or if its structural and mechanistic similarity to Sts1 instead leads to ubiquitin-independent targeting. I expressed Cut8 as a GFP fusion protein under the control of the *MET25* promoter in *S. cerevisiae* bearing the temperature-sensitive *cim3-1* allele which blocks proteasome activity at nonpermissive temperatures (Ghislain et al., 1993). Cut8 was strongly stabilized in *cim3-1* cells, suggesting that Cut8 is a proteasome substrate in budding yeast (Figure 6.4A). Additionally, to test for ubiquitin-dependent degradation, I similarly expressed Cut8-GFP in yeast impaired for ubiquitin-activation (*uba1-204*). I observed that Cut8-GFP was stabilized in this mutant compared to WT yeast, suggesting that Cut8 is still ubiquitylated when expressed heterologously in *S. cerevisiae* (Figure 6.4B). We did not test whether Ubr1 is the relevant E3 ligase in *S. cerevisiae* Cut8 ubiquitylation. Together, these results suggest that Cut8 and Sts1, while predicted to be highly structurally similar, may function differently or may simply not interact properly with the evolutionarily distinct host import or proteasome machinery.

6.2.2 Cut8 can bind to karyopherin- α proteins

Sts1 specifically binds to karyopherin- α through an NLS-dependent interaction of its unstructured N-terminal domain. As discussed in Chapter 3, the preservation of the Sts1 NLS appears pivotal to the proper nuclear localization of the proteasome and cell survival. Similarly, the sister factor AKIRIN2 in mammalian cells associates with the import receptor IPO9 for proteasome transport, likely via a bipartite nuclear localization signal (de

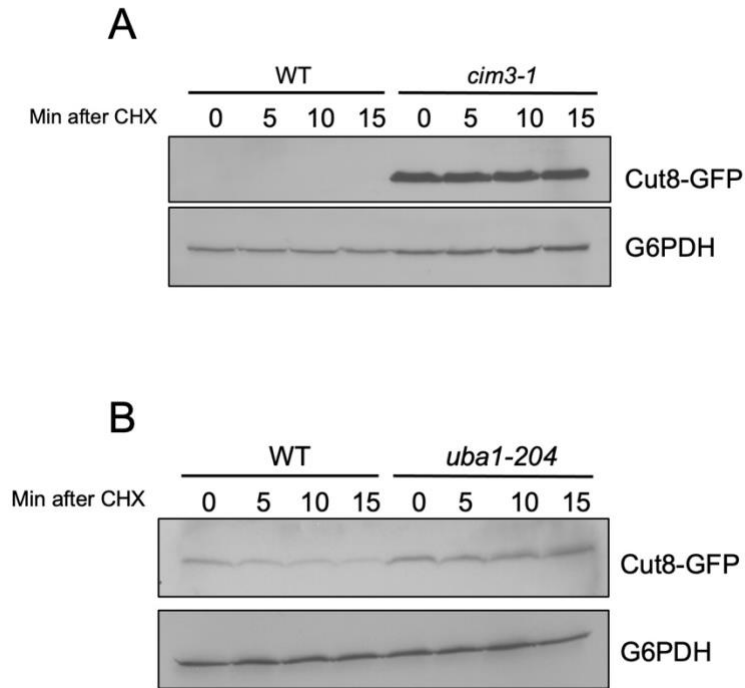


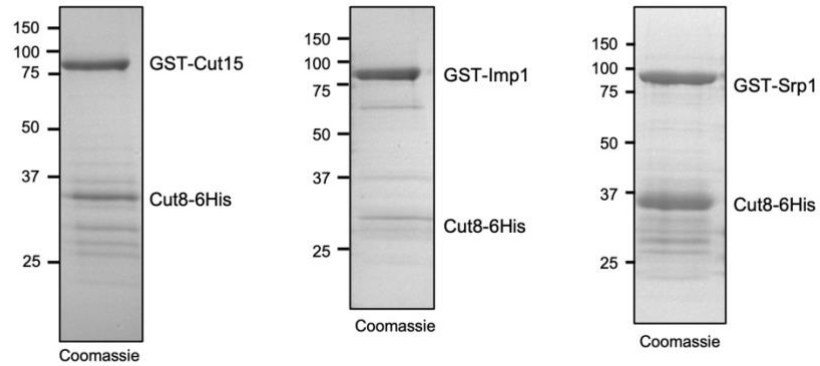
Figure 6.4: Cut8 is degraded in a ubiquitin-dependent manner in *S. cerevisiae*.

(A) Cut8 is a proteasome substrate in *S. cerevisiae*. Cycloheximide-chase analysis in yeast bearing the temperature-sensitive RP *cim3-1* mutation that were transformed with pRS415MET25-Cut8-GFP. (B) Cut8 is degraded in a ubiquitin-dependent manner in *S. cerevisiae*. Cycloheximide-chase analysis performed in yeast bearing the temperature-sensitive *uba1-204* mutation and transformed with pRS415MET25-Cut8-GFP. For (A) and (B), cells were grown at 37°C for the duration of the time-course and cell extracts from each timepoint were separated by SDS-PAGE. Cut8 levels were analyzed by anti-GFP immunoblotting (anti-G6PDH loading control).

Almeida et al., 2021). Structural analysis of Cut8 indicated that it also includes an unstructured N-terminal domain; the Cut8 N-terminus contains a lysine-rich region that has been identified as its primary ubiquitylation site, which must be ubiquitylated for its interaction with the proteasome and for proteasomal nuclear envelope anchoring (Takeda et al., 2011; Takeda and Yanagida, 2005). Importantly, the sequence of this lysine-rich ubiquitylation site (KKRK) resembles the patches of basic amino acids that are characteristic of nuclear localization signals. While no evidence has yet linked Cut8 to nuclear transport in fission yeast, its role as an INM tether and the presence of a putative NLS led us to examine whether Cut8 is able to interact with karyopherin- α proteins, as Sts1 does.

There are two paralogous karyopherin- α proteins in *S. pombe* fission yeast, Imp1 and Cut15, compared to a single factor in budding yeast, Srp1 (Umeda et al., 2005). While both Imp1 and Cut15 are classified as importin- α 1 proteins, they have been associated with distinct functions in cell cycle progression and may participate in the nuclear transport of both separate and overlapping pools of NLS-containing target proteins (Umeda et al., 2005). Our work has previously shown that co-purification of Sts1 and Srp1 from bacterial extracts was sufficient to discern binding *in vitro*, and we thus began by examining Cut8 interaction with its native karyopherin- α proteins. We expressed recombinant Cut8-6His in the presence of GST-Cut15 or GST-Imp1 in bacteria and co-purified the complexes using the GST tag on each karyopherin protein (Figure 6.5A). Cut8 was able to bind both Cut15 and Imp1 *in vitro*. Co-purification of Cut8-6His and GST-Srp1 showed substantial interaction as well (Figure 6.5A). These data suggest that Cut8, presumably via its N-terminal KKRK sequence, can be recognized by karyopherin- α proteins *in vitro*.

A



B

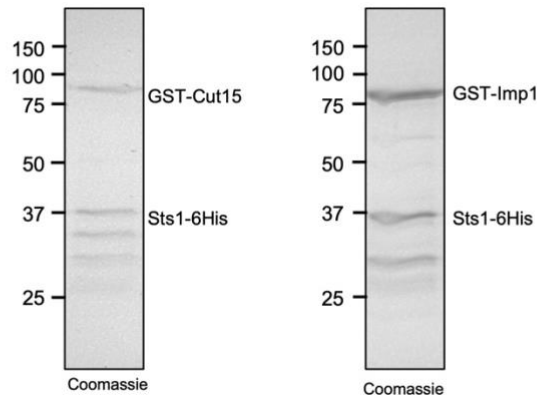


Figure 6.5: Cut8 can bind to karyopherin- α proteins.

(A) Cut8 binds to karyopherin- α proteins. The indicated recombinant species were co-purified from *E. coli* using GST-binding glutathione resin. Bound proteins were analyzed by SDS-PAGE and Coomassie staining.

(B) Sts1 can bind to Cut15 and Imp1, karyopherin- α proteins from *S. pombe*. The indicated recombinant species were co-purified from *E. coli* using GST-binding glutathione resin. Bound proteins were analyzed by SDS-PAGE and Coomassie staining.

Similar experiments with Sts1-6His co-expressed with recombinant GST-Cut15 or GST-Imp1 also demonstrated that both karyopherin- α proteins could bind Sts1 *in vitro* (Figure 6.5B).

It is important to note that Cut8 has not been identified as a participant in nuclear import, nor has its N-terminal sequence been formally characterized as an NLS. It is possible that *in vitro* binding with karyopherin- α proteins occurs in the absence of Cut8 ubiquitylation. However, our results indicate that Cut8 may associate with karyopherin- α proteins in *S. pombe* and this may be connected to its role in proteasome nuclear accumulation.

6.2.3 Conservation of proteasome nuclear import adaptors

I also conducted *in silico* studies of Sts1, Cut8, and AKIRIN2. Various database searches have shown that Cut8 and proteins possessing a similar fold and domain architecture (such as Sts1) are found in many eukaryotic lineages; based on this broad conservation, Cut8/Sts1 is believed to have been present in the last eukaryotic common ancestor (Takeda et al., 2011; Keeling et al., 2005; Koonin 2010; Budenholzer et al., 2020). Studies of sequence homology to Sts1 have identified potential homologs in a wide range of organisms including lancelets, flies, and bony fishes; the latter finding indicates the presence of Sts1/Cut8 in vertebrates, but the gene sequence was lost in early tetrapods (Budenholzer et al., 2020). Mammalian cells utilize a nonhomologous AKIRIN2-based karyopherin-mediated transport mechanism, a mechanism that appears to be similar in many ways to that observed for Sts1 (de Almeida et al., 2021).

It is noteworthy that genomic sequence searches reveal that some species possess both Cut8/Sts1-like and AKIRIN2-like proteins. A notable example comes from the fruit fly *Drosophila melanogaster*, though it is not clear that both proteins function in nuclear transport of proteasomes. The *D. melanogaster* Cut8-like uncharacterized protein CG5199 is localized to the nuclear periphery *in vivo* and is required for the accumulation of proteasomes at the nuclear periphery, as is true for Cut8 (Takeda and Yanagida, 2005). However, the fruit fly protein akirin has yet to be directly linked to proteasome nuclear localization. Akirin has been implicated in embryogenesis and has specifically been characterized as an adaptor or bridging factor in a variety of protein complexes, approximating the function observed for Sts1 and AKIRIN2 (Nowak et al., 2012). In mammalian cells, AKIRIN2 binds to the karyopherin protein IPO9 for proteasome nuclear transport; the IPO9 homolog in *Drosophila* has also been implicated in proteasome nuclear import, suggesting that this nuclear transport function of mammalian AKIRIN2 may be conserved in the akirin protein of flies (Palacios et al., 2021). While it is not yet clear why both classes of proteasome transport factors might be necessary to insects like *Drosophila*, the conservation of these protein classes indicates the important role of proteasome adaptor proteins for physiological function in a very broad range of eukaryotes.

Chapter 7: Conclusions and Outlook

7.1 Conclusions

The ubiquitin-proteasome system is a well-characterized cellular pathway that is responsible for mediating the degradation of unfolded and unneeded proteins in cells (Varshavsky, 2012). This pathway is conserved across eukaryotes and represents a pivotal process for the maintenance of cell health. Nevertheless, many unanswered questions about the UPS remain; in particular, this study has centered upon understanding the necessity and mechanism of proteasome nuclear accumulation. Proteasomes localize to the nucleus in various species and are likely responsible for clearance of the high volume of degradation targets in this compartment (Wójcik et al., 2003; Laporte et al., 2008; Pack et al., 2014). However, the fully assembled 26S proteasome is a massive protein complex that would not be able to passively diffuse through the nuclear pore complex unassisted, and the mechanism by which it enters the nucleus has remained elusive (Förster et al., 2013). The results presented here identify the small essential yeast protein Sts1 as a proteasome nuclear import adaptor protein that operates in a karyopherin-dependent manner.

Though an essential protein in *S. cerevisiae*, the structure of Sts1 has not been solved; our analysis has demonstrated that Sts1 likely possesses several distinct functional domains that each contribute to its unique cellular function. We have shown that the N-terminus of Sts1 contains a non-canonical bipartite nuclear localization signal that is sufficient for interaction with the budding yeast karyopherin- α protein Srp1. This connection to the karyopherin proteins has been noted in the literature, but our study has identified that this is entirely NLS-dependent (Tabb et al., 2000). Additionally, like its fission yeast counterpart, Sts1 likely homodimerizes via a central three-helix domain.

Dimerization ensures the recruitment of two Srp1 monomers, possibly to mediate nuclear entry of such a large cargo as a single proteasome more efficiently. Recruitment of the proteasome occurs in the Sts1 six-helix bundle domain, though this interaction appears to be blocked in the full-length Sts1 protein if Srp1 has not pre-bound.

We have also shown that Sts1 mediates proteasome nuclear import in a classical karyopherin-mediated pathway. Sts1 can form a ternary complex with Srp1 and the karyopherin- β protein Kap95, consistent with NLS-cargo nuclear import. Additionally, this complex is selectively disrupted by RanGTP, the nuclear form of the small GTPase. The inability of RanGDP to disassemble the Sts1/Srp1/Kap95 complex *in vitro* indicates that this complex is likely stable in the cytoplasm and is disrupted only in the nucleus once proteasome nuclear transport has been completed. Interestingly, Sts1-mediated import appears to be specific to fully assembled 26S proteasomes, though other subcomplexes are reportedly able to enter the nucleus independently of the full complex (Isono et al., 2007). This confirms the previous notion in the field that Sts1 acts as an “NLS-donor” for the proteasome lid which does not contain a recognizable NLS sequence. Additionally, Sts1 import can occur without any cargo bound, suggesting that the assembly of the karyopherin- α/β ternary complex occurs prior to proteasome recruitment. It is possible that Sts1 only transports proteasomes that it stochastically interacts with, rather than occurring in a regulated or directed pathway, though regulators of Sts1 have not yet been identified.

Perhaps most importantly, this study has shown that Sts1 ubiquitin-independent degradation is directly related to the successful completion of proteasome nuclear import. As a ubiquitin-independent degradation substrate, Sts1 directly binds to the proteasome and is able to initiate its proteolysis via its disordered N-terminal domain, consistent with

previous reports of intrinsically disordered ubiquitin-independent degradation substrates (Erales and Coffino, 2014; Yu et al., 2016). Degradation is blocked by the presence of the karyopherin- α/β heterodimer bound to the Sts1 NLS, thereby preventing premature Sts1 proteolysis in the cytoplasm or before nuclear import has concluded. The high concentration of RanGTP in the nucleus is sufficient to remove the karyopherin proteins, freeing Sts1 for degradation. This suggests that Sts1 does not participate in repeated rounds of transport and likely mediates proteasome nuclear import in a unidirectional mechanism, similar to the behavior observed for AKIRIN2 (de Almeida et al., 2021). Though not yet tested, it is possible that Cse1 (the yeast Exportin-2) and the nucleoporin protein Nup2 may similarly have a role in disassembly of the transport complex. Importantly, our study has shown that some aspects of Sts1 facilitated transport may be conserved in other species, though distinct pathways for proteasome nuclear import appear to have evolved between yeast and higher eukaryotes. A summary of these findings and our model for Sts1-mediated karyopherin-dependent proteasome nuclear import are depicted in Figure 7.1.

7.2 Future Studies

This study has sought to understand the mechanism by which proteasomes are actively transported through the nuclear pore complex for accumulation in the nucleus. We have demonstrated that the essential protein Sts1 facilitates this import in concert with the karyopherin- α/β heterodimer in a one-way mechanism that terminates with its RanGTP-dependent ubiquitin-independent proteasomal degradation. However, many questions remain surrounding how this import mechanism takes place and is regulated, as well as whether this nuclear import mechanism is the only cellular function for Sts1. Though

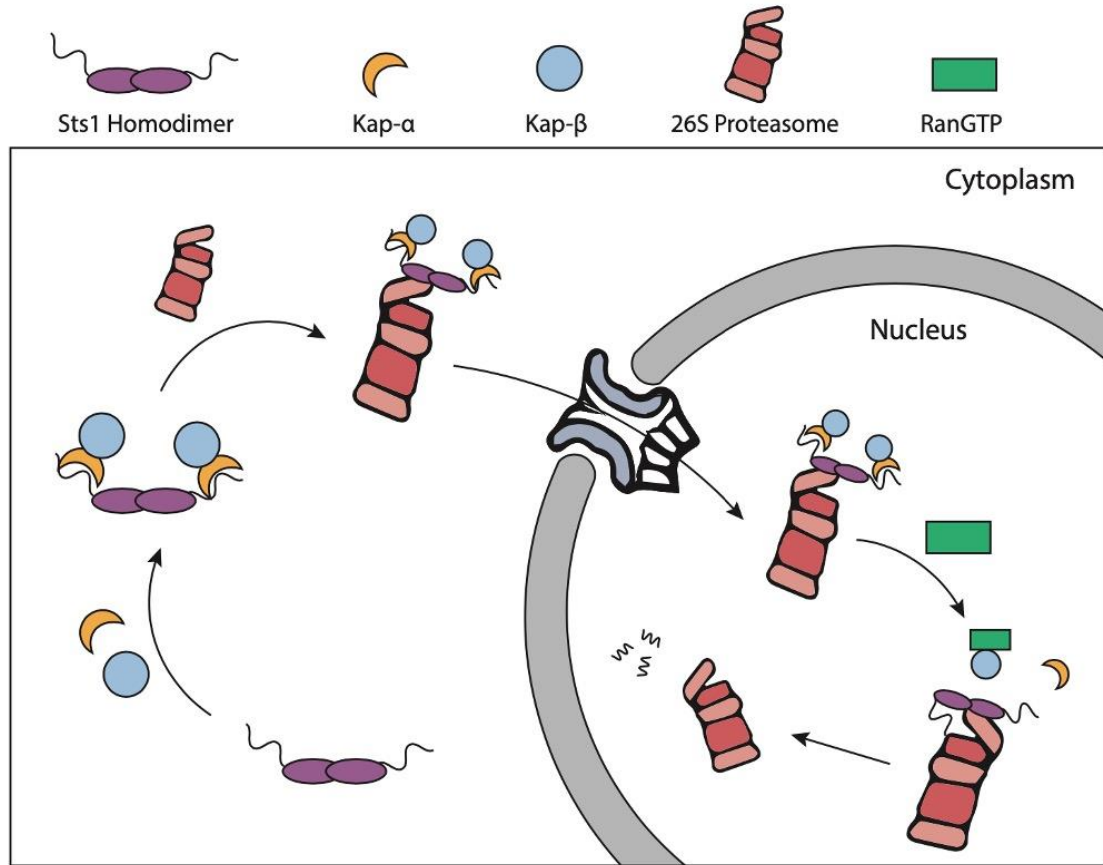


Figure 7.1: Model of Sts1 and karyopherin- α/β mediated nuclear import of 26S proteasomes and subsequent Sts1 ubiquitin-independent degradation in the nucleus.

In the cytoplasm, Sts1, likely a homodimer, binds to karyopherin- α via interaction with the bipartite NLS sequence at the Sts1 N-terminus. Karyopherin- α recruits karyopherin- β and Sts1 subsequently binds to the 26S proteasome. This complex is imported into the nucleus via the nuclear pore complex. In the nucleus, RanGTP is sufficient to promote removal of the karyopherin proteins from the Sts1 N-terminus. Once available, the unstructured Sts1 N-terminus is taken up by the proteasome RP and translocated into the CP to initiate ubiquitin-independent degradation of Sts1. This system occurs in a one-way mechanism and only during proliferative yeast growth.

mutations to the Sts1 NLS appear to have a significant impact on proteasome accumulation, merely alleviating this localization defect by appending the SV40 NLS to the proteasome lid is not sufficient to fully overcome the yeast growth defects (Budenholzer et al., 2020). This implies that Sts1 may be more than simply a nuclear import factor, possibly sensing proteolytic load or interacting with other pathways.

A central finding of this study is that Sts1 degradation likely proceeds immediately following nuclear entry and removal of the karyopherin heterodimer from the Sts1 NLS by RanGTP. This degradation appears opportunistic given Sts1 interaction with the proteasome and the availability of the Sts1 disordered N-terminus. However, we have not been able to determine whether a population of Sts1 is able to shuttle back to the cytoplasm via exportin proteins, as do the karyopherins (Kobe, 1999; Matsuura and Stewart, 2004; Nachury and Weis, 1999). We believe that Sts1 forms a homodimer that is integral to facilitating nuclear import, but it is not yet known whether one or both Sts1 monomers make contact with the proteasome. It is possible that a single Sts1 monomer binds to the proteasome and is proteolyzed following karyopherin dissociation while the second Sts1 monomer is detached and deposited in the nucleoplasm for recycling. Yeast studies to assess nuclear shuttling require the formation of yeast heterokaryons, a process that can take several hours (Dilworth et al., 2001; Feng and Hopper, 2002; Belanger et al., 2009). In our hands, Sts1 turnover is too rapid and has been incompatible with this analysis, though its observed nuclear-specific proteolysis would weigh against repeated rounds of import. However, a contribution of the exportin protein Cse1 to the Sts1/karyopherin complex may imply the possible export of a population of Sts1, and we have not yet been able to rule out this possibility (Hirano et al., 2017).

Despite the identified associations between Sts1, the karyopherin heterodimer, and the 26S proteasome, it is not yet known how Sts1-mediated import is initiated or regulated. Our results suggest that Sts1 binds to the karyopherin proteins prior to the proteasome as GST-Sts1 *in vitro* is insufficient for proteasome binding unless Srp1 is prebound. Additionally, Sts1 can accumulate in the cell nucleus even when proteasomes are excluded from the nucleus, as evidenced by our *in vivo* Anchor Away analysis. It is possible that Sts1 acts as a regulator of proteasome populations in the cell. Sts1 or an associated factor may be responsible for sensing the proteolytic load in the nucleus or cytoplasm and triggering proteasome import to the nucleus to address increased substrate volume. Though no such factor has yet been discovered, our truncation analysis showed that the Sts1 C-terminal tail does not affect cell growth yet leads to mislocalization of proteasomes to the cytoplasm compared to wild-type cells. It is possible that the C-terminal tail is responsible for gating proteasome interaction in response to cellular conditions or the contribution of an unknown factor. The deletion of the C-terminal tail may cause non-specific interactions between Sts1 and the proteasome, particularly in the cytoplasm, but the nuclear import function of Sts1 is otherwise unaffected; this may allow for a sufficient population of proteasomes to still enter the nucleus and support homeostasis, despite the localization defect *in vivo*. It remains to be seen how the C-terminal tail contributes to proteasome nuclear import, and what conditions may trigger Sts1-mediated import.

Our results have shown that Sts1 does not contribute to the rapid reimport of proteasomes from proteasome storage granules following exit from quiescence. We have shown that Sts1 is not expressed under glucose starvation conditions, nor is it expressed for several hours following glucose recovery and proteasome import. This is most likely

explained by the relatively inefficient mechanism of Sts1-mediated import—unidirectional import followed by Sts1 degradation. With such a large volume of proteasomes to be imported, the cell may favor a more efficient import mechanism rather than expending energy for repeated translation and degradation of Sts1. However, most proteasomes are typically reimported from PSGs within ~10 min, and we did not observe recovery of Sts1 levels for several hours following glucose recovery (Peters et al., 2006; Laporte et al., 2008; Li and Hochstrasser, 2021). It is not clear why Sts1-based import would be disfavored for so long after cells have returned to exponential growth. What conditions or transcription factors that are responsible for triggering a switch back to the Sts1 import mechanism also remain unknown, and it is possible that there are unidentified factors involved in or regulating this mechanism.

The outstanding questions surrounding Sts1-mediated nuclear import imply the contribution of outside factors, most intriguingly the possibility of regulatory factors. This also leaves open the possibility of Sts1 involvement in other cellular pathways. Previous scholarship has implicated Sts1 in a variety of roles outside of proteasome localization, particularly in association with the ribosome. Sts1 dysfunction has been associated with cell division defects as well as ribosome dysfunction, and one study has linked Sts1 to co-translational degradation (Houman and Holm, 1994; Romero-Perez et al., 2007; Ha et al., 2014). Additionally, in a sequence homology search for Cut8-like proteins, several proteins that incorporate a Cut8-like fold also contain RNA recognition motifs (RRMs) and Rad52/Rad22-like domains, possibly indicating associated roles for Sts1 (our observations). However, it is not clear if these defects are simply downstream effects of proteasome dysfunction or represent additional functions of Sts1 with or without the

proteasome. It would therefore be useful to perform a whole-lysate pull-down in search of Sts1 interaction partners, possibly including chemical cross-linking if Sts1 interactions are transient and in the presence of a proteasome inhibitor to block Sts1 degradation. The identification of new interaction partners for Sts1 will help to understand the impact that Sts1 has on cell health, and whether its essential function is limited to proteasome nuclear import.

To understand the essential role of Sts1, we have also investigated its structural and functional homologs in other species. A central question that we have not yet sufficiently answered is the extent of the differences between these various factors. Though we have shown that they are not interchangeable *in vivo*, our analysis has raised new questions about the overlap between Sts1 and its *S. pombe* homolog Cut8. Cut8 has consistently been treated as a nuclear membrane tethering protein for the proteasome without any contribution to prior import of the proteasome. However, we have demonstrated that Cut8 can bind to the karyopherin- α proteins Imp1 and Cut15 *in vitro*. This may be opportunistic binding due to a coincidental lysine-rich ubiquitylation site on Cut8, but it is possible that Cut8 participates in nuclear import before anchoring the proteasome to the inner nuclear membrane. Studies into the relationship between Cut8 and Imp1/Cut15 would be important to a deeper understanding of proteasome import in fission yeast. It is striking that two otherwise highly similar proteins like Sts1 and Cut8 should have such divergent approaches towards the same goal, but it is possible that their cellular behavior is more closely related than we yet realize.

The evolutionary divergence between the Cut8/Sts1-like and AKIRIN2-like lineages of proteasome-associated factors has also raised many interesting questions about

the importance of proteasome nuclear import. The evidence currently available suggests that Sts1 and AKIRIN2 function in remarkably similar mechanisms, yet Sts1-like structural domains do not appear to extend into tetrapods. It is peculiar that these karyopherin-dependent proteasome import proteins should have developed in parallel yet do not share any structural similarity. This may stem from the preference of AKIRIN2 for core particle binding, while Sts1 and Cut8 likely interact with the proteasome regulatory particle (de Almeida et al., 2021; Takeda and Yanagida, 2005). The significance of these different interaction surfaces remains to be seen but may ultimately be suggestive of functional nuance. As discussed previously, it is possible that each of these factors may partake in other processes that have necessitated these structural differences, despite their functional overlap. The possibility of functional divergence may explain why species such as *Drosophila melanogaster* appear to express proteins belonging to either structural class. If Cut8/Sts1-like or AKIRIN2-like factors participate in disparate functions outside of proteasome transport, it is possible that either factor in fruit flies may be specialized in other functions, rather than being functionally redundant for proteasome import.

Finally, much of the work discussed in this study relies upon AI-based predictions of Sts1 structure and the close similarity of Sts1 to Cut8 (Jumper et al., 2021; Varadi et al., 2022). Though Sts1 is predicted to share the Cut8 structure, we cannot know the full extent of Sts1 function without an understanding of its native structure. Structural analysis of Sts1 has presented a challenge as it is unstable in solution without bulky fusion proteins or its binding partners. However, we have shown that the complex of Sts1/Srp1/Kap95 is highly stable and is likely able to interact with the 26S proteasome *in vitro*. Altogether, this complex in the absence of the proteasome should alone be of a sufficient size for structure

work if the interactions occur in a 2:2:2 assembly. Furthermore, the purified Sts1/Srp1/Kap95 complex bound to the proteasome would likely be an ideal target for negative stain microscopy and cryo-electron microscopy. The large size of the karyopherin complex should be distinguishable from the densities of proteasome subunits and make for easier particle-picking compared to unbound-26S particles. Structures of the 26S proteasome, karyopherin- α , and karyopherin- β have been previously published and should be useful in assigning densities to the unknown structure of Sts1 (Luan et al., 2016; Conti et al., 1998; Forwood et al., 2010). Similarly, the predicted structural homology to Cut8 should aid Sts1 reconstruction in this endeavor. Analysis of a structure of Sts1/Srp1/Kap95 in complex with the 26S proteasome would be the most advantageous as it would provide a snapshot of the physiologically relevant transport complex.

This study has uncovered details about the importance of the proteasome nuclear import adaptor protein Sts1 and the contribution of the karyopherin- α/β heterodimer to this process. We have demonstrated that Sts1 import is directly related to its ubiquitin-independent degradation, and that certain aspects of this mechanism may be conserved in other eukaryotic organisms. Though many interesting questions about the regulation of Sts1 transport, the structure of the transport complex, and the relationship with its functional homologs persist, we believe this model represents an important contribution to the ubiquitin-proteasome field.

Appendix 1: Yeast strains used in this study

Strain	Genotype	Source
MHY500	<i>MATa his3-Δ200 leu2-3,112 ura3-52 lys2-801 trp1-1 gal2</i>	(Chen et al., 1993)
MHY690	<i>MATa ade2-1 ura3-1 his3-11 trp1-1 leu2-3,112 can1-100</i> (W303 background)	R. Rothstein
MHY5012	<i>MATalpha ade2-1 ura3-1 his3-11 his3-15 leu2-3,112 can1-100 trp1-1 uba1Δ::kanMX6/pRS313-uba1-204</i>	R. DeShaie
MHY5841	<i>MATa his3-Δ200 leu2-3,112 ura3-52 lys2-801 trp1-1 gal2 RPN11-6xGly-3xFLAG::kanMX6</i>	(Li et al., 2015)
MHY6493	<i>MATa his3-Δ200 leu2-3,112 ura3-52 lys2-801 trp1-1 gal2 RPN5-6xGly-3xFLAG::kanMX6 rpn10Δ::HIS</i>	(Li et al., 2015)
MHY6940	<i>MATa his3-Δ200 leu2-3,112 ura3-52 lys2-801 trp1-1 gal2 RPN2-mCherry::natMX4</i>	R. Tomko, MH lab strain
MHY6952	<i>MATa his3-Δ200 leu2-3,112 ura3-52 lys2-801 trp1-1 gal2 PRE1-6xGly-3xFLAG::kanMX6</i>	(Li et al., 2015)
MHY6966	<i>MATa his3-Δ200 leu2-3,112 ura3-52 lys2-801 trp1-1 gal2 RPN5-GFP(S65T)::HIS3MX6 RPN2-mCherry::natMX4</i>	R. Tomko, MH lab strain
MHY8344	<i>MATalpha ade2-1 ura3-1 his3-11,15 trp1-1 leu2-3,112 can1-100 TOR1-1 fpr1::natMX4 RPN11-FRB-GFP::kanMX6</i> (W303)	(Tsuchiya et al., 2013)
MHY8345	<i>MATa ade2-1 ura3-1 his3-11,15 trp1-1 leu2-3,112 can1-100 TOR1-1 fpr1::natMX4 RPN11-FRB-GFP::kanMX6 PMA1-2xFKBP12::TRP1</i> (W303)	(Tsuchiya et al., 2013)
MHY8346	<i>MATa ade2-1 ura3-1 his3-11,15 trp1-1 leu2-3,112 can1-100 TOR1-1 fpr1::natMX4 RPN11-FRB-GFP::kanMX6 RPL13A-2xFKBP12::TRP1</i> (W303)	(Tsuchiya et al., 2013)

MHY8347	<i>MATa ade2-1 ura3-1 his3-11,15 trp1-1 leu2-3,112 can1-100 TOR1-1 fpr1::natMX4 RPN11-FRB-GFP::kanMX6 HTB2-FKBP12::HIS3 (W303)</i>	(Tsuchiya et al., 2013)
MHY9579	<i>MATalpha his3-Δ200 leu2-3,112 ura3-52 lys2-801 trp1-1 gal2 sts1Δ::hphMX6/pRS316-STS1</i>	(Budenholzer et al., 2020)
MHY9580	<i>MATa his3-Δ200 leu2-3,112 ura3-52 lys2-801 trp1-1 gal2 sts1Δ::hphMX6/pRS316-STS1</i>	(Budenholzer et al., 2020)
MHY9690	<i>MATalpha ade2-1 his3-11,15 leu2-3,112 trp1 ura3-1 can1-100 STS1 (W303)</i>	(Budenholzer et al., 2020)
MHY9691	<i>MATalpha ade2-1 his3-11,15 leu2-3,112 trp1 ura3-1 can1-100 sts1-2 (W303)</i>	(Budenholzer et al., 2020)
MHY9692	<i>MATa ade2-1 his3-11,15 leu2-3,112 trp1 ura3-1 can1-100 STS1 (W303)</i>	(Budenholzer et al., 2020)
MHY9693	<i>MATa ade2-1 his3-11,15 leu2-3,112 trp1 ura3-1 can1-100 sts1-2 (W303)</i>	(Budenholzer et al., 2020)
MHY10019	<i>MATalpha his3-Δ200 leu2-3,112 ura3-52 lys2-801 trp1-1 gal2 atg8Δ::hphMX4</i>	(Li and Hochstrasser, 2022)
MHY10148	<i>MATalpha his3-Δ200 leu2-3,112 ura3-52 lys2-801 trp1-1 gal2 cue5Δ::hphMX4</i>	J. Li, MH lab strain
MHY4464	<i>MATa ura3-52 leu2Δ1 his3-Δ200 trp1Δ63 lys2-801 ade2-101 cim3-1 (YPH500)</i>	Minoru Funakoshi
MHY11357	<i>MATa his3-Δ200 leu2-3,112 ura3-52 lys2-801 trp1-1 RPN2-mCherry::natMX4 sts1Δ::hphMX6/pRS316-STS1</i>	This study
MHY12557	<i>MATa ade2-1 ura3-1 his3-11,15 trp1-1 leu2-3,112 can1-100 TOR1-1 fpr1::natMX4 RPN11-FRB-GFP::kanMX6 STS1-3xFLAG::hphMX4 (W303)</i>	This study
MHY12558	<i>MATa ade2-1 ura3-1 his3-11,15 trp1-1 leu2-3,112 can1-100 TOR1-1 fpr1::natMX4 RPN11-FRB-</i>	This study

	<i>GFP::kanMX6 PMA1-2xFKBP12::TRP1 STS1-3xFLAG::hphMX4 (W303)</i>	
MHY12559	<i>MATa ade2-1 ura3-1 his3-11,15 trp1-1 leu2-3,112 can1-100 TOR1-1 fpr1::natMX4 RPN11-FRB-GFP::kanMX6 RPL13A-2xFKBP12::TRP1 STS1-3xFLAG::hphMX4 (W303)</i>	This study
MHY12660	<i>MATa ade2-1 ura3-1 his3-11,15 trp1-1 leu2-3,112 can1-100 TOR1-1 fpr1::natMX4 RPN11-FRB-GFP::kanMX6 HTB2-FKBP12::HIS3 STS1-3xFLAG::hphMX4 (W303)</i>	This study
MHY12577	<i>ade3 ade3 leu3 ura3 lys2 prp20-1 [PRP20 ADE3 URA3]</i>	Michael Rosbash

Appendix 2: Plasmids used in this study

Plasmid	Description	Source
19-6-1	pRS415MET25	(Sikorski et al., 1989)
23-4-7	pET42b(+)	Novagen
57-1-4	pRS314-RPN5-GFP-FLAG	(J. Li, MH lab)
57-4-2	pRS316-RPN5-GFP-FLAG	(J. Li, MH lab)
60-8-6	pRS313-uba1-204	(R. Tomko, MH lab)
65-6-5	pET42b(+)-6His-MBP-STS1	(R. Tomko, MH lab)
78-6-2	pGEX6P1	(Smith & Johnson, 1988)
80-3-7	pGEX6P1-SRP1	(J. Ronau, MH lab)
90-9-6	pRS316-STS1	(Budenholzer et al., 2020)
91-2-5	pRS415MET25-STS1-GFP	(Budenholzer et al., 2020)
91-2-6	pRS415GPD-STS1-GFP	(Budenholzer et al., 2020)
91-2-7	pRS424-SRP1	(Budenholzer et al., 2020)
91-3-7	pRS415MET25-sts1(R38D)-GFP	(Budenholzer et al., 2020)
91-3-8	pRS415MET25-sts1(C194Y)-GFP	(Budenholzer et al., 2020)
91-3-9	pRS415GPD-sts1(R38D)-GFP	(Budenholzer et al., 2020)
91-4-3	pRS314-STS1	(Budenholzer et al., 2020)
91-4-4	pRS314-sts1(R38D, R65D)	(Budenholzer et al., 2020)
91-4-6	pRS414GPD-sts1(R38D, R65D)	(Budenholzer et al., 2020)
91-5-5	pRS315-STS1prom[536]-STS1-6xGly-3xFLAG	(Budenholzer et al., 2020)
91-6-4	pET42b(+)-STS1-6His	(Budenholzer et al., 2020)
91-7-9	pRS314-sts1(R38D)	(Budenholzer et al., 2020)
91-8-5	P415GPD-sts1(R38D, R65D)-GFP	(Budenholzer et al., 2020)
91-9-8	pRS415GPD-sts1(R65D)-GFP	(Budenholzer et al., 2020)
94-3-2	pRS415MET25-sts1(1-116)-GFP	(Budenholzer et al., 2020)
94-5-3	pRS415MET25-sts1(R38D, R65D)-GFP	(Budenholzer et al., 2020)
94-5-4	pRS415MET25-sts1(R65D)-GFP	(Budenholzer et al., 2020)
94-6-3	pRS415MET25-sts1(L80E)-GFP	This study
94-6-4	pRS415MET25-sts1(L95E)-GFP	This study

94-6-9	pET42b(+)-sts1(1-116)-6His	This study
94-9-5	pGEX6P1-sts1(116-276)	This study
94-9-6	pGEX6P1-sts1(116-319)	This study
95-5-1	pET42b(+)-sts1(C194Y)-6His	(Budenholzer et al., 2020)
95-6-6	pET42b(+)-sts1(R38D, R65D)-6His	(Budenholzer et al., 2020)
98-7-1	pRS314-sts1(R65D)	(Budenholzer et al., 2020)
100-3-2	pET42b(+)-SRP1-6His	This study
101-6-6	pMET25-GFP-GFP	Anita Corbett
101-6-7	pMET25-GFP-GFP-IN NLS	Anita Corbett
102-1-6	pMET25-sts1(1-76)-GFP-GFP	This study
102-1-7	pMET25-sts1(1-76, R38D)-GFP-GFP	This study
102-1-8	pMET25-sts1(1-76, R65D)-GFP-GFP	This study
102-1-9	pMET25-sts1(1-76, R38D, R65D)-GFP-GFP	This study
102-4-9	pMW172-KAP95	Anita Corbett
102-5-1	pGEX4T-1-GST-KAP95	Anita Corbett
102-5-3	pET15b-His6-GSP1	Anita Corbett
102-8-3	pRS415MET25-sts1(L80E, L95E)-GFP	This study
104-9-3	pRS415MET25-STs1	This study
108-9-1	pGEX-6P1-GST-IMP1	This study
108-9-2	pGEX-6P1-GST-CUT15	This study
108-9-3	pET42b(+)-CUT8-6His	This study
108-9-8	pRS415MET25-CUT8	This study
108-9-9	pRS415MET25-AKIRIN2	This study
109-6-7	pRS415MET25-STs1-mCherry-FLAG	This study
109-6-8	pGEX6P1-STs1	This study
109-7-2	pRS416MET25-STs1-GFP	This study
109-7-3	pET42b(+)-sts1(L80E)-6His	This study
109-7-4	pET42b(+)-sts1(L95E)-6His	This study
109-7-5	pET42b(+)-sts1(L80E, L95E)-6His	This study
109-7-6	pRS415MET25-CUT8-GFP	This study

References

- Aebi M, Clark MW, Vijayraghavan U, Abelson J.** (1990). A yeast mutant, PRP20, altered in mRNA metabolism and maintenance of the nuclear structure, is defective in a gene homologous to the human RCC1 which is involved in the control of chromosome condensation. *Molecular Genetics and Genomics* **224**, 72-80.
- Albert S, Schaffer M, Beck F, Mosalaganti S, Asano S, Thomas HF, Pitzko JM, Beck M, Baumeister W, Engela BD.** (2017). Proteasomes tether to two distinct sites at the nuclear pore complex. *Proceedings of the National Academy of Science USA* **114**, 13726–13731.
- Amrani N, Dufour ME, Bonneaud N and Lacroute F.** (1996). Mutations in STS1 suppress the defect in 3' mRNA processing caused by the rna15-2 mutation in *Saccharomyces cerevisiae*. *Molecular Genetics and Genomics* **252**, 552-562.
- Atkinson NS, Dunst RW, Hopper AK.** (1985). Characterization of an essential *Saccharomyces cerevisiae* gene related to RNA processing: cloning of RNA1 and generation of a new allele with a novel phenotype. *Molecular and Cellular Biology* **5**, 907–15.
- Babbitt SE, Kiss A, Deffenbaugh AE, Chang YH, Bailly E, Erdjument-Bromage H, Tempst P, Buranda T, Sklar LA, Baumler J, et al.** (2005). ATP hydrolysis-dependent disassembly of the 26S proteasome is part of the catalytic cycle. *Cell* **121**, 553–565.
- Baugh JM, Viktorova EG, Pilipenko EV.** (2009). Proteasomes can degrade a significant proportion of cellular proteins independent of ubiquitination. *Journal of Molecular Biology* **386**, 814–827.
- Bayliss R, Corbett AH, Stewart M.** (2000). The Molecular Mechanism of Transport of Macromolecules Through Nuclear Pore Complexes. *Traffic* **1**, 448-456.
- Bayliss R, Littlewood T, Stewart M.** (2000). Structural basis for the interaction between FxFG nucleoporin repeats and importin-beta in nuclear trafficking. *Cell* **102**, 99–108.
- Becker J, Melchior F, Gerke V, Bischoff FR, Ponstingl H, Wittinghofer A.** (1995). RNA1 encodes a GTPase-activating protein specific for Gsp1p, the Ran/TC4

- homologue of *Saccharomyces cerevisiae*. *Journal of Biological Chemistry* **270**, 11860-11865.
- Belanger KD, Walter D, Henderson TA, Yelton AL, O'Brien TG, Belanger KG, Geier SJ, Fahrenkrog B.** (2009). Nuclear localization is crucial for the proapoptotic activity of the HtrA-like serine protease Nma111p. *Journal of Cell Science* **122**, 3931-3941.
- Bemassola F, Karin M, Ciechanover A, Melino G.** (2008). The HECT Family of E3 Ubiquitin Ligases: Multiple Players in Cancer Development. *Cancer Cell* **74**, 10-21.
- Ben-Nissan G & Sharon M.** (2014). Regulating the 20S proteasome ubiquitin-independent degradation pathway. *Biomolecules* **23**, 862-864.
- Bischoff FR, Krebber H, Kempf T, Hermes I, Pongstingl H.** (1995). Human RanGTPase-activating protein RanGAP1 is a homolog of yeast RNA1 involved in messenger RNA processing and transport. *Proceedings of the National Academy of Sciences USA* **92**, 1749-1753.
- Breckel C & Hochstrasser M.** (2021). Ubiquitin Ligase Redundancy and Nuclear-Cytoplasmic Localization in Yeast Protein Quality Control. *Biomolecules* **11**, 1821.
- Budenholzer L, Breckel C, Hickey CM, Hochstrasser M.** (2020). The Sts1 nuclear import adaptor uses a non-canonical bipartite nuclear localization signal and is directly degraded by the proteasome. *Journal of Cell Science* **133**, jcs236158.
- Budenholzer L, Cheng CL, Li Y, Hochstrasser M.** (2017). Proteasome structure and assembly. *Journal of Molecular Biology* **429**, 3500-3524.
- Burrows JF, Johnston JA.** (2012) Regulation of cellular responses by deubiquitinating enzymes: an update. *Frontiers in Bioscience (Landmark Ed)* **17**, 1184-200.
- Cadwell K & Coscoy L.** (2005). Ubiquitination on nonlysine residues by a viral E3 ubiquitin ligase. *Science* **309**, 127-30.
- Cautain B, Hill R, de Pedro N, Link W.** (2014). Components and regulation of nuclear transport processes. *FEBS Journal* **282**, 445-462.
- Chen X, Barton LF, Chi Y, Clurman BE, Roberts JM.** (2007). Ubiquitin-independent degradation of cell cycle inhibitors by the REGgamma proteasome. *Molecular Cell* **26**, 843-852.

- Chen P, Johnson P, Sommer T, Jentsh S, Hochstrasser M.** (1993). Multiple ubiquitin-conjugating enzymes participate in the in vivo degradation of the yeast MAT alpha 2 repressor. *Cell* **74**, 357-369.
- Chen L & Madura K.** (2014). Degradation of specific nuclear proteins occurs in the cytoplasm in *Saccharomyces cerevisiae*. *Genetics* **197**, 193-197.
- Chen L, Romero L, Chuang SM, Tournier V, Joshi KK, Lee JA, Kovvali G, Madura K.** (2011). Sts1 plays a key role in targeting proteasomes to the nucleus. *Journal of Biological Chemistry* **286**, 3104-3118.
- Chook YM & Süel KE.** (2011). Nuclear Import by Karyopherin-Bs: Recognition and Inhibition. *Biochimica et Biophysica Acta* **1813**, 1593-1606.
- Chowdhury M & Enenkel C.** (2015). Intracellular dynamics of the ubiquitin-proteasome-system. *F1000 Research* **4**, 367.
- Cingolani G, Petosa C, Weis K.** (1999). Structure of importin-beta bound to the IBB domain of importin-alpha. *Nature* **399**, 221–229.
- Clarkson WD, Kent HM, & Stewart M.** (1996). Separate binding sites on nuclear transport factor 2 (NTF2) for GDP-Ran and the phenylalanine-rich repeat regions of nucleoporins p62 and Nsp1p. *The Journal of Molecular Biology* **263**, 517-524.
- Cokol M, Nair R, Rost B.** (2000). Finding nuclear localization signals. *EMBO Reports* **1**, 411–415.
- Conti E & Kuriyan J.** (2000). Crystallographic analysis of the specific yet versatile recognition of distinct nuclear localization signals by karyopherin alpha. *Structure* **8**, 329–338.
- Conti E, Uy M, Leighton L, Blobel G, Kuriyan J.** (1998). Crystallographic analysis of the recognition of a nuclear localization signal by the nuclear import factor karyopherin alpha. *Cell* **94**, 93–204.
- Coux O, Tanaka K, Goldberg AL.** (1996). Structure and Functions of the 20S and 26S Proteasomes. *Annual Review of Biochemistry* **65**, 801–847.
- de Almeida M, Hinterdorfer M, Brunner H, Grishkovskaya I, Singh K, Schleiffer A, Jude J, Deswal S, Kalis R, Vunjak M, et al.** (2021). AKIRIN2 controls the nuclear import of proteasomes in vertebrates. *Nature* **599**, 491-496.

- de Boor S, Knyphausen P, Kuhlmann N, Wroblowski S, Brenig J, Scislowski L, Baldus L, Nolte H, Kruger M, Lammers M.** (2015). Small GTP-binding protein Ran is regulated by posttranslational lysine acetylation. *Proceedings of the National Academy of Sciences USA* **112**, E3679-E3688.
- Deshaies RJ & Joazeiro CA.** (2009). RING domain E3 ubiquitin ligases. *Annual Review of Biochemistry* **78**, 399-434.
- Dilworth DJ, Suprpto A, Padovan JC, Chait BT, Wozniak RW, Rout MP, Aitchison JD.** (2001). Nup2p dynamically associates with the distal regions of the yeast nuclear pore complex. *The Journal of Cell Biology* **153**, 1465-1478.
- Dingwall C & Laskey RA.** (1991). Nuclear targeting sequences--a consensus? *Trends in Biochemical Science* **16**, 478-481.
- Dworetzky SI & Feldherr CM.** (1988). Translocation of RNA-coated gold particles through the nuclear pores of oocytes. *Journal of Cell Biology* **106**, 575-584.
- Enenkel C.** (2014). Nuclear transport of yeast proteasomes. *Biomolecules* **4**, 940-955.
- Enenkel C.** (2018) The paradox of proteasome granules. *Current Genetics* **64**, 137-140.
- Enenkel C, Blobel G, Rexach M.** (1995). Identification of a Yeast Karyopherin Heterodimer That Targets Import Substrate to Mammalian Nuclear Pore Complexes. *Journal of Biological Chemistry* **270**, 16499-16502.
- Erales J & Coffino P.** (2014). Ubiquitin-Independent Proteasomal Degradation. *Biochimica et Biophysica Acta* **1843**, 216-221.
- Expand RM.** (2006). Cholesterol and the interaction of proteins with membrane domains. *Progress in Lipid Research* **45**, 279-294.
- Fan X, Geisberg JV, Wong KH, Jin Y.** (2011). Conditional Depletion of Nuclear Proteins by the Anchor Away System (ms# CP-10-0125). *Current Protocols in Molecular Biology* Chapter 13, Unit 13.10B.
- Feldherr CM & Akin D.** (1997). The location of the transport gate in the nuclear pore complex. *Journal of Cell Science* **110**, 3065-3070.
- Feldherr CM, Kallenbach E, Schultz N.** (1984). Movement of a karyophilic protein through the nuclear pores of oocytes. *Journal of Cell Biology* **99**, 2216-2222.

- Feldherr C, Akin D, Moore MS.** (1998). The nuclear import factor p10 regulates the functional size of the nuclear pore complex during oogenesis. *Journal of Cell Science* **111**, 1889-1896.
- Feng W & Hopper AK.** (2002). A Los1p-independent pathway for nuclear export of intronless tRNAs in *Saccharomyces cerevisiae*. *Proceedings of the National Academy of Sciences USA* **99**, 5412-5417.
- Finley D.** (2009). Recognition and processing of ubiquitin-protein conjugates by the proteasome. *Annual Review of Biochemistry* **78**, 477–513.
- Finley D, Ulrich HD, Sommer T, Kaiser P.** (2012). The ubiquitin-proteasome system of *Saccharomyces cerevisiae*. *Genetics* **192**, 319-60.
- Fischer U, Huber J, Boelens WC, Mattaj JW, Luhrmann R.** (1995) The HIV-1 Rev activation domain is a nuclear export signal that accesses an export pathway used by specific cellular RNAs. *Cell* **82**, 475–483.
- Fleishmann M, Clark MW, Forrester W, Wickens M, Nishimoto T, Aebi M.** (1991). *Molecular Genetics and Genomics* **227**, 417-423.
- Folger A & Wang Y.** (2021). The cytotoxicity and clearance of mutant Huntington and other misfolded proteins. *Cells* **10**, 2835.
- Fontes MR, Teh T, Kobe B.** (2000). Structural basis of recognition of monopartite and bipartite nuclear localization sequences by mammalian importin- α . *Journal of Molecular Biology* **297**, 1183–1194.
- Förster F, Unverdorben P, Sledz P, Baumeister W.** (2013). Unveiling the long-held secrets of the 26S proteasome. *Structure* **21**, 1551–1562.
- Forwood JK, Lange A, Zachariae U, Marfori M, Preast C, Grubmuller H, Stewart M, Corbett AH, Kobe B.** (2010). Quantitative structural analysis of importin- β flexibility: paradigm for solenoid protein structures. *Structure* **18**, 1171-1183.
- Fredrickson EK & Gardner RG.** (2012). Selective destruction of abnormal proteins by ubiquitin-mediated protein quality control degradation. *Seminars in Cell and Developmental Biology* **23**, 530–37.
- Gall JG.** (1964). Electron microscopy of the nuclear envelope. *Protoplasmatologia* **5**, 4–25.

- Ghislain M, Udvardy A, Mann C.** (1993). *S. cerevisiae* 26S protease mutants arrest cell division in G2/metaphase. *Nature* **366**, 358-362.
- Glickman MH, Rubin DM, Fried VA, Finley D.** (1998). The Regulatory Particle of the *Saccharomyces Cerevisiae* Proteasome. *Molecular and Cellular Biology* **18**, 3149-3162.
- Gödderz D, Schäfer E, Palanimurugan R, Dohmen RJ.** (2011). The N-Terminal Unstructured Domain of Yeast ODC Functions as a Transplantable and Replaceable Ubiquitin-Independent Degron. *Journal of Molecular Biology* **407**, 354–367.
- Goldberg A.** (2003). Protein degradation and protection against misfolded or damaged proteins. *Nature* **426**, 895-899.
- Goldfarb DS, Corbett AH, Mason DA, Harreman MT, Adam SA.** (2004). Importin alpha: a multipurpose nuclear-transport receptor. *Trends in Cell Biology* **14**, 505-514.
- Gorlich D & Kutay U.** (1999). Transport between the cell nucleus and the cytoplasm. *Annual Review of Cell and Developmental Biology* **15**, 607–660.
- Gorlich D, Pante N, Kutay U, Aebi U, Bischoff FR.** (1996). Identification of different roles for RanGDP and RanGTP in nuclear protein import. *EMBO Journal* **15**, 5584–5594.
- Guthrie C & Fink GR. (eds)** (2004). *Guide to Yeast Genetics and Molecular and Cell Biology*, pp. 1-933. Elsevier.
- Ha SW, Ju D, Xie Y.** (2012). The N-terminal domain of Rpn4 serves as a portable ubiquitin- independent degron and is recognized by specific 19S RP subunits. *Biochemical and Biophysical Research Communications* **419**, 226–231.
- Ha SW, Ju D, Xie Y.** (2014). Nuclear import factor Srp1 and its associated protein Sts1 couple ribosome-bound nascent polypeptides to proteasomes for cotranslational degradation. *Journal of Biological Chemistry* **289**, 2701-2710.
- Haruki H, Nishikawa J, Laemmli UK.** (2008). The Anchor-Away Technique: Rapid, Conditional Establishment of Yeast Mutant Phenotypes. *Molecular Cell* **31**,925–932.
- Hickey CM & Hochstrasser M.** (2015). STUbL-mediated degradation of the transcription factor MAT α 2 requires degradation elements that coincide with corepressor binding sites. *Molecular Biology of the Cell* **26**, 3401-3412.

- Hickey CM, Xie Y, Hochstrasser M.** (2018). DNA binding by the Mat alpha2 transcription factor controls its access to alternative ubiquitin-modification pathways. *Molecular Biology of the Cell* **29**, 542–556.
- Hirano H, Kobayashi J, Matsuura Y.** (2017). Structures of the karyopherins Kap121p and Kap60p bound to the nuclear pore targeting domain of the SUMO protease Ulp1p. *Journal of Molecular Biology* **429**, 249-260.
- Hochstrasser M.** (1996). Ubiquitin-Dependent Protein Degradation. *Annual Review of Genetics* **30**, 405– 439.
- Hochstrasser M.** (2009) Origin and function of ubiquitin-like proteins. *Nature* **458**, 422–429.
- Hodel AE, Harreman MT, Pulliam KF, Harben ME, Holmes JS, Hodel MR, Berland KM, Corbett AH.** (2006). Nuclear localization signal receptor affinity correlates with in vivo localization in *Saccharomyces cerevisiae*. *Journal of Biological Chemistry* **281**, 23545-23556.
- Hopper AK, Traglia HM & Dunst RW.** (1990). The yeast RNA1 gene product necessary for RNA processing is located in the cytosol and apparently excluded from the nucleus. *Journal of Cell Biology* **111**, 309–321.
- Houman F & Holm C.** (1994). DBF8, an essential gene required for efficient chromosome segregation in *Saccharomyces cerevisiae*. *Molecular and Cellular Biology* **14**, 6350-6360.
- Isono E, Nishihara K, Saeki Y, Yashiroda H, Kamata N, Ge L, Ueda T, Kikuchi Y, Tanaka K, Nakano A, et al.** (2007). The assembly pathway of the 19S regulatory particle of the yeast 26S proteasome. *Molecular Biology of the Cell* **18**, 569-580.
- Jackson PK, Eldridge AG, Freed E, Furstenthal L, Hsu JY, Kaiser BK, Reimann JD.** (2000). The lore of the RINGs: substrate recognition and catalysis by ubiquitin ligases. *Trends in Cell Biology* **10**, 429-439.
- Jariel-Encontre I, Bossis G, Piechaczyk M.** (2008). Ubiquitin-independent degradation of proteins by the proteasome. *Biochimica et Biophysica Acta* **1786**, 153-177.
- Ju D, Xie Y.** (2004). Proteasomal degradation of RPN4 via two distinct mechanisms, ubiquitin-dependent and -independent. *Journal of Biological Chemistry* **279**, 23851–23854.

- Ju D, Xie Y.** (2006). Identification of the preferential ubiquitination site and ubiquitin-dependent degradation signal of Rpn4. *Journal of Biological Chemistry* **281**, 10657–10662.
- Jumper J, Evans R, Pritzel A, Green T, Figurnov M, Ronnenberger O, Tunyasuvunakool K, Bates R, Zidek A, Potapenko A, et al.** (2021). Highly accurate protein structure prediction with AlphaFold. *Nature* **596**, 583-589.
- Kafri, M., Metzl-Raz, E., Jona, G., Barkai, N.** (2016). The Cost of Protein Production. *Cell Reports* **14**, 22-31.
- Kalderon D, Richardson WD, Markham AF, Smith AE.** (1984). Sequence requirements for nuclear location of simian virus 40 large-T antigen. *Nature* **311**, 33–38.
- Kalderon D, Roberts BL, Richardson WD, Smith AE.** (1984). A short amino acid sequence able to specify nuclear location. *Cell* **39**, 499–509.
- Keeling PJ, Burger G, Durnford DG, Lang BF, Lee RW, Pearlman RE, Roger AJ, Gray MW.** (2005) The tree of eukaryotes. *Trends in Ecology and Evolution* **20**, 670–676.
- Koonin EV.** (2010). The origin and early evolution of eukaryotes in the light of phylogenomics. *Genome Biology* **11**, 1-12.
- Kobe B.** (1999). Autoinhibition by an internal nuclear localization signal revealed by the crystal structure of mammalian importin-alpha. *Nature Structural Biology* **6**, 388–397.
- Kosugi S, Hasebe M, Tomita M, Yanagawa H.** (2009). Systematic identification of cell cycle-dependent yeast nucleocytoplasmic shuttling proteins by prediction of composite motifs. *Proceedings of the National Academy of Sciences USA* **106**, 10171-10176.
- Kunjappu MJ & Hochstrasser M.** (2014). Assembly of the 20S Proteasome. *Biochimica et Biophysica Acta* **1843**, 2-12.
- Kunzler M, Gerstberger T, Stutz F, Bischoff FR, Hurt E.** (2000). Yeast Ran-binding protein 1 (Yrb1) shuttles between the nucleus and cytoplasm and is exported from the nucleus via a CRM1 (XPO1)-dependent pathway. *Molecular Cellular Biology* **20**, 4295–4308.

- Kushnirov VV.** (2000). Rapid and reliable protein extraction from yeast. *Yeast* **16**, 857-860.
- Lange A, McLane LM, Mills RE, Devine SE, Corbett AH.** (2010). Expanding the Definition of the Classical Bipartite Nuclear Localization Signal. *Traffic* **11**, 311-323.
- Laporte D, Salin B, Daignan-Fornier B, Sagot I.** (2008). Reversible cytoplasmic localization of the proteasome in quiescent yeast cells. *Journal of Cell Biology* **181**, 737–745.
- Lee SJ, Matsuura Y, Liu SM, Stewart M.** (2005). Structural basis for nuclear import complex dissociation by RanGTP. *Nature* **435**, 693–696.
- Lehmann A, Janek K, Braun B, Kloetzel PM, Enenkel C.** (2002). 20S proteasomes are imported as precursor complexes into the nucleus of yeast. *Journal of Molecular Biology* **317**, 401-413.
- Leung SW, Harreman MT, Hodel MR, Hodel AE, Corbett AH.** (2003). Dissection of the Karyopherin Nuclear Localization Signal (NLS)-binding Groove Functional Requirements for NLS Binding. *Journal of Biological Chemistry* **273**, 41947–41953.
- Li J & Hochstrasser M.** (2021). Microautophagy regulates proteasome homeostasis. *Current Genetics* **66**, 683-687.
- Li J & Hochstrasser M.** (2022). Selective microautophagy of proteasomes is initiated by ESCRT-0 and is promoted by proteasome ubiquitylation. *Journal of Cell Science* **135**, jcs259393.
- Li SC & Kane PM.** (2009). The Yeast Lysosome-Like Vacuole: Endpoint and Crossroads. *Biochimica et Biophysica Acta* **1793**, 650-63.
- Li Y, Tomko RJ, Hochstrasser M.** (2015). Proteasomes: Isolation and Activity Assays. *Current Protocols in Cell Biology* **67**, 1–20.
- Liang S, Lacroute F, Képeš F.** (1993). Multicopy STS1 restores both protein transport and ribosomal RNA stability in a new yeast sec23 mutant allele. *European Journal of Cell Biology* **62**, 270-281.
- Liu C, Corboy MJ, DeMartino GN, Thomas PJ.** (2002). Endoproteolytic Activity of the Proteasome. *Science* **299**, 408-411.

- Liu C, Li X, Thompson D, Wooding K, Chang T, Tang Z, Yu H, Thomas PJ, DeMartino GN.** (2006). ATP Binding and ATP Hydrolysis Play Distinct Roles in the Function of 26S Proteasomes. *Molecular Cell* **24**, 39-50.
- Lott K, Bhardwaj A, Mitrousis G, Pante N, Cingolani G.** (2010). The Importin Binding Domain Modulates the Avidity of Importin-Beta for the Nuclear Pore Complex. *Journal of Biological Chemistry* **285**, 13769–13780.
- Lu Y, Lee BH, King RW, Finley D, Kirschner MW.** (2015). Substrate Degradation by the Proteasome: a Single-Molecule Kinetic Analysis. *Science* **348**, 1250834-1250834.
- Luan B, Huang X, Wu J, Mei Z, Wang Y, Xue X, Yan C, Wang J, Finley DJ, Shi Y, Wang F.** (2016). Structure of an Endogenous Yeast 26S Proteasome Reveals Two Major Conformational States. *Proceedings of the National Academy of Sciences USA* **113**, 2642-2647.
- Ma CP, Slaughter CA, DeMartino GN.** (1992). Identification, purification, and characterization of a protein activator (PA28) of the 20S proteasome (macropain). *Journal of Biological Chemistry* **267**, 10515–10523.
- Majumder P, Rudack T, Beck F, Danev R, Pfeifer G, Nagy L, Baumeister W.** (2019). Cryo-EM Structures of the Archaeal PAN-Proteasome Reveal an Around-the-Ring ATPase Cycle. *Proceedings of the National Academy of Sciences* **116**, 534-539.
- Mapa CE, Arsenault HE, Conti MM, Poti KE, Benanti JA.** (2018). A balance of deubiquitinating enzymes controls cell cycle entry. *Molecular and Cellular Biology* **29**, 2821-2834.
- Matsuura Y, Lange A, Harreman MT, Corbett AH, Stewart M.** (2003). Structural basis for Nup2p function in cargo release and karyopherin recycling in nuclear import. *EMBO Journal* **22**, 5358-5369.
- Matsuura Y & Stewart M.** (2004). Structural basis for the assembly of a nuclear export complex. *Nature* **432**, 872–877.
- McCann TS & Tansey WP.** (2014). Functions of the proteasome on chromatin. *Biomolecules* **4**, 1026-1044.

- Metzger MB, Pruneda JN, Klevit RE, Weissman AM.** (2013). RING-type E3 ligases: Master manipulators of E2 ubiquitin-conjugating enzymes and ubiquitination. *Biochimica et Biophysica Acta* **1843**, 47-60.
- Moore MS.** (1998). Ran and nuclear transport. *Journal of Biological Chemistry* **273**, 22857–22860.
- Müller AU & Weber-Ban E.** (2019). The Bacterial Proteasome at the Core of Diverse Degradation Pathways. *Frontiers in Molecular Bioscience* **6**, 23.
- Mumberg D, Muller R, Funk M.** (1995). Yeast vectors for the controlled expression of heterologous proteins in different genetic backgrounds. *Gene* **156**, 119-122.
- Nachury MV & Weis K.** (1999). The direction of transport through the nuclear pore can be inverted. *Proceedings of the National Academy of Science USA* **96**, 9622–9627.
- Nakagowa H, Suzuki K, Kamada Y, Ohsumi Y.** (2009). Dynamics and diversity in autophagy mechanisms: lessons from yeast. *Nature Reviews Molecular and Cellular Biology* **10**, 458-67.
- Nakai K & Horton P.** (1999). PSORT: a program for detecting sorting signals in proteins and predicting their subcellular localization. *Trends in Biochemical Science* **24**, 34–36.
- Nowak SJ, Aihara H, Gonzalez K, Nibu Y, Baylies MK.** (2012). Akirin links twist-regulated transcription with the Brahma chromatin remodeling complex during embryogenesis. *PLoS Genetics* **8**, e1002547.
- Paci G, Zheng T, Caria J, Zilman A, Lemke E.** (2020). Molecular determinants of large cargo transport into the nucleus. *eLife* **9**, e55963.
- Pack CG, Yukii H, Toh-e A, Kudo T, Tsuchiya H, Kaiho A, Sakata E, Murata S, Yokosawa H, Sako Y, et al.** (2014). Quantitative live-cell imaging reveals spatio-temporal dynamics and cytoplasmic assembly of the 26S proteasome. *Nature Communications* **5**, 3396.
- Paine PL, Moore LC, Horowitz SB.** (1975). Nuclear envelope permeability. *Nature* **254**, 109-114.
- Palacios V, Kimble GC, Tootle TL, Buszczak M.** (2021). Importin-9 regulates chromosome segregation and packaging in *Drosophila* germ cells. *Journal of Cell Science* **134**, jcs258391.

- Peters LZ, Karmon O, Miodownik S, Ben-Aroya S.** (2016). Proteasome storage granules are transiently associated with the insoluble protein deposit in *Saccharomyces cerevisiae*. *Journal of Cell Science* **129**, 1190–1197.
- Pickart CM.** (2000). Ubiquitin in chains. *Trends in Biochemical Sciences* **25**, 544-8.
- Pohl C & Dikic I.** (2019). Cellular quality control by the ubiquitin-proteasome system and autophagy. *Science* **366**, 818-822.
- Radu A, Blobel G, Moore MS.** (1995). Identification of a protein complex that is required for nuclear protein import and mediates docking of import substrate to distinct nucleoporins. *Proceedings of the National Academy of Sciences USA* **92**, 1769-1773.
- Ravid T & Hochstrasser M.** (2008). Diversity of degradation signals in the ubiquitin-proteasome system. *Nature Reviews Molecular and Cellular Biology* **9**, 679-90.
- Ribbeck K & Görlich D.** (2002). The permeability barrier of nuclear pore complexes appears to operate via hydrophobic exclusion. *EMBO Journal* **21**, 2664–2671.
- Robbins J, Dilworth SM, Laskey RA, Dingwall C.** (1991). Two interdependent basic domains in nucleoplasmin nuclear targeting sequence: identification of a class of bipartite nuclear targeting sequence. *Cell* **64**, 615–623.
- Romero-Perez L, Chen L, Lambertson D, Madura K.** (2007). Sts1 can overcome the loss of Rad23 and Rpn10 and represents a novel regulator of the ubiquitin/proteasome pathway. *Journal of Biological Chemistry* **282**, 35574-35582.
- Sadowski M, Suryadinata R, Tan AR, Roesley SN, Saracevic B.** (2012). Protein monoubiquitination and polyubiquitination generate structural diversity to control distinct biological processes. *IUBMB Life* **64**, 136-42.
- Saeki Y.** (2017). Ubiquitin Recognition by the Proteasome. *Journal of Biochemistry* **161**, 113-124.
- Sánchez-Lanzas R & Castaño JG.** (2014). Proteins directly interacting with mammalian 20S proteasomal subunits and ubiquitin-independent proteasomal degradation. *Biomolecules* **4**, 1140-1154.
- Schneider CA, Rasband WS, Eliceiri KW.** (2012). NIH Image to ImageJ: 25 years of image analysis. *Nature Methods* **9**, 671-675.

- Schwoebel ED, Talcott B, Cushman I, Moore MS.** (1998). Ran-dependent signal-mediated nuclear import does not require GTP hydrolysis by Ran. *Journal of Biological Chemistry* **273**, 35170-35175.
- Sharp PM & Li WH.** (1987). Molecular evolution of ubiquitin genes. *Trends in Ecology & Evolution* **2**, 328–332.
- Shulga N, Roberts P, Gu Z, Spitz L, Tabb MM, Nomura M, Goldfarb GS.** (1996). In vivo nuclear transport kinetics in *Saccharomyces cerevisiae*: A role for heat shock protein 70 during targeting and translocation. *The Journal of Cell Biology* **135**, 329-339.
- Sikorski RS & Hieter P.** (1989). A system of shuttle vectors and yeast host strains designed for efficient manipulation of DNA in *Saccharomyces cerevisiae*. *Genetics* **122**, 19-27.
- Smith DB & Johnson KS.** (1988). Single-step purification of polypeptides expressed in *Escherichia coli* as fusions with glutathione-S-transferase. *Gene* **67**, 31-40.
- Stewart M.** (2007). Molecular mechanism of the nuclear protein import cycle. *Nature Reviews Molecular and Cellular Biology* **8**, 195-208.
- Strombio-de-Castillia C & Rout MP.** (2002). The Structure and Composition of the Yeast NPC. In: Weis K (ed) Nuclear Transport. *Results and Problems in Cell Differentiation* **35**, 1-23.
- Suntharalingam M & Wente SR.** (2003). Peering Through the Pore: Nuclear Pore Complex Structure, Assembly, and Function. *Developmental Cell* **4**, 775-789.
- Suskiewicz MJ, Sussman JL, Silman I, Shaul Y.** (2011). Context-dependent resistance to proteolysis of intrinsically disordered proteins. *Protein Science* **20**, 1285-1297.
- Tabb MM, Tongaonkar P, Vu L, Nomura M.** (2000). Evidence for separable functions of Srp1p, the yeast homolog of importin alpha (Karyopherin alpha): role for Srp1p and Sts1p in protein degradation. *Molecular and Cellular Biology* **20**, 6062-6073.
- Takeda K & Yanagida M.** (2005). Regulation of nuclear proteasome by Rhp6/ Ubc2 through ubiquitination and destruction of the sensor and anchor Cut8. *Cell* **122**, 393-405.
- Takeda K, Tonthat NK, Glover T, Xu W, Koonin EV, Yanagida M, Schumacher MA.** (2011). Implications for proteasome nuclear localization revealed by the

- structure of the nuclear proteasome tether protein Cut8. *Proceedings of the National Academy of Science USA* **108**, 16950-16955.
- Tanaka K, Yoshimura T, Tamura T, Fujiwara T, Kumatori A, Ichihara A.** (1990). Possible mechanism of nuclear translocation of proteasomes. *FEBS Letters* **271**, 41-46.
- Tatebe H & Yanagida M.** (2000). Cut8, essential for anaphase, controls localization of 26S proteasome, facilitating destruction of cyclin and Cut2. *Current Biology* **10**, 1329-1338.
- Thrower JS, Hoffman L, Rechsteiner M, Pickart CM.** (2000). Recognition of the polyubiquitin proteolytic signal. *EMBO Journal* **19**, 94-102.
- Tomko RJ Jr & Hochstrasser M.** (2011). Incorporation of the Rpn12 subunit couples completion of proteasome regulatory particle lid assembly to lid-base joining. *Molecular Cell* **44**, 907-917.
- Tomko RJ Jr & Hochstrasser M.** (2013). Molecular Architecture and Assembly of the Eukaryotic Proteasome. *Annual Review of Biochemistry* **82**, 415-445.
- Tsuchiya H, Arai N, Tanaka K, Saeki Y.** (2013). Cytoplasmic proteasomes are not indispensable for cell growth in *Saccharomyces cerevisiae*. *Biochemical and Biophysical Research Communications* **436**, 372–376.
- Ulrich HD & Walden H.** (2010). Ubiquitin signalling in DNA replication and repair. *Nature Review Molecular Cell Biology* **11**, 479–489.
- Umeda M, Izaddoost S, Cushman I, Moore MS, Sazer S.** (2005). The fission yeast *Schizosaccharomyces pombe* has two importin- α proteins, Imp1p and Cut15p, which have common and unique functions in nucleocytoplasmic transport and cell cycle progression. *Genetics* **171**, 7-21.
- Valas RE & Bourne PE.** (2008). Rethinking proteasome evolution: two novel bacterial proteasomes. *Journal of Molecular Evolution* **66**, 494–504.
- Varadi M, Anyango S, Deshpande M, Nair S, Natassia C, Yordanova G, Yuan D, Stroe O, Wood G, Laydon A, et al.** (2022). AlphaFold Protein Structure Database: massively expanding the structural coverage of protein-sequence space with high-accuracy models. *Nucleic Acids Research* **50**, D439-D444.

- Varshavsky A.** (2012). The Ubiquitin System, an Immense Realm. *Annual Review of Biochemistry* **81**, 167–176.
- Verma R, Aravind L, Oania R, Hayes McDonald W, Yates III JR, Koonin EV, Deshaies RJ.** (2002) Role of Rpn11 metalloprotease in deubiquitination and degradation by the 26S proteasome. *Science* **298**, 611-5.
- Vijayraghavan U, Company M, Abelson J.** (1989). Isolation and characterisation of pre-mRNA splicing mutants in *Saccharomyces cerevisiae*. *Genes and Development* **3**, 1206-1216.
- Weberruss MH, Savulescu AF, Jando J, Bissinger T, Harel A, Glickman MH, Enenkel C.** (2013). Blm10 facilitates nuclear import of proteasome core particles. *EMBO Journal* **32**, 2697–2707.
- Wen W, Meinkoth JL, Tsien RY, Taylor SS** (1995) Identification of a signal for rapid export of proteins from the nucleus. *Cell* **82**, 463–473.
- Wendler P & Enenkel C.** (2019). Nuclear transport of yeast proteasomes. *Frontiers in Molecular Bioscience* **6**, 34.
- Wendler P, Lehmann A, Janek K, Baumgart S, Enenkel C.** (2004). The bipartite nuclear localization sequence of Rpn2 is required for nuclear import of proteasomal base complexes via karyopherin alpha and proteasome functions. *Journal of Biological Chemistry* **279**, 37751-37762.
- Wente SR & Rout MP.** (2010). The nuclear pore complex and nuclear transport. *Cold Spring Harbor Perspectives in Biology* **2**, a000562.
- Wenzel DM & Klevit RE.** (2012). Following Ariadne's thread: a new perspective on RBR ubiquitin ligases. *BMC Biology* **10**, 24.
- Wilkinson CR, Wallace M, Morpew M, Perry P, Allshire R, Javerzat JP, McIntosh JR, Gordon C.** (1998). Localization of the 26S proteasome during mitosis and meiosis in fission yeast. *EMBO Journal* **17**, 6465–6476.
- Wójcik C & DeMartino GN.** (2003). Intracellular localization of proteasomes. *International Journal of Biochemistry and Cell Biology* **35**, 579–589.
- Xie Y & Varshavsky A.** (2001). RPN4 is a ligand, substrate, and transcriptional regulator of the 26S proteasome: A negative feedback circuit. *Proceedings of the National Academy of Science USA* **98**, 3056-3061.

- Xu P, Duong DM, Seyfried NT, Cheng D, Xie Y, Robert J, Rush J, Hochstrasser M, Finley D, Peng J.** (2009). Quantitative proteomics reveals the function of unconventional ubiquitin chains in proteasomal degradation. *Cell* **137**, 133-45.
- Yang H & Hu HY.** (2016). Sequestration of cellular interacting partners by protein aggregates: implication in loss-of-function pathology. *FEBS Journal* **283**, 3705-17.
- Yau R & Rape M.** (2016). The increasing complexity of the ubiquitin code. *Nature Cell Biology* **18**, 579-86.
- Yu H, Kago G, Yellman CM, Matouschek A.** (2016). Ubiquitin-like domains can target to the proteasome but proteolysis requires a disordered region. *EMBO Journal* **35**, e201593147-e1536.
- Zhu YJ, Lin H, & Lal R.** (2000). Fresh and nonfibrillar amyloid beta protein(1-40) induces rapid cellular degeneration in aged human fibroblasts: Evidence for AbetaP-channel-mediated cellular toxicity. *FASEB Journal* **14**, 1244–1254.
- Zimmerli CE, Allegretti M, Rantos V, Goetz SK, Obarska-Kosinska A, Zagoriy I, Halavatyi A, Hummer G, Mahamid J, Kosinski J, Beck M.** (2021). Nuclear pores dilate and constrict in cellulo. *Science* **374**, eabd9776.